# Electrochemistry and separation of transition metals with biodegradable ligands

Lebogang Katata

Thesis presented in partial fulfillment for the degree of

Magister Scientiae (Chemistry/Chemie)

At the Faculty of Science at the University of Stellenbosch,

Republic of South Africa


Supervisor: Prof. Andrew. M. Crouch

December 2001

**"Declaration**

I, the undersigned, hereby declare that the work contained in this thesis is my own original work and that I have not previously in its entirety or in part submitted it at any university for a degree.

Signature:

Date:

# ABSTRACT

The electrochemical analysis of selected metal ions with the newly biodegradable chelating agents, Iminodisuccinic acid (IDS) and Polyaspartic acid (PASP) was performed by cyclic voltammetry using a thin mercury film glassy carbon microelectrode. IDS and PASP are of interest from an environmental perspective. They were introduced as alternatives to chelants and dispersants.

The thermodynamic stability constants of these selected metal complexes were determined by cyclic voltammetry (CV). A comparison with similar data obtained using potentiometric methods shows a good correlation between the two methods. This reaffirms that CV is a useful and facile means for evaluating metal-ligand complex thermodynamic data. Furthermore, our results were used to validate the predicted models obtained using an Equilibrium Speciation model JESS program.

Capillary Electrophoresis (CE) was used to separate metal-IDS and metal-PASP complexes at different pH's. The separation of these chelates was achieved within 7 minutes. The obtained results were compared with speciation and a reasonable agreement was observed, although the separation of metal-PASP showed poor broad peaks.

# OPSOMMING

Die elektrochemiese analise van geselekteerde metaal-ione met nuwe biodegredeerbare chelate, Iminodisuksien suur (IDS) en Polyaspartiese suur was gedoen met sikliese voltametrie deur gebruik te maak van 'n dun laag kwik glasagtige koolstof mikroelektrode. Vanaf 'n omgewingsstandpunt is IDS en PASP van belang. Hulle was voorgestel as alternatiewe vir chelate en verspreidingsagente.

Die termodinamies stabiliteits konstantes van hierdie uitgesoekte metal komplekse was bepaal deur middel van sikliese voltametrie (CV). 'n Vergelyking met soortgelyke data, wat met potensiometriese metodes bepaal was, dui 'n goeie korrelasie aan tussen die twee metodes bepaal was. Dit bevestig die feit dat CV 'n bruikbare en maklike manier is om metal ligand komplekse se termodiniese data te evalueer. Die resultate was ook gebruik om die voorspelde model, wat verkry was deur gebruik te maak van "Equilibrium Speciation model JESS program, te bevestig.

Kapillere elektroforese (CE) was gebruik om metal-IDS en metal-PASP komplekse by verskillende pH's te skei. Die skeiding van hierdie chelate was binne sewe minute verkry. Hierdie resultate was vergelyk met die spesiasie data en 'n aanvaarbare ooreenstemming was waargeneem, alhoewel die skeiding van die Metaal-PASP swak pieke toon.

# *ACKNOWLEDGEMENTS*

First and foremost I would like to thank The Almighty for all his blessings. NRF financial support is gratefully acknowledged. Special thanks are due to my supervisor Prof A.M. Crouch for his support and guidance throughout this project and sincere gratitude to my family. Finally I would like to thank my friends and colleagues.

Dedicated to my Late Grandfather, who will always be part of my life.

# LIST OF ABBREVIATIONS

| | |
|---|---|
| AAS | - Atomic Absorption Spectroscopy |
| ASP | - Aspartic Acid |
| ASV | - Anodic Stripping Voltammetry |
| CE | - Capillary Electrophoresis |
| CTAB | - Cetyltrimethylammonium bromide |
| CV | - Cyclic Voltammetry |
| CZE | - Capillary zone electrophoresis |
| DCTA | - Trans-1, 2-diaminocyclohexane-N, N, N', N'-tetraacetic |
| DME | - Dropping Mercury Electrode |
| DTPA | - Diethylenetriamine pentaacetic acid |
| E | - Potential |
| EC | - Electrochemical |
| EDDM | - Ethylenediamine dimalonic acid |
| EDDS | - Ethylenediamine disuccinic acid |
| EDTA | - Ethylenediamine tetraacetic acid |
| EGTA | - Ethyleneglycolcolbis (2-aminoethyl ether) N, N, N', N'-tetraacetic acid |
| EN | - Ethylenediamine |
| GC | - Gas Chromatography |
| HMDE | - Hanging Mercury Dropping Electrode |
| $HNO_3$ | - Nitric acid |

| | |
|---|---|
| HPCE | - High Performance Capillary Electrophoresis |
| HPLC | - High Performance Liquid Chromatography |
| i | - Current |
| ICP | - Inductively Coupled Plasma |
| ICP-AES | - Inductively Coupled plasma source with atomic emission spectrometry |
| ICP-MS | - Inductively Coupled Plasma source with a Mass Spectrometer |
| IDS | - Iminodisuccinic acid |
| ISE | - Ion Selective Electrode |
| JESS | - Joint Expert Speciation System |
| M | - Marker |
| MECC | - Micellar Electrokinetic Capillary Chromatography |
| NTA | - Nitrilotriacetic acid |
| PASP | - Polyaspartic acid |
| PSA | - Potentiometric Stripping Analysis |
| RDE | - Rotating Disk Electrode |
| SMDE | - Static Mercury Drop Electrode |
| TTHA | - Triethylenetetramine-N, N, N', N", N"', N"'-hexaacetic acid |
| UV | - Ultraviolet |
| XRF | - X-ray Fluorescence |

# CONTENTS

**Chapter 6**

# LIST OF FIGURES

## CHAPTER 3

## CHAPTER 4

## CHAPTER 5

# LIST OF TABLES

## CHAPTER 3



## CHAPTER 4



## CHAPTER 5

# ANNEXURES

# CHAPTER 1

## Aims and Objectives

The objectives of this study were the following:

- To determine the equilibrium constants of selected metal complexes of Iminodisuccinic acid (IDS) and Polyaspartic acid (PASP) using cyclic voltammetry. IDS and PASP are new biodegradable ligands and their equilibrium behaviour needs to be known for speciation prediction
- Compare the obtained stability behaviour with those reported in the literature using potentiometric methods
- To use speciation modelling to compare and validate the presence and distribution of metal-ligand species
- Separation of biodegradable complexes by Capillary Electrophoresis will be used to further validate the electrochemical studies.

# CHAPTER 2

## 2.1 Sequestering of metal ions

### 2.1.1 Uses of metals

In general metal complexes have received a great deal of attention in environmental and ecotoxicological sciences [5]. This is all owing to the increasing of metal contaminants in the environment, which has focussed attention on their determination and characterisation[6]. The most important feature distinguishing most pollutants is that they are not biodegradable but interaction of these metals with (biodegradable) ligands transforms them from a relatively toxic state to an essentially non-toxic bound state. This parameter is called the complexation capacity [7].

The predominant sources of metals before the industrial revolution were in ore deposits and volcanoes. Dumps of metal mines and mills can contaminate ground and surface waters so those reservoirs for drinking water have to avoid such mining areas[8]. Metals are released into the atmosphere, both as particles and as vapors, as a result not only of fossil fuel (coal, oil and natural gas) combustion but also of cement production and extractive metallurgy[8]. Living organisms are exposed to them through respiration, skin contact and consumption. Metals are essential and non-essential for some organisms.

Among the most hazardous metals are Pb, Cd and Hg. Inhalation of fumes or dusts containing cadmium compounds produce symptoms suggestive of food poisoning of microbial origin. The alkyl compounds of mercury and lead are especially dangerous because they are lipid soluble [5] and materials such as lead halide aerosol emitted by automobiles can enter the lungs and be absorbed directly into the blood stream.

Many catalysts for important industrial reactions involve transition elements, especially those that form coordinate covalent bonds with molecules or anions having lone pairs of electrons, such as hexadentate polyaminocarboxylate ligands like EDTA, DTPA and EDDS.

Some of the biochemical essential elements are Cu, Zn, Co, Ni, V, Se, Cr, Fe and Mn, though become progressively toxic above certain levels. Some of these metals are for example Ni, Cr, Cu and Se are known to display carcinogenic effects [6] due to their interaction with nucleic acids. In general, the toxicity of metals stems from the fact that they are biologically non-degradable and have a tendency to accumulate in vital organs e.g. brain, liver or bones of man and their accumulation becomes progressively more toxic. However, the degree of toxicity exerted on a biological system depends on the chemical form or oxidation state of the particular heavy metal [5,9]. For example studies have revealed that ionic copper is far more toxic towards aquatic organisms than organically bound copper and that the more stable the copper complex, the lower is its toxicity[10]. It is important to have knowledge of chemical state of metal in natural waters and biological fluids in order to understand their reactivity, transport and toxicity.

Transitional elements studied in this project are $Cu^{2+}$, $Pb^{2+}$, $Zn^{2+}$, $Cd^{2+}$, $Fe^{3+}$, $Fe^{2+}$, $Cr^{3+}$ and $Mn^{2+}$, of which the first four are of prime environmental concern. The first four are referred to as heavy metals[7] and certain heavy metals such as Hg, Cd and Pb are generally toxic even at very low concentration levels. In most cases the biological activity of the transition elements and their role in human nutrition depend on the formation of complexes or coordination compounds. The transition element is central to the structure and function of the biological molecule. Hemoglobin and Myoglobin are examples of metal complexes or coordination compounds where oxygen molecule bonds to the iron atom. Hemoglobin, a complex of iron, is vital to the transport of oxygen from lungs to other body tissues by red blood cells[11].

### 2.1.2 Ligands for metal complexation

Many metal ions of transition elements form coordinate covalent bonds with molecules or anions having lone pairs of electrons thus the metal ion acts as a Lewis acid (electron pair acceptor) and the molecule or anion having the lone pair of electrons acts as a Lewis base (electron pair donor). Complex ions are formed from a metal ion with Lewis bases attached to it by coordinate covalent bonds [11]. The stability of complex ions is expressed by means of stability constant. The more stable the complex, the greater is the stability constant that is the smaller the tendency of the complex ion to dissociate into its constituent ions [12]. A complex formed by polydentate ligands is frequently quite stable and is called a chelate. Because of the stability of chelates, polydentate ligands are often used to remove metal ions from a chemical system [11].

The aminopolycarboxylic acids are excellent complexing agents: the most important of these is EDTA. Other complexing agents are sometimes used including nitrilotriacetic acid (NTA), trans-1, 2-diaminocyclohexane-N, N, N', N'-tetraacetic (DCTA), ethyleneglycolcolbis (2-aminoethyl ether) N, N, N', N'-tetraacetic acid (EGTA), triethylenetetramine-N, N, N', N'', N''', N'''-hexaacetic acid (TTHA) and diethyllenetriaminepentaacetate (DTPA).

DCTA often forms stronger metal complexes than does EDTA and thus finds applications in analysis, but the metal complexes are formed rather more slowly than with EDTA. EGTA finds analytical application mainly in the determination of calcium in a mixture of calcium and magnesium and is probably superior to EDTA in the calcium/magnesium water-hardness titration. TTHA forms 1:2 complexes with many trivalent cations and with some divalent metals. However, EDTA has the widest general application in analysis because of its powerful complexing action and commercial availability. EDTA reacts with all metals in a 1:1 ratio.

The non-biodegradable chelating agents like ethylenediaminetetraacetate (EDTA) **(1)** and diethylenetriaminepentaacetate (DTPA) **(2)** are being used in everyday consumer products, i.e. food, cleaning and photographic applications [13], as well as in some medicinal and personal care products [14]. Metal complexes of EDTA because they are soluble, form anionic complexes and their changes in redox potential [14]. The main purpose of these chelating agents is to mask the interfering metals by converting them into forms that lack the ability to cause undesirable effects. The metal ions can lead to

undesirable effects in water and play a leading role in household, trade and industry, being essential for many processes.

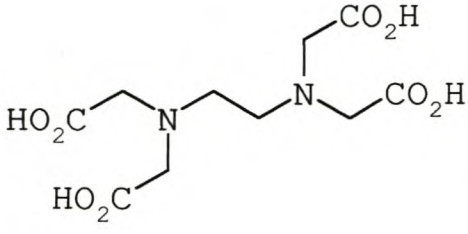

(1)

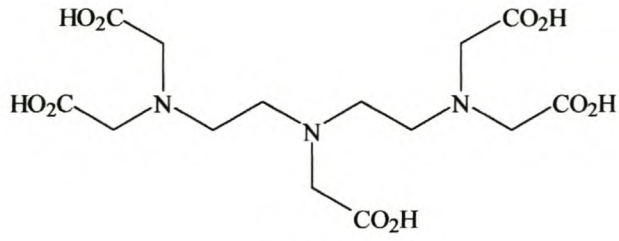

(2)

Aminopolycarboxylic acid chelating agents, such as NTA, EDTA and DTPA are known to efficiently oxidize the hydrosulfide ion to elemental sulfur in the pH range 8.0-8.5 when chelated to aqueous solutions of Fe (III). This reaction has been utilized in the desulfurization of fuel gases [15]. Lead poisoning is commonly administered either by intravenous infusion or by intramuscular injection, after which the lead-EDTA complex is excreted in urine [16]. The pulp and paper industry is the dominant user of EDTA and DTPA. They utilise EDTA and DTPA to inactivate metal ions that catalyze the decomposition of added bleach [17].

The disadvantages of these commonly used chelating agents i.e. EDTA and DTPA is their poor biodegradability and thus tend to accumulate in the biosphere [18]. It is becoming necessary to replace some of the ligands currently preferred in industrial processes.

## 2.1.3 Biodegradable ligands

The most important properties of biodegradable ligands is their ready biodegradability and its ability to form water soluble complexes with Fe, Cu and other polyvalent metal ions over a wide pH range [19]. Biodegradability of a substance is a key property in the environmental hazard and risk assessment of organic chemicals. Biodegradable chelating agents have to be powerful, and chemically resistant to oxidative process itself and yet easily broken down when released to the environment. Biodegradation models could be a useful in the early development of new chemicals because biodegradability could then become an integral part of the design process itself [20].

Current environmental legislation is increasingly moving towards the phasing out of potentially harmful non-biodegradable chelating agents and the introduction of environmentally more benign readily biodegradable sequestering agents. The viable alternatives to these ubiquitous ligands are ethylenediamine disuccinic acid (EDDS) **(3)**, ethylenediamine dimalonic acid (EDDM) **(4)**, iminodisuccinic acid (IDS) **(5)** and polyaspartic acid (PASP) **(6)**. These are chelating agents that display ready biodegradability not apparent in EDTA and DTPA.

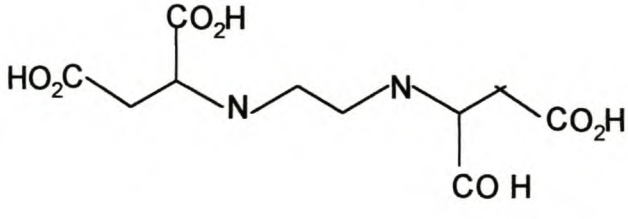


**(3)**

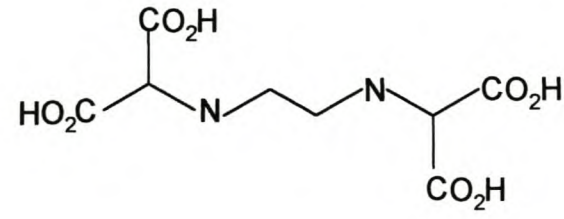


**(4)**

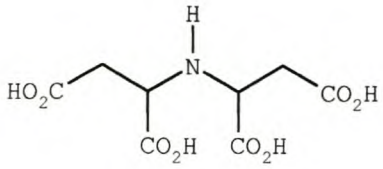

(5)

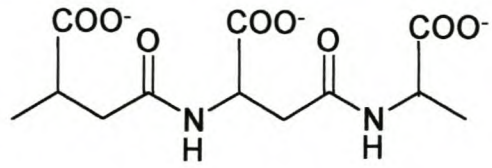

(6)

EDDS is proposed to replace EDTA as a chelating agent due to the disadvantages posed by EDTA. EDDS and its complexes with transitional metal ions biodegrade more readily than does EDTA [21]. EDDM chelate weakly with alkaline earth metals but strongly with transition metals [22]. EDDS is an effective biodegradable chelating agent for pulp and paper, metal treatment, photographic, agricultural, cleaning and personal care applications. It can produce a pulp with comparable properties to that produced using DTPA. It is also a powerful chelate to be used in pulp bleaching with hydrogen peroxide. Being readily biodegradable makes it an additional benefit over chelants such as EDTA or DTPA. It has the potential to be mixed with other biodegradable chelants without significant loss of performance to further reduce the potential environmental burden of the bleaching process. It can effectively replace EDTA and can be used as a low-corrosive cleaning additive in metal cleaning formulations for use in iron, copper, zinc and aluminum. Plant Growth trials have indicated that EDDS is as effective as EDTA in delivering iron metal to soybean and maize plants in foliar feeding applications.

Other biodegradable ligands that were recently developed include PASP Na-salt [23] and IDS Na-salt [24]. These ligands are environmentally friendly and can be used in a wide

variety of applications, including laundry and dishwashing detergents. They show great promise as successor ligands to EDTA and DTPA.

IDS Na-salt is obtained by reacting maleic anhydride with water, ammonia and sodium hydroxide, according to the reaction below.

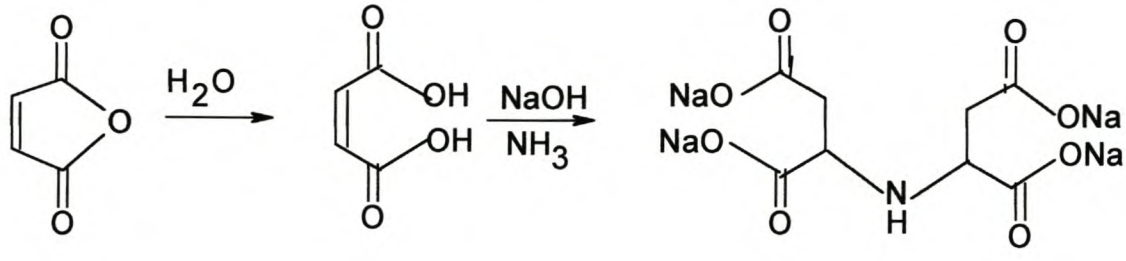


It is available in two forms i.e. a clear or yellowish liquid with a 40 % minimum content and as a white odourless powder, minimum 85 % content. IDS Na-salt is a pentadentate ligand because it can form complexes with metal ions in which bonds are formed with the nitrogen atom and all four carboxyl groups. In the usual octahedral system the sixth bond is formed with water.

IDS combines with metal ions in a 1:1 ratio. The pK values for IDS with these metals are as follows: $Fe^{2+}$ = 8.2, $Cu^{2+}$ = 14.3, $Cd^{2+}$ = 13.5, $Zn^{2+}$ = 13.0 and $Mn^{2+}$ = 7.3. The transition metal ions mainly bind nitrogen and oxygen-containing ligands. According to the Irving and Williams series the order of complex-forming ability is as follows: $Mn^{2+} < Fe^{2+} < Co^{2+} < Ni^{2+} < Cu^{2+} > Zn^{2+}$ [25].

## 2.2 Methods of metal complex detection

### 2.2.1 AA, UV-Vis, ICP, XRF and Electrochemical techniques.

Analytical applications capable of quantifying trace elements at low levels include atomic absorption spectrometry (AAS), inductively coupled plasma (ICP) combined with atomic emission spectrometry (ICP-AES) or with mass spectrometry (ICP-MS). Other methods include electrochemical, neutron activation, isotope-dilution mass spectrometry, flame atomic fluorescence spectrometry, molecular absorption spectrometry and the non-invasive technique, X-ray fluorescence and radiochemical procedures. All these methods must be species sensitive rather than element sensitive. The qualitative and quantitative nature of the metal must also be considered. In order to judge the suitability of a specific technique the following factors must be considered i.e. detection limits, instrumentation costs, analysis time, sample preparation and selectivity and precision, because in various matrices, the normal concentration of important metals is often near the detection limits of some of the techniques.

The majority of these methods however are not used for routine applications. Neutron activation is sensitive but access to a nuclear reactor is required and therefore is not in general use. ICP-MS is a technique well suited for speciation measurement and screening purposes because it offers extreme sensitivity and selectivity [26]. However this technique suffers from interferences which cannot be resolved by quadruple instruments. AAS is

the most widely used analytical technique for the determination of trace elements in biological materials [26].

Atomic absorption (AA) and inductively coupled plasma (ICP) spectrometries have been increasingly accepted as the standard methods in the recent years for trace metal analysis in seawater. However, AA can measure only one element at a time and the ICP, besides being prohibitively expensive, lacks sensitivity for certain elements such as Cu, Pb, Ti and Cd. Flame emission spectroscopy is limited to the determination of the alkali and alkaline earth elements. ICP-AES eliminates chemical interference, the high temperature leads to multiplicity of intense emission lines in the spectrum. XRF's application does not normally extent to the trace elements. AAS has both excellent resolution and good sensitivity for selected metals i.e. Cu, Pb, and Cd. All these methods are characterised by good selectivity and sensitivity and can be applied to a very wide range of sample types.

These constraints led to the suggestion that an electrochemical analytical method for heavy metals is still indispensable. Electrochemical stripping techniques, like anodic stripping voltammetry (ASV), have been considered most suitable for the analysis of trace or ultra-trace heavy metals. The main advantages of electrochemical methods are their simplicity, inexpensiveness, rapid analysis and sensitivity [27]. The main advantage of voltammetric methods is the possibility to distinguish between metals in different oxidation states e.g.Cr (III) and Cr (IV).

Interest in stripping analysis has been sparked by it's ability to measure four to six trace metals simultaneously at concentration levels down to the fractional parts per billion (sub-ppb), i.e. utilising inexpensive instrumentation. Among it's spectroscopic competitors only flameless atomic absorption has nearly the same sensitivity, but at much higher costs. The relevant modes of AAS are to be considered as an alternative. The difference between voltammetry and AAS is that AAS need more test measurements than voltammetry if comparable precision is to be achieved. The potential of voltammetry for simultaneous determination balances the faster measurement rate of AAS for a single element. However, the AAS technique has the advantage i.e. very sensitive for a greater number of metals, for e.g. the continued high level of interest in the problem of environmental pollution by lead compounds has resulted in many reports [28].

The availability of simple, reliable electrochemical instrumentation makes polarography and voltammetry favourable analytical tools. Heyrovsky first described Voltammetric analysis in 1922 [29]. Voltammetry stands for voltamperometry, which means the recording of current-voltage curves at small electrodes with radii in the nm to mm range. Voltage ramp is applied to the electrode and current is measured. The metal ions are reduced and dissolved in mercury. Advantages of voltammetry against spectroscopic methods include: There is less problem with high salt matrices compared to ICP and AAS, speciation is possible (distinguish between ions), low detection limits even at ppt range, capital outlay i.e. low price, low running costs (using nitrogen gas), no extensive laboratory infrastructure (no expensive gases, no fume cabinet), versatility (inorganic e.g. anions and organics), alternative and complementary method to AAS/ICP, simultaneous

determination of metals(up to seven metals in one run) and results are very reliable. Voltammetry uses a three electrode system i.e. working electrode where the reaction takes place, a reference electrode where the potential is stable and an auxiliary electrode where the current flows between working and counter electrodes.

Voltammetric techniques such as polarography use the dropping mercury electrode (DME, SMDE) and stripping voltammetry uses a stationary electrode (HMDE, RDE), this increases sensitivity. Polarographic analysis involves direct reduction or oxidation at the electrode and its sensitivity is limited. Stripping voltammetry involves a two step measurement i.e. an electrochemical deposition (enrichment) step and determination or analysis (stripping step). It has high sensitivity due to the enrichment of the analyte, for trace analysis even down to ppt range and used mainly for metal analysis Potentiometric Stripping Analysis (PSA) involves potentiostatic accumulation, chemical stripping or constant current stripping and analysis.

Voltammetry has the advantage of being a species sensitive method, not just an element-sensitive, providing many opportunities for studies of heavy metal speciation [30]. Voltammetric determinations of trace metals require prior preconcentration for very low levels of concentrations in the same way as other instrumental methods [31]. This is where the electrochemical approach provides its greatest inherent advantage because the preconcentration can be done electrochemically in the same cell as the final measurement. Common chemical preconcentration procedures, for example, separation

procedures such as solvent extraction, ion exchange, coprecipitation or co-crystallization is both time consuming and open to additional contamination of samples.

Potentiometry remains the method of choice for determining complex formation constants, with the majority of constants reported in the literature having been obtained using potentiometric titration. However, the use of a glass electrode limits the effective pH window in which these data can be recorded, and as such analyses are also quite laborious and time-consuming. Cyclic voltammetry offers a reliable and reasonably rapid means of determining complex stability constants, and also allows the researcher to examine the behaviour of the complex in a wider pH window than in the potentiometric titrations.

Voltammetry offer the following advantages: the voltammetric instrument can be installed in small even mobile laboratories without any problems. The investment and operating costs are comparatively low. It's used in environment analysis and also in the analysis of seawater, brine and ultrapure chemicals, in electroplating technology and in chemical industry.

## 2.3 Speciation of complexes of metals with ligands

### 2.3.1 General

According to the IUPAC speciation of an individual element refers to its occurrence in or distribution among different species. Chemical speciation defines the oxidation state, concentration and composition of each of the species actually present in a chemical sample. Speciation analysis is the analytical activity of identifying and quantifying one or more chemical species of an element present in a sample. An understanding of chemical speciation is important for at least two reasons. First, the toxicity caused by ingestion and inhalation of a metal is independent on its chemical form. Secondly, chemical speciation strongly influences environmental pathways, transport and fate of a metal [32].

The speciation of a compound is important as this provides insight into its distribution, for example, in the human body at physiological pH, as well as its possible modes of complexing with metal ions. At low pH the protonated form of a ligand will obviously be less efficient at complexing than the deprotonated form found at higher pH. The chemical speciation of trace metals is the most important concern in the field of marine and terrestrial chemistry because the bioavailability and scavenging of metals are closely related to the chemical forms of the metals [33].

Speciation may also be useful in studying element toxicokinetics, for e.g. the toxicity of the three-oxidation states of mercury differs considerably [34]. Since it is well known that

hexavalent Cr is taken up more than the trivalent form and that species of the same metal are differently partitioned in blood. These examples show the great potential for developing and applying speciation in order to better understand the role of elements in both the environment and in biological systems.

In biochemistry it is known that speciation should be considered in order to elucidate the role of the metal. The rapidly growing interest in elemental speciation has brought the development of a new generation of analytical techniques, which enable the discrimination among different forms of a metal [35].

In general, looking at the toxicological relevance of oxidation states and organometallic compounds, the removal or addition of electrons to the metal atom influences the chemical activity and therefore the ability of the metal to interact with tissue ligands. A difference in ionic action may help to explain the finding that neuromuscular weakness can occur in patients poisoned by methylmercury, but not in those poisoned by inorganic mercury [36].

The casual links between a chemical and its environmental/healthcare influence have increasingly being shown to be related to the presence of a specific chemical species rather than to the total presence [37]. For the production of fine chemicals not only the quantity of product but also its purity is dependent upon the chemical species present in the reaction vessel rather than the total amounts of the reactants used. The knowledge of speciation has improved efficiency, yields and profits. This has been shown by many

examples in literature. A simple example may be seen in the use of EDTA and of its more readily biodegradable replacement, EDDS to sequester copper ions from copper, iron and nickel solution [37].

The environment contains a myriad of ligands and of metal complexes arising endogenous and exogenous sources. Coordination compounds involve both ligands and metal ions. An exciting new development involves ligands that are designed to replace EDTA after 60 years of intensive and essential use [38]. The chemical industry produces 166 000 tonnes EDTA and NTA per annum. The majority of these chelates are discharged into sewers. Environmental concerns, which have banned EDTA etc, in some states/countries, have led to drives to find readily biodegradable replacement ligands which have parity in terms of chelating power and are not considerably more expensive than traditional ligands.

The newly biodegradable ligands include EDDS, EDDM, IDS and PASP. EDDS is up to four times as efficient as EDTA at sequestering the nominated metal ion and thus can be used at lower concentrations, in addition to enhanced efficiency this also reduces the environmental cost of disposal of unused ligands. Manganese ions are considered to be the most detrimental in pulp processes. The speciation of EDDS and EDTA were compared for manganese, it showed to chelate all of the Mn at higher pH and have significant benefits for instance in the pulping process.

Speciation measurements are not readily accessible but have improved markedly with conceptual advances in analytical methodology over the last 25 to 30 years. Nowadays, modern computers can extrapolate chemical speciation knowledge down to well below parts per billion. The chemical speciation analysis is beset with many problems, not the least of which is that of lability. Changing the prevailing conditions by, for example, concentrating the solution or maybe extracting it into an organic solvent, the existing equilibria is disturbed and so the species eventually detected instrumentally may not be representative of those occurring at the steady state during the industrial or biological process. It is preferable to use computer simulation of the chemical speciation present. This is a non-disturbing approach that also lends itself to accumulating a wide databank of knowledge that can be used collectively to develop an understanding of any problem at an early stage. To be successful a manufacturing industry needs to maximize product yields, minimise undesirable byproducts and impurities, operate efficient processes, satisfy current legislation and be financially profitable [39].

Gas chromatography (GC) has been used for speciation of inorganic analytes and has been relatively limited. This possibly reflects that most GC detectors are not element specific, and that there may be problems associated with transferring the analyte from the end of the GC column to the atom/ion source when atomic spectroscopy is used for detection [40]. Many elements exist as different species; however, few examples where there has been extensive environmental interest have been considered i.e. mercury and lead for instance. Lead and mercury are poisonous regardless of the chemical form in which they are present, but the degree of toxicity will again depend on the species.

Methylmercury for example is substantially more toxic than inorganic mercury. The concentration of lead in the environment has increased substantially over the last fifty years largely because of its use in antiknock additives in petroleum. The alkylated lead compounds used for this purpose are extremely toxic and therefore legislation has been introduced in many countries to reduce the amount of leaded petrol. Between 0.1-0.2% of the organolead in petrol passing the engine is not combusted and thus ends up in the environment.

High performance liquid chromatography (HPLC) has been used for speciation although it is not the premier technique. However when HPLC is coupled with element-selective detectors like ICP-AES and ICP-MS, it is more suited for speciation analysis than for total metal or non-metal determination [41]. Metal speciation is now well established in many areas of chemistry. Although a lot has been achieved in terms of increasing our knowledge of the behavior of some elements in the environment, much still needs to be done. Thus the whole area of metal speciation continues to provide an exciting and challenging arena for research in the future [40].

Anodic stripping voltammetry (ASV) is the technique, which is commonly used for speciation of heavy metals because of its high sensitivity. However for elements such as mercury, selenium and arsenic, gas chromatography or atomic absorption spectroscopy (AAS) are used. The only analytical technique, which may measure a particular metal species without affecting the solution equilibria, is potentiometry with ion-selective

electrode (ISE). Unfortunately, ISE measurements are unreliable below $1\times10^{-6}$M concentrations for most elements in natural waters which is far too insensitive.

The speciation of trace metals in waters has been studied using the following techniques i.e. computer modelling and experimental measurement. The computer modelling approach involves the use of published stability-constant data, together with known concentrations of various ions and suspended solids in the water, to compute the equilibrium concentrations of the species. The main obstacle to the successful use of computer modelling of trace metal speciation in waters is the lack of reliable thermodynamic data. The experimental procedures mainly used to study trace metal speciation in waters are anodic stripping voltammetry, ion-exchange chromatography, ultrafiltration, dialysis and bioassay. It is inevitable that in the near future, water-quality legislation for heavy metals will include statements relating to their speciation. Unfortunately, trace metal speciation techniques have not yet been developed to the stage where any one method is completely acceptable for routine use [9].

Ligand exchange with EDTA and differential pulse anodic stripping voltammetry was a technique used to determine free zinc ion concentration and zinc speciation in lake waters. Using ligand-exchange techniques, metal ions bound to exchangeable ligands can be determined and free metal ion concentrations can be calculated at the low levels of total metal concentrations in natural waters. Total dissolved Zn in lake waters includes voltammetrically labile and inert species [42]. The improvement in the determination of

complexation parameters was demonstrated by a modified version of the van der Berg/Ruzic method using EDTA as a model ligand. [43].

# CHAPTER 3

## Electrochemistry and speciation of Iminodisuccinic acid with Cd, Cu, Fe, Pb and Zn

## 3.1 EXPERIMENTAL PROCEDURES

### 3.1.1 Apparatus

The BAS C2 cell stand with a pre-amplifier, connected to a BAS 100B system tower stand was used to determine the voltammetric measurements. Thin mercury film glassy carbon microelectrode, Ag/AgCl and platinum wire were used as the working, reference and auxiliary electrodes, respectively. The pH values were recorded using a Hanna PC turtle pH meter.

The following instrumental parameters were generally used throughout:

| | |
|---|---|
| Initial potential | : -200mV |
| Start Potential | : -200mV |
| End potential | : -2000mV |
| Scan rate | : 100 mV/s |
| Initial Direction | : Negative |
| No. of Segments | : 2 |

Sensitivity : 100nA/V

### 3.1.2 Reagents and chemicals

All chemicals were of reagent grade. They were purchased commercially and used as received. The ultra pure water obtained using a Milli-Q Millipore water purification system was used for all solutions.

| CHEMICALS | MANUFACTURER AND GRADE |
|---|---|
| Zinc solution (1000ppm) | Merck (Spectrosol) |
| Lead solution (1000ppm) | Merck (Spectrosol) |
| Copper solution (1000ppm) | Merck (Spectrosol) |
| Cadmium solution (1000ppm) | Merck (Spectrosol) |
| Iron solution (1000ppm) | Merck (Spectrosol) |
| Chromium solution (1000ppm) | Merck (Spectrosol) |
| Manganese solution (1000ppm) | Merck (Spectrosol) |
| Ammonia | Merck (33%) |
| IDS | Bayer |
| PASP | Bayer |
| NaOH | Holpro Lovasz (Analytical Reagent) |
| Nitric acid | Riedel-de Haen (65%) |
| Mercury metal triple-distilled | SAAR Chem (Univar) |
| Iron(II) Chloride | Merck (Pro analysis) |
| Sodium Acetate | Holpro Lovasz (Analytical Reagent) |

**Preparation of Buffer solution**, 0.1M $NH_3$ as $NH_4OH$. Dilute 1.87ml of the ammonia solution with distilled water in a 100ml volumetric flask.

**Preparation of Acetate Buffer solution**, 0.2M $CH_3COONa.3H_2O$. Dissolve 2.72g of acetate with an appropriate amount of distilled water and dilute to 100ml volumetric flask using the same solvent.

**Preparation of HCl solution**, 0.1M. Dilute 0.98ml of HCl (37%) with distilled water in a 100ml volumetric flask.

**Preparation of Stock solution**, 0.015M $Hg^{2+}$. 0.3g of triple distilled mercury was dissolved with several drops of concentrated nitric acid (in the hood) and diluted to 100ml with distilled water in a volumetric flask.

### 3.1.3 Standard preparations.

**Cadmium**, $8.90\times10^{-4}$M. Dilute 1.0ml of cadmium (1000ppm) with 0.1M ammonia solution in a 100ml volumetric flask.

**Copper**, $1.57\times10^{-4}$. Dilute 1.0ml of copper (1000ppm) with 0.1M ammonia solution in a 100ml volumetric flask.

**Iron**, $1\times10^{-2}$M. Dissolve 0.199g of $FeCl_2.4H_2O$ with an appropriate amount of acetate solution and dilute to 100ml volumetric flask using the same solvent.

**Lead**, $4.83\times10^{-4}$M. Dilute 1.0ml of lead (1000ppm) with 0.1M ammonia solution in a 100ml-volumetric flask.

**Zinc** $1.52\times10^{-4}$M. Dilute 1.0ml of zinc (1000ppm) with 0.1M ammonia solution in a 100ml-volumetric flask.

**IDS**, 0.01M. Dilute 1.67ml of IDS with an appropriate amount of 0.1M ammonia solution and dilute to 200ml volumetric flask.

## 3.2 RESULTS AND DISCUSSION

### 3.2.1 Voltammetric analysis of $H_4$IDS with Cd, Cu, Fe, Pb and Zn

The background voltammogram was obtained for, firstly the 0.1M $NH_3$ and then for the 0.01M solution of $H_4$IDS. Metal-ligand complexation was then examined as follows: $Cd^{2+}$, $Cu^{2+}$, $Pb^{2+}$, $Fe^{2+}$and $Zn^{2+}$ stock solutions (10ml) each were used, to which 100µl aliquots of the appropriate ligand standard solutions were added to ensure a 1:1 ratio of metal: ligand. The pH of the solutions were then adjusted by the addition of 100µl aliquots of 0.1M HCl and the voltammograms were recorded for the corresponding pH values of the solutions. The electrolyte mixture was stirred and purged with nitrogen prior to analysis. During the analysis, the sample was covered with a nitrogen blanket.

A series of studies had been completed on $H_4$EDDS, where the stability constants of complexes between $H_4$EDDS and selected transition metal ions were measured by cyclic voltammetry [44].

The metal-ligand complexes dealt with in this project form a 1:1 complex between the iminodisuccinic acid anion $IDS^{m-}$ and a metal cation $M^{n+}$. The 1:1 complex formation can be represented by the following equation:

$$IDS^{m-} + M^{n+} \leftrightarrow IDSM^{(m-n)-}$$

The stability constant, $K_{IDSM}$, is given by:

$$K_{IDSM} = \frac{[IDSM^{(m-n)}]}{[IDS^{m-}][M^{n+}]}$$

Iminodisuccinic acid is capable of forming five coordinate bonds in an octahedral geometry around the metal ion and this is shown schematically below.

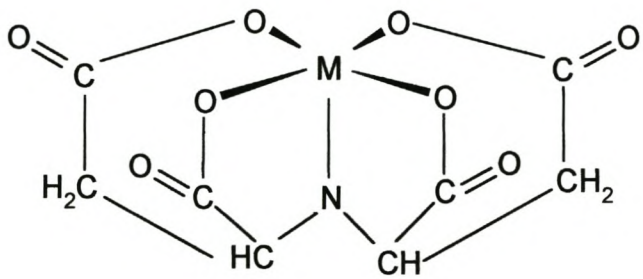


A typical cyclic voltammogram recorded in figure 3.1 shows the reduction current observed at +110mV and oxidation potential at +8mV. These positions are ascribed to the presence of $H_4IDS$ and $IDS^{4-}$, respectively. The cyclic voltammogram displayed in figure 3.1 is very similar to the corresponding voltammograms recorded for $H_4EDDS$ [40] and $H_4EDDM$ [18].

Figure 3.1: Cyclic voltammogram of 0.01M $H_4IDS$ at pH ≈11.25 (T = 25°C)

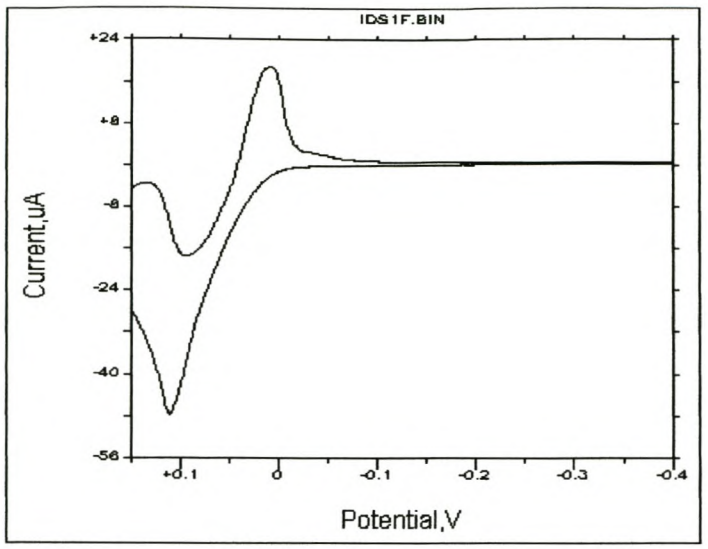


The ligand protonation constants of $H_4IDS$ ($logK_P$), which provide a direct measure for determining its speciation, were determined by plotting the change in reduction potential as a function of pH. A modified Lingane equation can be used to calculate the value of the stability constants [45]. The plot is based upon the "Lingane Equation" [46]

$$\Delta E = -\frac{RT}{nF}\ln\frac{[ML]}{[M][LH_x]} + \frac{2.303x}{n}pH$$

The Lingane Modified Equation was derived from the following equations:

$$\Delta E = -\frac{RT}{nF}\ln K (NerstEquation)$$

$$M^+ + LH_x \rightarrow ML + xH^+$$

where $K = \frac{[ML][H^+]^x}{[M][LH_x]}$

$$\Delta E = -\frac{RT}{nF}\ln\frac{[ML][H^+]^x}{[M][LH_x]}$$

$$\Delta E = -\frac{RT}{nF}\ln\frac{[ML]}{[M][LH_x]} - \frac{RT}{nF}\ln[H+]^x$$

$$\Delta E = -\frac{RT}{nF}\ln\frac{[ML]}{[M][LH_x]} - \frac{2.303x}{n}\log[H^+]$$

$$\Delta E = -\frac{RT}{nF}\ln\frac{[ML]}{[M][LH_x]} + \frac{2.303.x}{n}pH$$

On rearranging the following is obtained:

$$\ln K = \frac{nF}{RT}\left[\frac{2.303x}{n}pH - \Delta E\right]$$

Cukrowski et.al used a similar approach relating to a modified Lingane equation in the polarographic determination of formation curves for metal-ligand complexes [47]. The changes in the gradient of such plots correspond to a logK value for the complex. In our case the logK values could be estimated directly from the graph since it has been proven by the above mentioned methods.

Figure 3.2 shows the graph of the change in reduction potential (ΔE) against pH for $H_4IDS$.

Figure 3.2: Plot of ΔE against pH for $H_4$IDS at T=25°C.

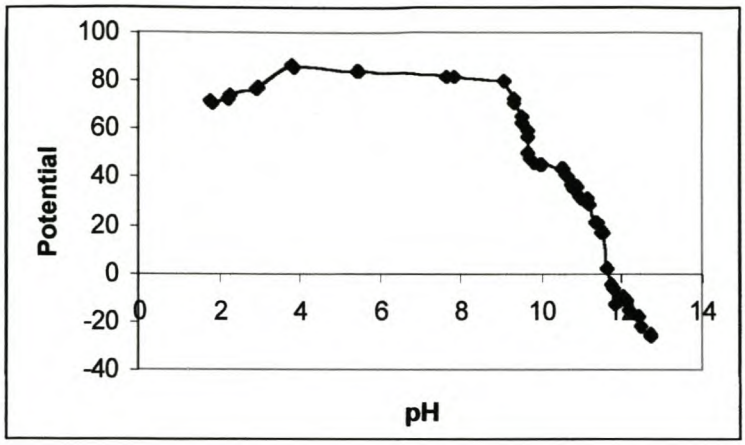


According to figure 3.2, it is observed that a change in the gradient of the plot signifies a change in the major components of the different species of the $H_4$IDS ligand. The first ligand protonation constant ($logK_{P1}$) is taken as 3.9 from the above figure. This value compares favourably with the $logK_{P2}$ value of 3.6 as determined by potentiometric titration [24]. In a similar manner, the second ligand protonation was found to be 10.8, which compared well with a $logK_{P4}$ value of 10.9,respectively. $LogK_{P1}$ = 2.8 and $logK_{P3}$ = 4.7 are the other protonation values of IDS determined using a potentiometric method. They were not observed by the voltammetric method, the reason being that at low pH more protonated species exist. Therefore it is difficult to determine protonation constants.

### 3.2.2 Complex stabilities of $H_4$IDS-metal complexes.

The complex formation stability constants of $H_4$IDS with $Cd^{2+}$, $Cu^{2+}$, $Pb^{2+}$, $Fe^{2+}$and $Zn^{2+}$ were determined at a thin Hg film coated on the glassy carbon microelectrode (11μm).

Using cyclic voltammetric analysis the corresponding change in reduction potential as a function of the pH of the solution was then taken into account. A generalized reaction for a metal with $H_4IDS$ is as follows:

$$M + H_4IDS \xrightarrow{k_1} MH_3IDS^- + H^+$$
$$MH_3IDS^- \xrightarrow{k_2} MH_2IDS^{2-} + H^+$$
$$MH_2IDS^{2-} \xrightarrow{k_3} MHIDS^{3-} + H^+$$
$$MHIDS^{3-} \xrightarrow{k_4} MIDS^{4-} + H^+$$

From this, the overall formation constant $K_f = k_1k_2k_3k_4$.

The voltammetric behaviour of $Cd^{2+}$ and Cd-$(IDS)_x$ (x = 1,2,3,4) is shown in figure 3.3 and 3.4.

Figure 3.3: Cyclic voltammogram of $Cd^{2+}$ in $NH_4OH$ at pH ≈10.5 (T = 25°C).

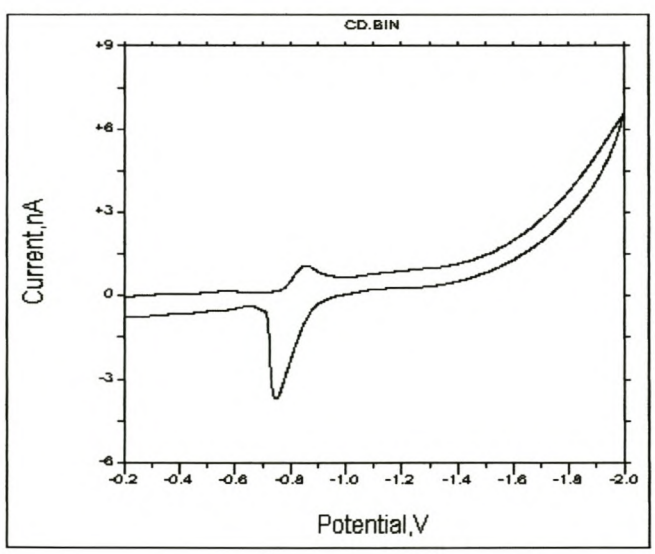

Figure 3.4: Cyclic voltammogram of Cd-IDS at pH ≈10.4 (0.1M, T = 25°C).

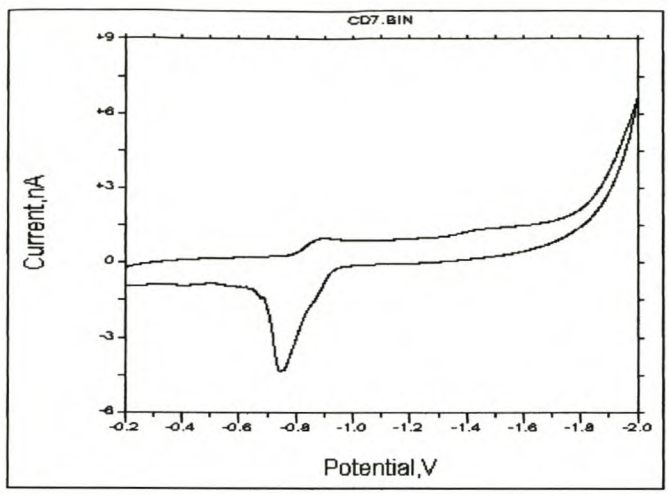


The voltammogram recorded impose a linear sweep in a negative direction which is called the cathodic or reductive sweep, followed by a reverse sweep in the positive direction and is hence called the anodic or oxidative sweep.

During the cathodic sweep, reduction of the Cd and the Cd-IDS is observed by increases in the cathodic reduction currents on the voltammogram at –892mV which is typical for the $Cd^{2+}$ ion and –1475mV for Cd-IDS at the pH of 10.4. Figure 3.3 shows a quasi-reversible behaviour for the $Cd^{2+}$/Cd redox couple. In figure 3.4 a Cd-$IDS^{2-}$ peak is observed. This peak is due to the complexation of $Cd^{2+}$ and the $IDS^{4-}$ ligand. A decrease in the cathodic metal peak was seen as the ligand was added to the metal. It also shifted to a more negative potential. The shift in the reduction potentials varies with a change in pH when aliquots of 0.1M HCl were added. A plot of the change in reduction potential with varying pH was used to directly determine the pK values for $(Cd\text{-}IDS)^{2-}$ complex

found in figure 3.5, since the pK value corresponds directly to the pH at which a change in the gradient of the plot is observed.

Figure 3.5: Plot of ΔE against pH for Cd-IDS at T=25°C.

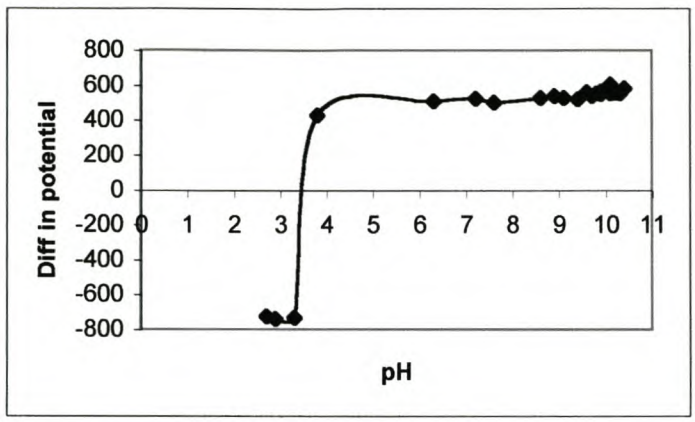


In figure 3.5, two changes of gradient correspond to a $\log K_1 = 4.0$ and $\log K_2 = 9.6$, with an overall formation constant of $\log K = 13.6$. This compares well with the potentiometrically determined value of $\log K = 13.5$ [24].

The same approach was followed for the other metal ions as in the cyclic voltammetry measurement of $Cd^{2+}$ and the Cd-IDS complex. A similar behaviour can be seen in figures 3.6 and 3.7. Figures 3.6 and 3.7 show the voltammograms of the $Cu^{2+}$ and the Cu-IDS complex in a 1:1 ratio at the potential of between –500mV and –1282.8mV, respectively. A quasi-reversible behaviour is also seen in figure 3.6 for the $Cu^{2+}$/Cu redox behaviour. The cathodic peak at –1282.8mV shows that complexation of $Cu^{2+}$ and IDS ligand has taken place. A similar behaviour was observed in the case of CuEDDS [43]. The major changes are at pH's of ≈ 4.4 and 9.7 as pointed out in figure 3.8.

Figure 3.6: Cyclic voltammogram of $Cu^{2+}$ in $NH_4OH$ at pH ≈10.3, T = 25°C.

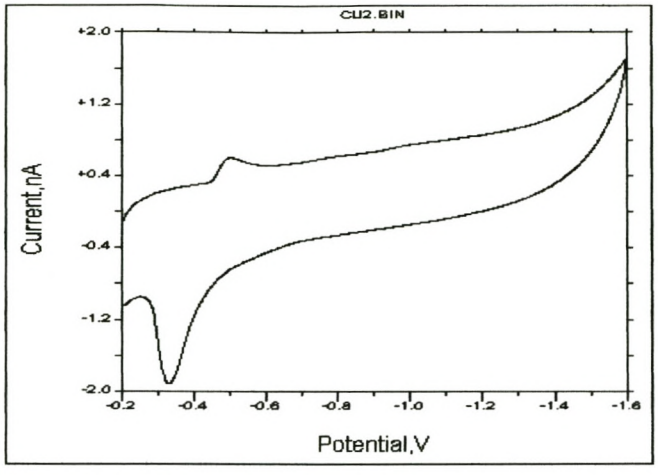


Figure 3.7: Cyclic voltammogram of Cu-IDS at pH ≈10.5 (0.1M, T = 25°C).

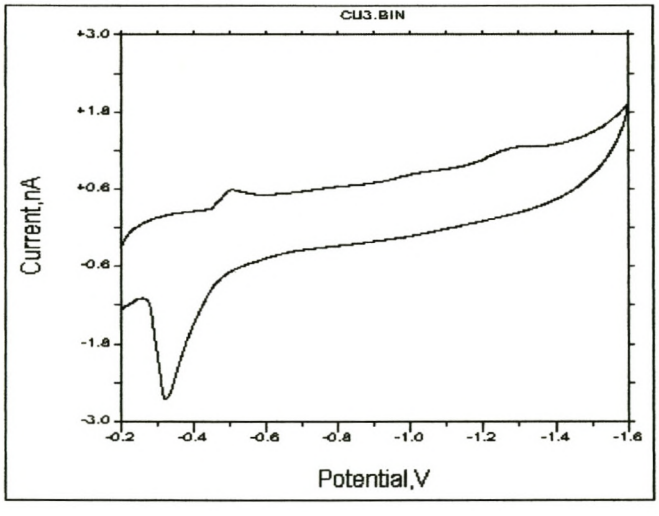

Figure 3.8: Plot of ΔE against pH for Cu-IDS at T=25°C.

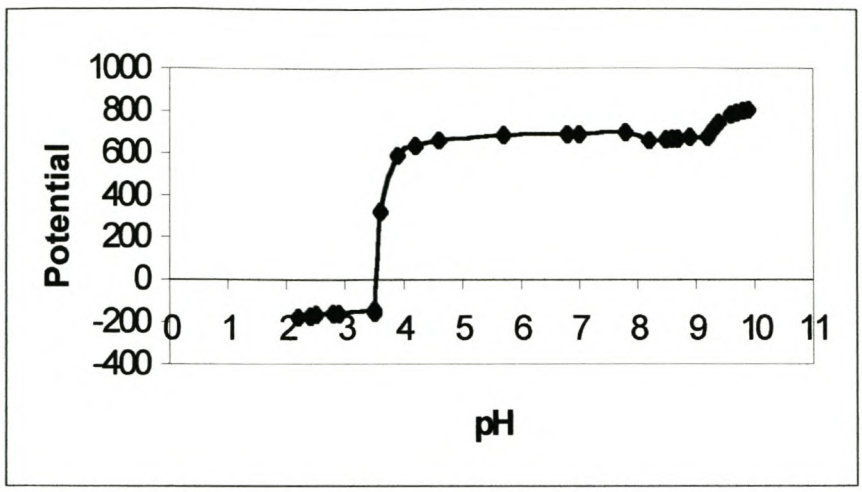


Figure 3.9 shows a quasi-reversible behaviour of the $Pb^{2+}/Pb$ redox reaction at the potential of –464mV. The cathodic peak of the Pb-IDS complex in the 1:1 ratio at the potential of –1337mV is shown in figure 3.10, respectively. In figure 3.10, the cathodic metal peak disappeared after the addition of the ligand and a new cathodic peak appeared. This new peak is the result of the complexation of the metal with the ligand. This is similar to what was observed for PbEDDS [44]. From figure 3.11, the major changes are at the pH's ≈ 4.4 and 8.0.

Figure 3.9: Cyclic voltammogram of Pb in $NH_4OH$ at pH ≈10.5, T = 25°C.

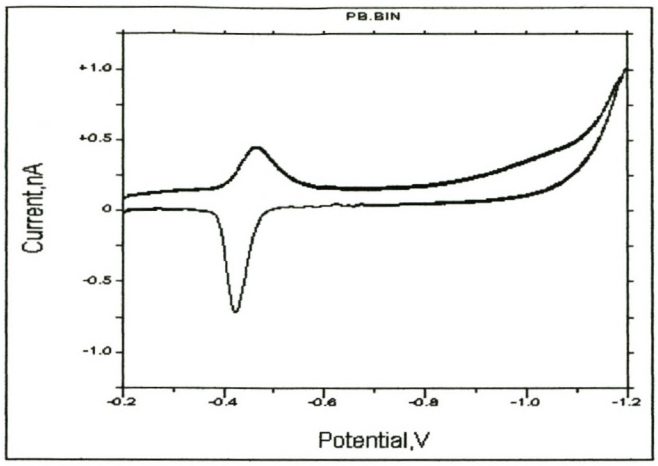


Figure 3.10: Cyclic voltammogram of Pb-IDS at pH ≈10.5 (0.1M, T = 25°C).

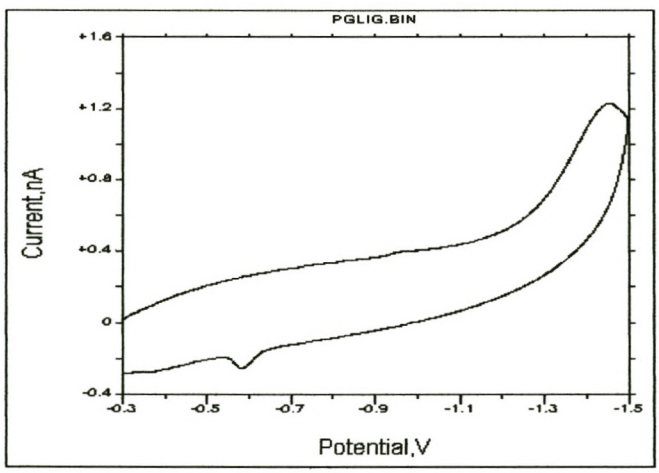

Figure 3.11: Plot of ΔE against pH for Pb-IDS at T=25°C.

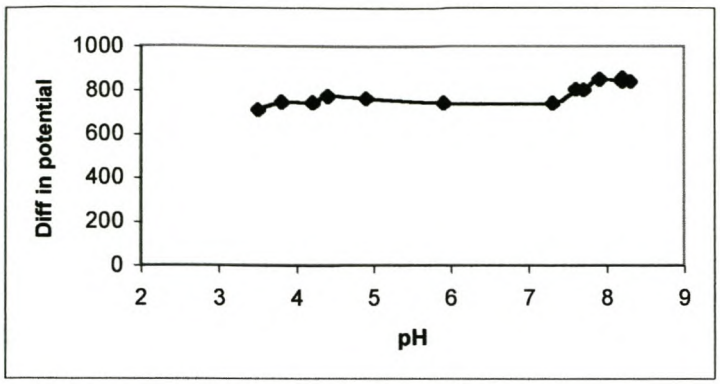


Figure 3.12 and 3.13 show the voltammograms of the Fe and Fe-IDS complex in the 1:1 ratio at the potential of –741mV and –1310mV, respectively. In figure 3.12 an irreversible behaviour of $Fe^{2+}/Fe^{3+}$ redox behaviour was observed. A broader peak was seen as the ligand was added and the peak also shifted to a more negative potential. The peak can be ascribed to be FeIDS peak. From figure 3.14, the major changes are at the pH's ≈ 4.4 and 8.0.

Figure 3.12: Cyclic voltammogram of Fe in $NH_4OH$ at pH ≈10.5, T = 25°C.

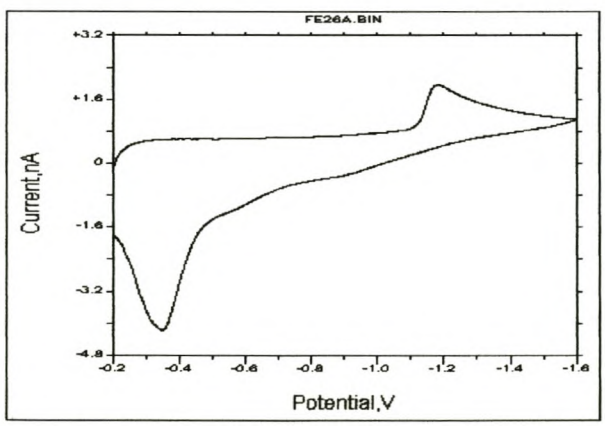

Figure 3.13: Cyclic voltammogram of Fe-IDS at pH ≈10.5 (0.1M, T = 25°C).

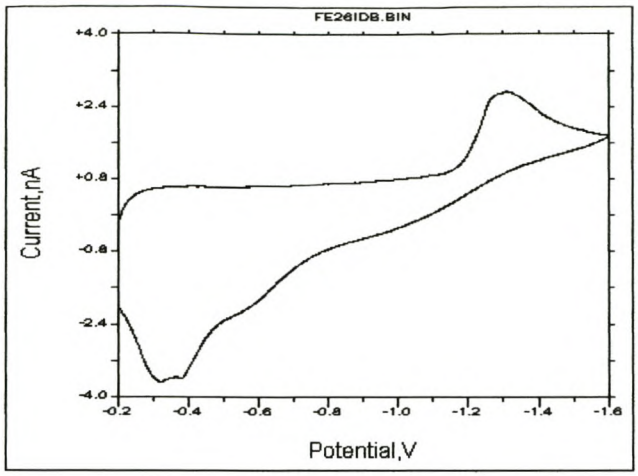


Figure 3.14: Plot of ΔE against pH for Fe-IDS at T=25°C.

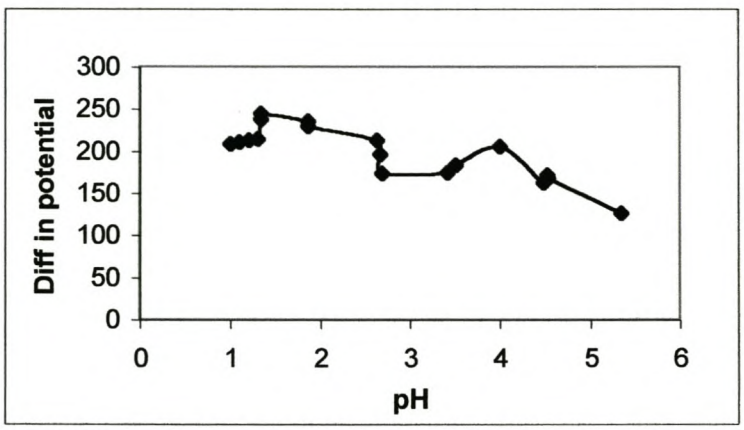


Figure 3.15 and 3.16 show the voltammograms of the Zn and Zn-IDS complex in the 1:1 ratio at the potential of –1332mV and –1533mV, respectively. A smooth quasi-reversible behaviour of $Zn^{2+}$/Zn was observed in figure 3.15. In figure 3.16, a second peak is due to the complexation, which has taken place. From figure 3.17, the major changes are at pH's

≈ 3.6 and 9.6. The large changes in the curve signify a change in the major components of the different species of Zn with the complex.

Figure 3.15: Cyclic voltammogram of Zn in $NH_4OH$ at pH ≈10.5, T = 25°C.

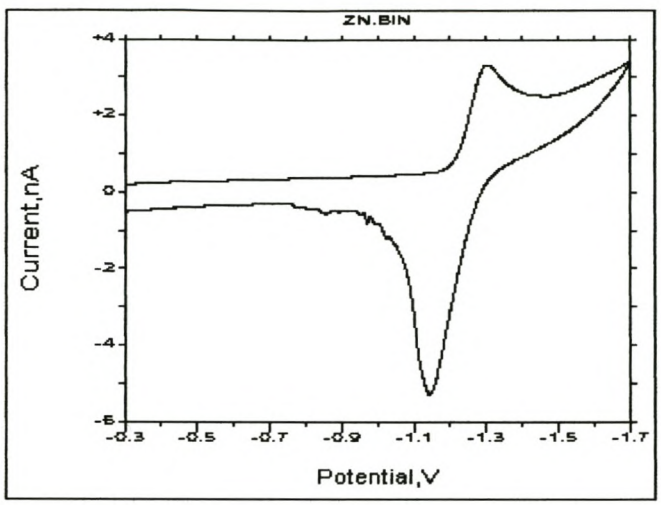


Figure 3.16: Cyclic voltammogram of Zn-IDS at pH ≈10.5 (0.1M, T = 25°C).

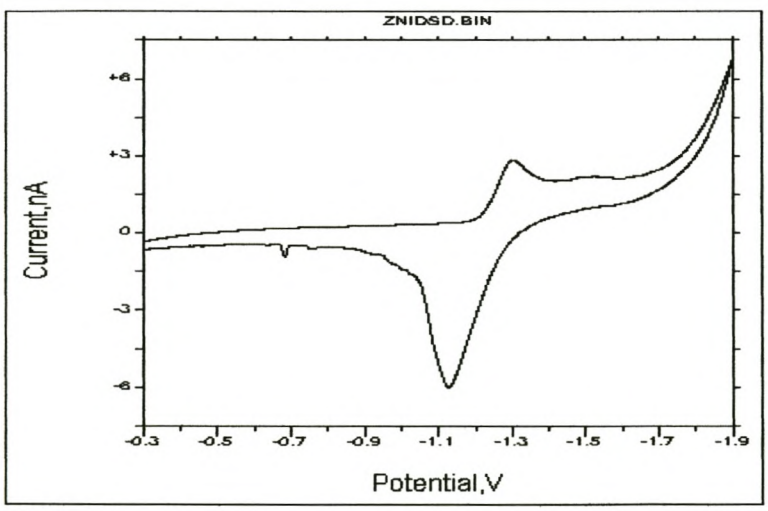

Figure 3.17: Plot of ΔE against pH for Zn-IDS at T=25°C.

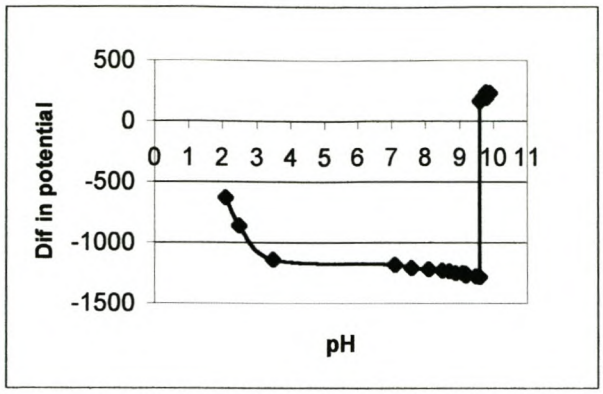


Table 3.1 displays a summary of the stepwise and overall formation constants for complexes between $H_4IDS$ and the selected transition metals. Literature values compared well with the voltammetrically determined values

Table 3.1:Complex stability constants for $H_4IDS$-metal complexes.

| **Metal** | **$pK_1$** | **$pK_2$** | **$pk_3$** | **ΣpK** | **Literature pK** |
|---|---|---|---|---|---|
| $Cd^{2+}$ | 4 | 9.6 | | 13.6 | 13.5 [24] |
| $Cu^{2+}$ | 4.4 | 9.7 | | 14.1 | 14.3 [24] |
| $Pb^{2+}$ | 4.4 | 8.0 | | 12.4 | |
| $Zn^{2+}$ | 3.6 | 9.6 | | 13.1 | 13.0[24] |
| $Fe^{2+}$ | 1.4 | 2.6 | 4.1 | 8.1 | 8.1[24] |

According to table 3.1, it is observed that $Cu^{2+}$ has the highest stability constant. This means that $Cu^{2+}$ ion react faster with IDS than the other metal ions. The order of stability constant of IDS with these metals is as follows $Cu^{2+}>Cd^{2+}>Zn^{2+}>Pb^{2+}>Fe^{2+}$. This agrees with the Irving and Williams series order of stability for complexation between transition metal ions and chelating ligands.

### 3.2.3 Experimental determination of speciation diagrams for metal-ligand complexes

The speciation diagrams depicted here were modelled using a speciation model known as the Joint Expert Speciation System (JESS) [48-50].

Speciation diagrams for metal-IDS complexes were determined from a thermodynamic database called Joint Expert Speciation System (JESS). JESS is a computer package written in Fortran 77, used for modelling chemical systems in solution and performing numerical analyses on the corresponding experimental data, for example input stability constants determined using potentiometric titration. The package has been designed to solve problems requiring specialist knowledge of chemical speciation and overcomes many existing problems with solution chemistry databases. The system is fully interactive. The reactions can be expressed in almost any form and can be associated with any number of equilibrium constants, enthalpy, entropy and Gibbs-free energy values. The supplementary data such as background electrolyte, ionic strength, temperature, method determination and original literature reference are also stored.

The thermodynamic database i.e. being distributed with JESS contains over 1200 reactions and over 20 000 equilibrium constants, with these data spanning interactions in aqueous solution of some 100 metal ions with more than 650 ligands.

This program calculates the speciation of a ligand from a database containing the relevant thermodynamic parameters for that ligand, and offers significant insight into the expected distribution behaviour of the ligand in different pH environments. The user can interactively select the desired ligand and metal(s), which must be speciated, given by a series of commands. The user can also specify the conditions under which the data is to be modelled, e.g. ionic strength of the medium, temperature, concentration of reactants and desired pH range over which the speciation is to be calculated. The final output data correspond to pH and the respective species that have been modelled over the pH range of interest. The output can then be readily manipulated and graphed in most spreadsheets and graphics programs for facile visual representation of the speciation curves.

### 3.2.3.1 Discussion of speciation of IDS with Cd, Fe, Pb and Zn

The complex stability constants for metal-IDS complexes obtained were utilised to generate and validate the predicted speciation models. Chemical speciation was done to generate distribution diagrams, which predicts the form of the species present at different pHs.

Figure 3.18: Speciation profile of $H_4IDS$ at T = 25, I = 0.1M

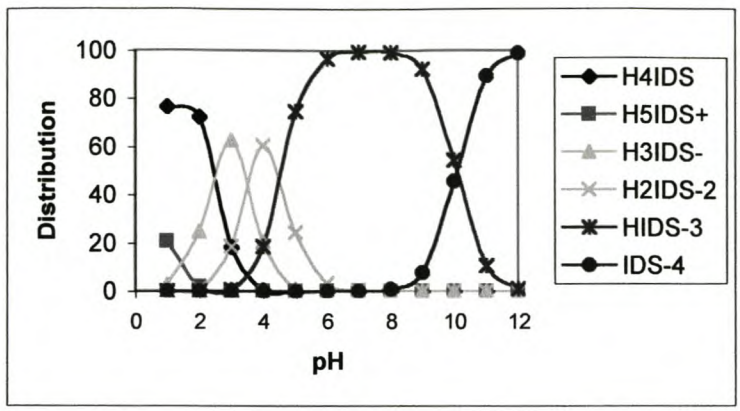


Figure 3.18 shows the speciation diagram for $H_4IDS$. According to modelled speciation data in figure 3.18, at pH $\geq\approx$ 10 the predominant species of $H_4IDS$ is $IDS^{4-}$. An agreement between the experimental (voltammetric) and predicted distribution values was found in an analysis of the speciation of $H_4IDS$, where the ratio of $IDS^{4-}$: $HIDS^{3-}$ at pH = 11.25 was 85:15 as determined voltammetrically, while the calculated speciation curve at pH = 11.25 afforded a ratio of 89:11. The cyclic voltammetric values were obtained by measuring the ratio of the reduction currents of $IDS^{4-}$ and $HIDS^{3-}$ species, which reflect the speciation of these two species. At pH$\geq\approx$ 10.9, it is observed that the $IDS^{4-}$ species is formed (found). This is in good agreement with the obtained by our voltammetric data, i.e. from figure 3.2; pH's 3.9 and 10.8 signifies the major changes in the $H_4IDS$ complex which showed that the optimum complexation took place.

Figure 3.19: Speciation profile of Cd-IDS at T = 25, I = 0.1M

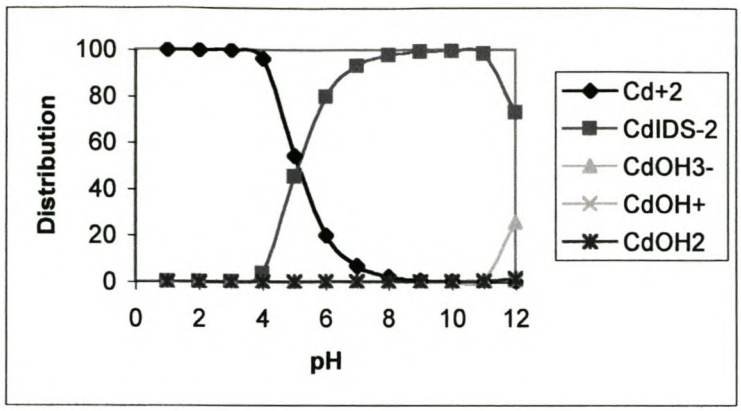


The Cd-IDS speciation curve shows that optimum complexation occurs between pH $\geq\approx$ 4.8 and 11, the predominant species is Cd-$IDS^{2-}$. This fit well with the voltammetric data (figure 3.5), which showed major changes at pH 4.0 and 9.6. Above pH 11, hydroxy species start to form for e.g. $CdOH_3^-$. This is also observed in the speciation curve of Fe-IDS where the main species found at pH 4.6 is Fe-$IDS^{2-}$. From the species distribution diagrams of the different metals with IDS, it was observed that optimum complexation occurs at pH>3.4. Any application involving the removal of the transitional metals from any process (for e.g. pulp and paper) should take this into consideration.

Figure 3.20: Speciation profile of Pb-IDS at T = 25, I = 0.1M

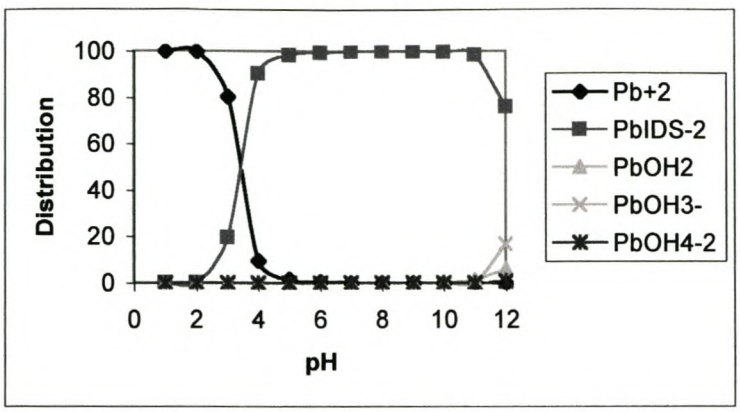


The Pb-IDS speciation curve shows that between pH's 1 and 3.5 the main species formed is the Pb. The Pb-IDS complex is stable between pH $>\approx$ 4.4 and 11. Hydroxy species start to form for e.g. $PbOH^{3-}$ and $PbOH_2$ above pH 10.

Figure 3.21: Speciation profile of Fe-IDS at T = 25, I = 0.1M

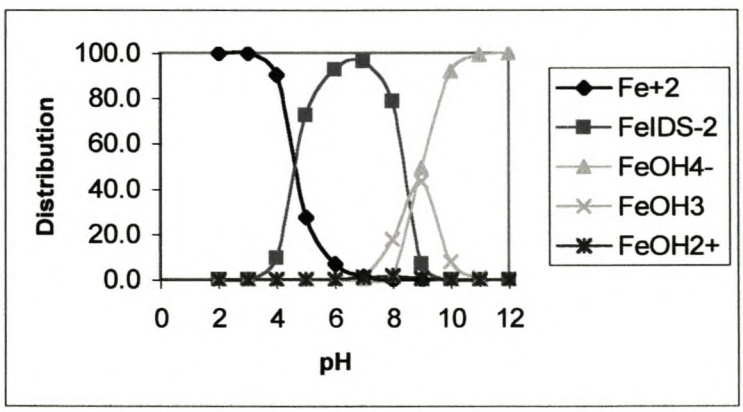


A similar behaviour is also seen in Fe, i.e. between pH 2 and 4, $Fe^{2+}$ is the dominant species in the solution. The Fe-IDS speciation curve shows that the main species of Fe-

IDS $^{2-}$ start to form at pH >≈ 3.6 and 9. Above pH 9, hydroxy species start to form for e.g. $FeOH_4^{2-}$, $FeOH_3$ etc.

Figure 3.22: Speciation profile of Zn-IDS at T = 25, I = 0.1M

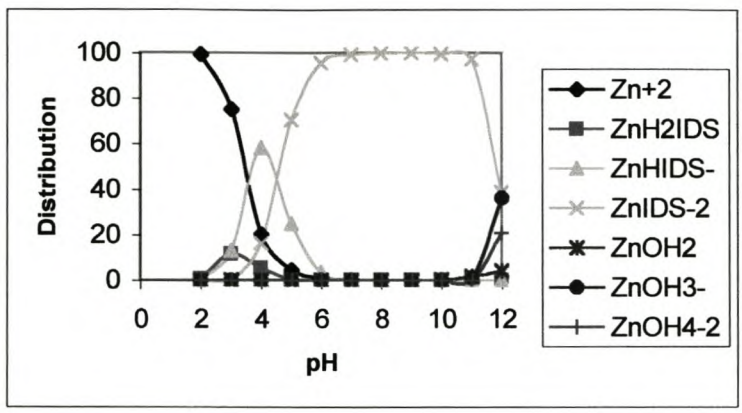


The Zn-IDS speciation curve shows that the main species of Zn-IDS start to form at pH >≈ 5 and 11. Hydroxy species start to form i.e. $ZnOH^{3-}$and $ZnOH_2$.

## 3.4 GENERAL CONCLUSION

A good agreement between potentiometric methods and cyclic voltammetric method shows the utility of cyclic voltammetry as a viable, facile and reliable means for determining complex stability thermodynamic data. This is true when the complex stability is in the domain of reasonably inert complexes. When lability is taken into account the reversibility of the complexes is a good indication. Cyclic voltammetry also offers several distinct advantages over potentiometry, notable ease of sample preparation,

rapidity and reproducibility of sample analysis and a wider pH range than potentiometric titration. The facility of cyclic voltammetry is also enhanced by the option of using macro- or microelectrode for complex stability measurements.

In this project a glassy carbon microelectrode was used instead of the carbon macroelectrode because of the following advantages: has smaller diameter, which lead to higher resolution and better-defined peaks are obtained, show fast electrode response, which led to the possibility of fast scan stripping voltammetry and this, shortens the time of analysis, very small currents (rates of reaction) as low as $\cong 10^{-17}$A can be measured with ease. This is important since the equilibrium is minimally disturbed. It also exhibits excellent signal-to-noise (S/N) characteristics as a consequence of reduced capacitative charging currents and increased mass transport rates. It is easily implemented and involves low costs[42].The trend in modern electrochemistry is to use microelectrodes.

All the metal ions were found to be quasi reversible except for the $Fe^{2+}$ which showed an irreversible behaviour in the voltammetric analysis results. The metal ligand peaks took a reasonable time to appear and all the complexes were found to be electrochemically (kinetically) labile compared to the $Fe^{2+}$.

Table 3.2 shows the different log K values obtained by voltammetry for the various metals with the range of other ligands. These include the common ligands EDTA and EN, as well as a biodegradable analogous EDDS and EDDM which was previously studied by

Crouch et al [45]. The log K values from table 3.2 were all determined by voltammetric methods and compare well with literature values determined by potentiometry.

From table 3.2, M-EDTA complexes have much higher stability constant values than M-IDS, however M-IDS complexes are biodegradable, environmentally friendly and acceptable while M-EDTA is not. The stability constant of Cu-EDDS is much higher than Cu-IDS. This shows that $Cu^{2+}$ complex more readily with EDDS than IDS and this makes EDDS a better ligand for complexing $Cu^{2+}$ than IDS. All the pK values of other metals were found to be comparable with the EDDS values. A recent theoretical study of IDS using a semi-empirical approach shows it's relative stability to that of it's homologues on the assumption that all six coordination centres of the ligand bind to the metal ions of interest [51].

The results obtained from voltammetric analysis of $H_4IDS$ and metal-IDS complexes were able to validate the predicted speciation models obtained using JESS. The speciation distribution diagrams were found to correlate well with the voltammetric $\Delta E$ vs pH curves, showing that this approach is useful for labile complexes at low pH.

Table 3.2: Table of stability constant values from potentiometry and voltammetry

| | **EDTA** | | **EN** | | **EDDS** | | **EDDM** | | **IDS** | |
|---|---|---|---|---|---|---|---|---|---|---|
| METAL | LIT. VALUE | EXP.VALUE | LIT. VALUE | EXP.VALUE | LIT. VALUE | EXP. VALUE | LIT. VALUE | EXP.VALUE | LIT. VALUE | EXP. VALUE |
| | | MICRO-ELECTRODE | | MICRO-ELECTRODE | | MICRO-ELECTRODE | | MICRO-ELECTRODE | | MICRO-ELECTRODE |
| $Cu^{2+}$ | 18.8 [52] | 18.7± [44] | 20.03 [52] | 20.1± [44] | 18.50 [44] | 18.3± [44] | 13.00 [44] | 13.01± [44] | 14.3 [24] | 14.1± |
| $Pb^{2+}$ | 17.9 [52] | 17.94± [44] | 5.05 [52] | 8.6± [44] | 12.3 [44] | 12.3± [44] | 11.1 [44] | 11.3± [44] | | 12.4± |
| $Zn^{2+}$ | 16.5 [52] | 16.7± [44] | 12..09 [52] | 12.16± [44] | 11.3 [44] | 11.5± [44] | 10.6 [44] | 10.7± [44] | 13.0 [24] | 13.1± |
| $Cd^{2+}$ | 16.5 [52] | 16.6± [44] | 13.52 [52] | 13.1± [44] | 13.1 [44] | 13.1± [44] | 10.8 [44] | 10.8± [44] | 13.5 [24] | 13.6± |
| $Fe^{2+}$ | | | | | | | | | 8.2 [24] | 8.1± |

# CHAPTER 4

## Electrochemistry and speciation of Polyaspartic acid with Cd, Cu, Mn, Pb and Zn

### 4.1 Polymeric biodegradable ligand

Polymers with carboxylic acid groups are one of the most important water-soluble polymers e.g. polyacrylic acid and polymethacrylic acid. Polyvinyl alcohol, polyethylene glycol and polyacrylic acid are water-soluble polymers that are widely used in cosmetics, paper additives, dispersants and detergent builders. The main concern of these polymers is that they are non-biodegradable i.e. they are rarely recovered after use and they tend to accumulate in the earth's environment after they've been released [53].

Polyamino acids having free carboxylic groups such as polyaspartic acid (PASP) and polyglutamic acid are best candidates for the biodegradable water-soluble polymer [53]. PASP Na-salt is synthesized by thermal polymerization of maleic acid anhydride in the presence of nitrogen containing compounds such as ammonia.

The ligand is available in solution and powder forms. The PASP enhance the ability to disperse the precipitation of salts which form the wash waters that degrade the cleaning

power of detergents and also affect machine parts with salt deposit build-up. PASP investigations revealed no toxic, sensitizing or mutagenic effects [23].

The salts of PASP are used as agents to assist in the milling of mineral materials to obtain aqueous suspensions of finely divided mineral materials. These mineral materials are pumpable and non-sedimenting. The salts of PASP have high concentrations of mineral materials that are useful in papermaking and paper coating [54]. PASP has potential biomedical applications including use as a material component in dialysis membranes, artificial skin, drug delivery and orthopedic implants [55].

## 4.2 EXPERIMENTAL PROCEDURES

### 4.2.1 Apparatus

The same apparatus were used as in the voltammetric analysis of metal-IDS complexes.

### 4.2.2 Reagents and chemicals

Note that the reagents and chemicals are the same as in the voltammetric analysis of metal-IDS complexes.

### 4.2.3 Standard preparations

**PASP**, 0.01M. Dilute 9.615ml of PASP with an appropriate amount of 0.2M acetate solution and dilute to 200ml volumetric flask.

The preparation of standard solutions is the same as in 3.1.3 (IDS).

## 4.3 RESULTS AND DISCUSSION

### 4.3.1 Complex stabilities of PASP-metal complexes

PASP is a novel biodegradable water-soluble polymer. The polymer chain contains potentially cleavable critical links in the form of amide bridges. The molecular mass distribution of the polymer was taken as 2250g/mol (average of total mass). This ligand complex with various transition metals in different molar ratios. PASP did not show any electrochemical activity (figure 1 in annexure) over the electrochemical window that was investigated.

Figure 4.1 shows a typical cyclic voltammogram of Cd and Cd-PASP. A quasi-reversible behaviour for the $Cd^{2+}$/Cd redox behaviour was observed.

Figure 4.1: Voltammogram of $Cd^{2+}$ and Cd-PASP complex at pH = 10.31

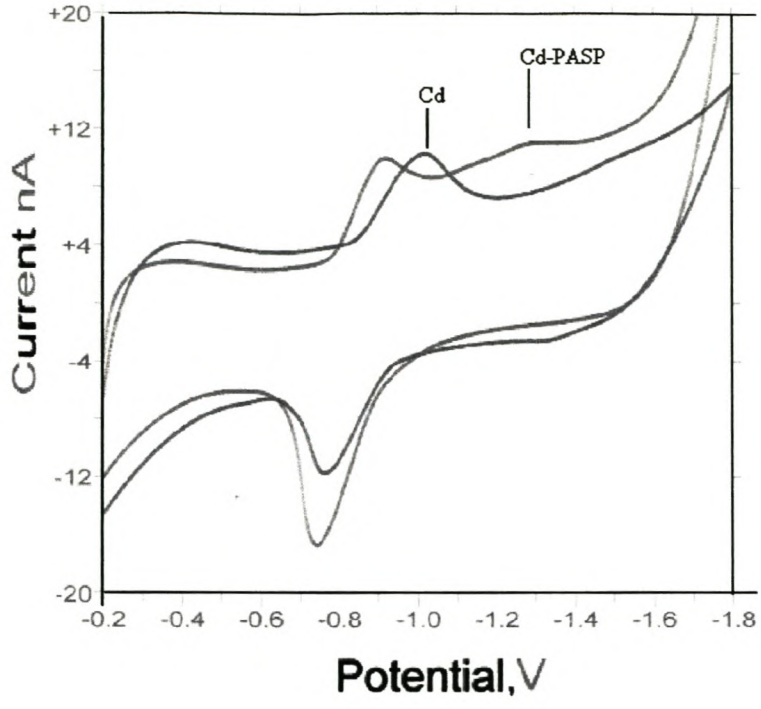


After the addition of the ligand, a decrease in the metal peak and a metal-ligand peak is observed. The metal peak shifted slightly to the negative potential. The metal reacted with the ligand in a 1:3.27 ratio at the potential of –1021mV and –1313mV, respectively. This behaviour was also seen in the complexation of CdIDS, where the metal-ligand peak is –1475mV. From figure 4.2, the major changes are at pH ≈ 3 and 8.

Figure 4.2: Plot of ΔE against pH for Cd-PASP at T=21.5°C.

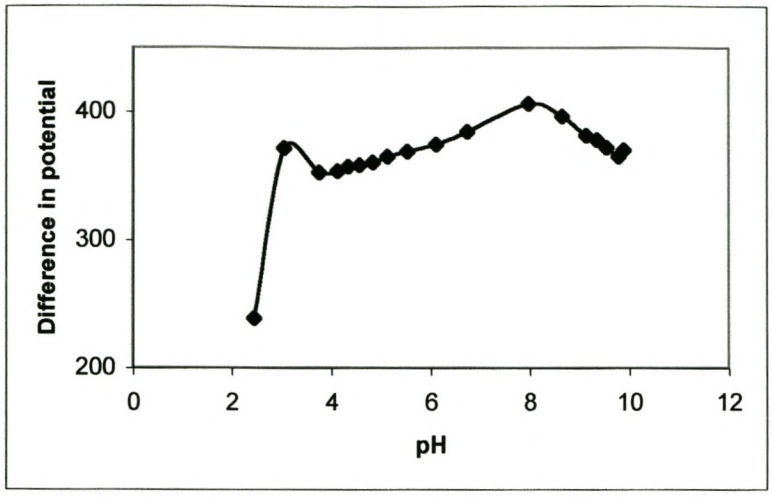


The cyclic voltammograms of Cu ion and CuPASP are shown in figure 4.3 and 4.4.

Figure 4.3: Voltammogram of $Cu^{2+}$ in $NH_4OH$ at pH = 10.96, T =21.5°C.

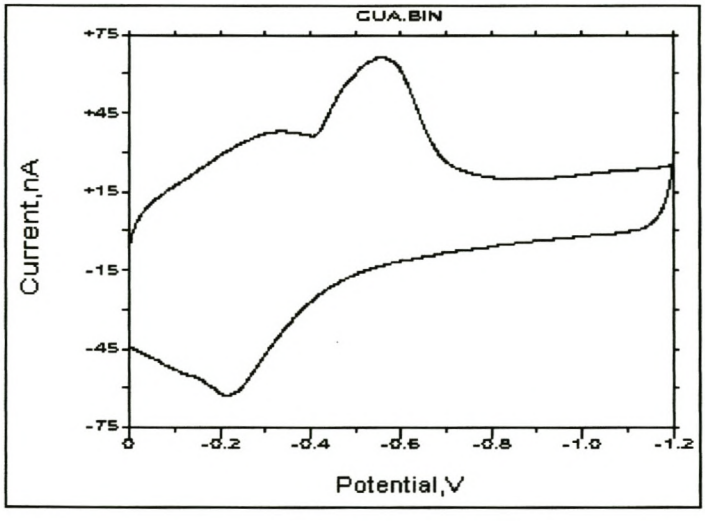

Figure 4.4: Voltammogram of CuPASP at pH = 10.33 (0.1M, T = 25°C).

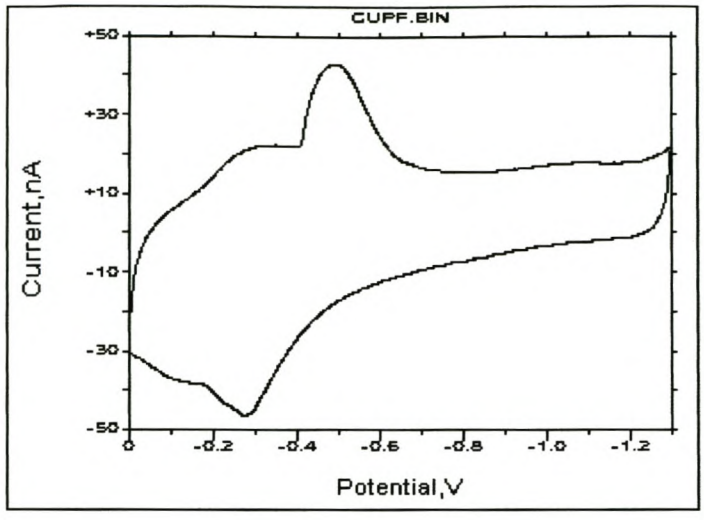


Figure 4.3 and figure 4.4 show the voltammograms of the Cu and CuPASP at the potential of -551mV and -1089mV, respectively. A quasi-reversible behaviour of the $Cu^{2+}$/Cu couple was observed. Figure 4.5 is a plot of the change in reduction potential against pH for CuPASP. The major changes are at pH's 8.2 and 9.5.

Figure 4.5: Plot of ΔE against pH for Cu-PASP at T=21.5°C.

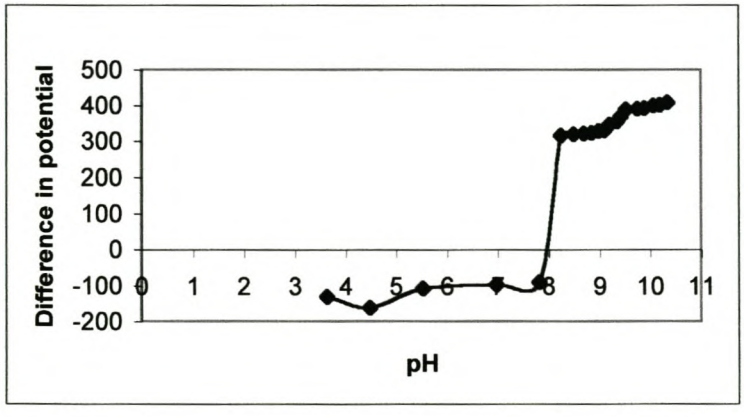

Figure 4.6 shows a typical cyclic voltammogram of the quasi-reversible behaviour of $Pb^{2+}$/Pb and Pb-PASP complex.

Figure 4.6: Voltammogram of $Pb^{2+}$ and Pb-PASP complex at pH = 10.31, T =21.5°C.

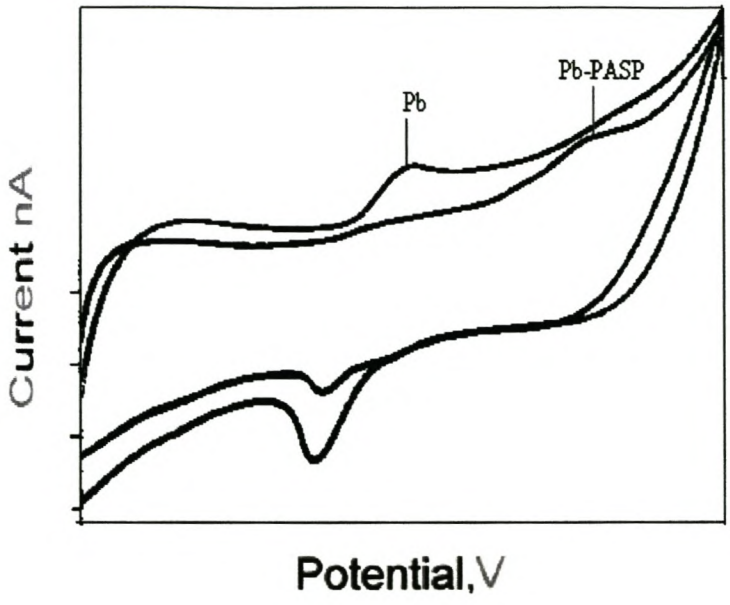


The Pb and PASP are in a 1:5.60 ratio at the potential of –1031mV and –1456.4mV, respectively. A similar behaviour as in Pb-IDS is also seen in Pb-PASP i.e. the metal peak disappeared completely as the complexation was reached. From figure 4.7, the major change is at pH ≈ 9.5, which is the log K value of Pb-PASP.

Figure 4.7: Plot of ΔE against pH for Pb-PASP at T=25.1°C.

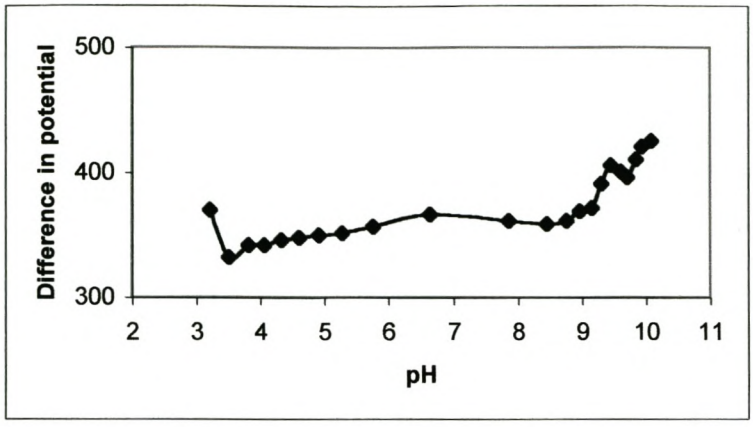


In figure 4.8, a cathodic peak of reduction of Zn (II) to Zn (Hg) appears at –1501mV and this resulted in a quasi-reversible characteristic process.

Figure 4.8: Voltammogram of $Zn^{2+}$ and Zn-PASP complex at pH = 10.31, T =21.5°C.

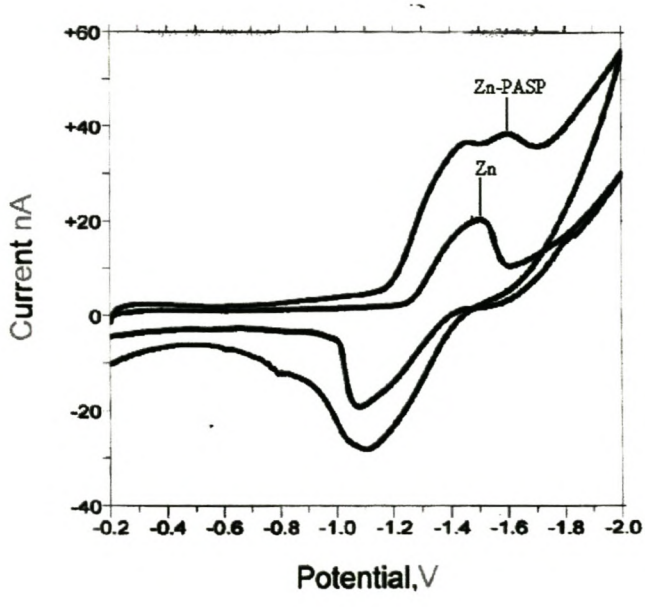

A quasi-reversible behaviour of $Zn^{2+}$/Zn redox reaction is observed. Complexation of Zn and PASP is seen by the formation of the new cathodic peak in the 1:1.11 ratio at the potential of –1356mV and –1598mV, respectively.

Figure 4.9: Plot of ΔE against pH for Zn-PASP at T=25.1°C.

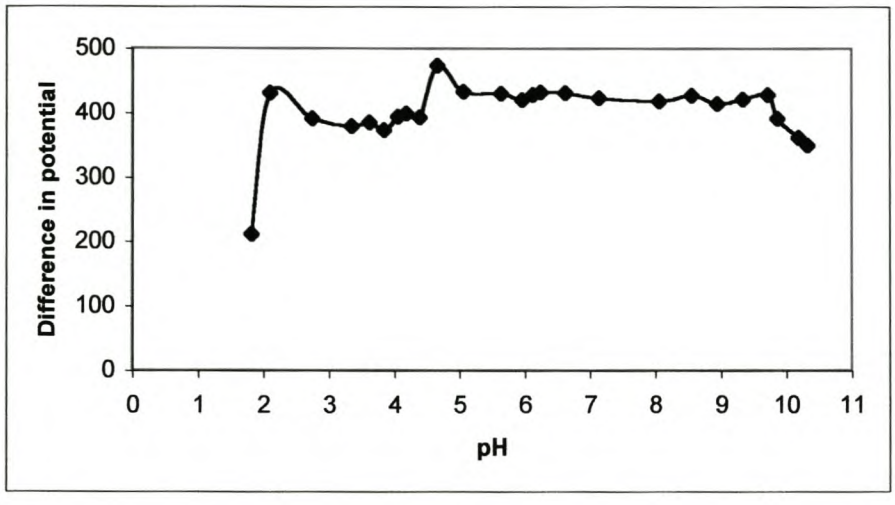


Figure 4.10 shows a cyclic voltammogram of $Mn^{2+}$ ion at the potential of –496mV respectively. $Mn^{2+}$ showed a quasi-reversible behaviour. The metal peak disappeared as PASP was added to the metal and the Mn-PASP peak was not observed because Mn is not electrochemically active within the selected window that was used for the analysis. This is seen in figure 4.11, which shows the overlap of the cyclic voltammograms of Mn-PASP complex. The cyclic voltammograms of Mn is shown and the others are due to the additions (100μl) of PASP to Mn. It was difficult to calculate the M:L ratios in this case because the amount of PASP added to form a metal-ligand peak is not known

Figure 4.10: Cyclic voltammogram of Mn in $NH_4OH$ at pH = 1.873, T = 21.7°C.

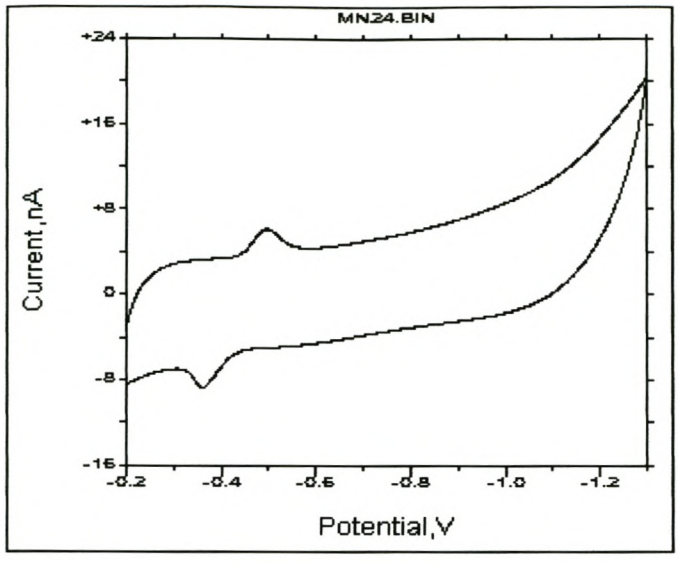


Figure 4.11: Cyclic voltammogram of Mn-PASP at pH = 10.31 (0.1M, T = 25°C).

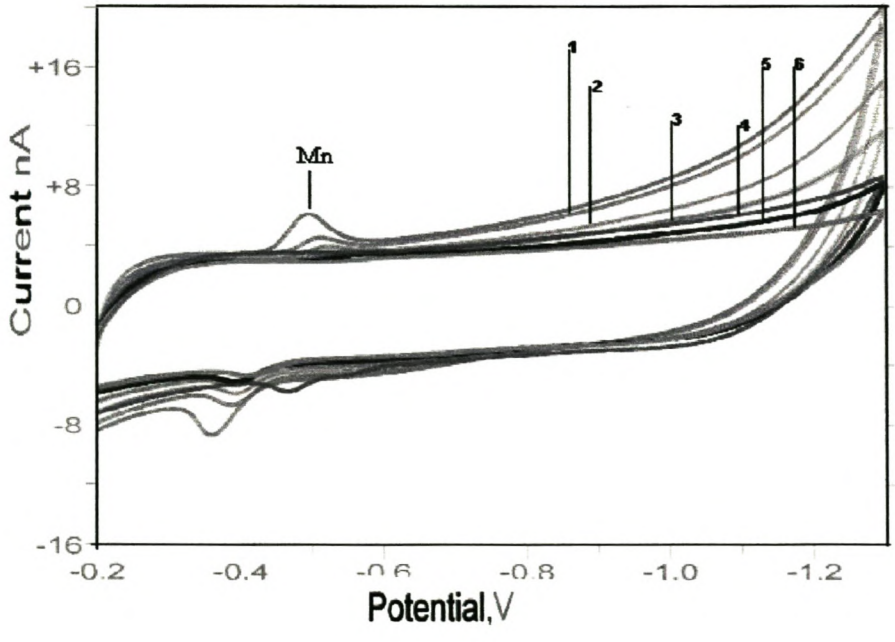

A summary of stepwise formation constants for complexes between PASP and selected transition metals is shown in table 4.1.

Table 4.1: Complex stability constants for PASP-metal complexes

| **Metal** | **$pK_1$** | **$pK_2$** | **$pk_3$** | **ΣpK** | **Literature pK** |
|---|---|---|---|---|---|
| Cd | 3 | 8 | | 11 | 1.7 [23] |
| Cu | 4.5 | 8.2 | 9.5 | 22.2 | 4.8 [23] |
| Pb | 3.2 | 9.3 | 9.8 | 22.3 | |
| Zn | 2.2 | 4.9 | 9.7 | 16.8 | 2.2[23] |

Literature values were not comparable with the voltammetrically determined values because CV can determine a wider pH range than potentiometric titration. The literature values for PASP are very low, (similar to the stepwise formation constant) so its apparent that the complex stability values determined by CV are more applicable. CV has been proposed as the preferred technique for determining equilibrium characteristics over potentiometry [2]. From table 4.1 the order of stability constants of M-PASP complexes is as follows Pb ≈ Cu > Zn >Cd. This agrees well with the order of the literature values even though they are small. Pb and Cu seem to react more readily with PASP since their stability constants are high.

The obtained complex stability constants (voltammetric data) of PASP are suppose to be used to generate and validate the predicted speciation models. These models predict the form of species present at different pH's. PASP is a polymer, which consist of aspartic acid units. It was difficult to interpret the speciation data of metal-PASP complexes because the complexes are labile. Aspartic acid is used as a model compound for the PASP because it is necessary to study the CV of aspartic acid with metals before predicting their speciation models. The cyclic voltammetry of ASP with transition metals was studied. This was done in order to observe the behaviour of species present at different pH's. The structure of aspartic acid is given below

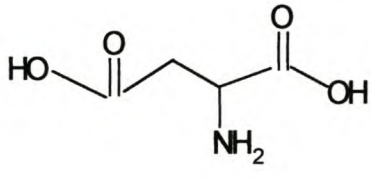


Aspartic acid reactions are kinetically slow. It does not complex with heavy metals[7] strongly but only with transition metals (preferably those with higher oxidation states for e.g. $Cr^{3+}$ is larger than $Cu^{2+}$). The theory of Hard and Soft Acid and Base (HSAB) developed by Pearson can be used to classify metals and ligands[56]. Hard acids are small metal ions that do not polarize easily[57]. These metal ions prefer hard ligands or bases, which are also small and are not very polarizable. Similarly, soft acids prefer soft bases or ligands. Soft bases are larger and more polarizable.

A typical cyclic voltammogram recorded in figure 4.11 shows the reduction current of ASP at -945mV and oxidation current at -784 mV. Figure 4.12 is a graph of the change in reduction potential against pH for aspartic acid. The major change is at pH 9.3, and this is the log K value of aspartic acid.

Figure 4.11: Cyclic voltammogram of 0.01M ASP at pH = 1.873, T = 21.7°C.

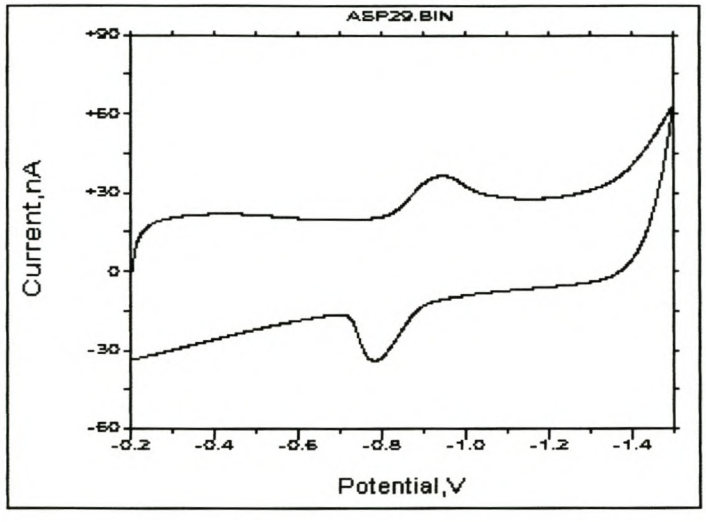


Figure 4.12: Plot of ΔE against pH for ASP at T=25.1°C.

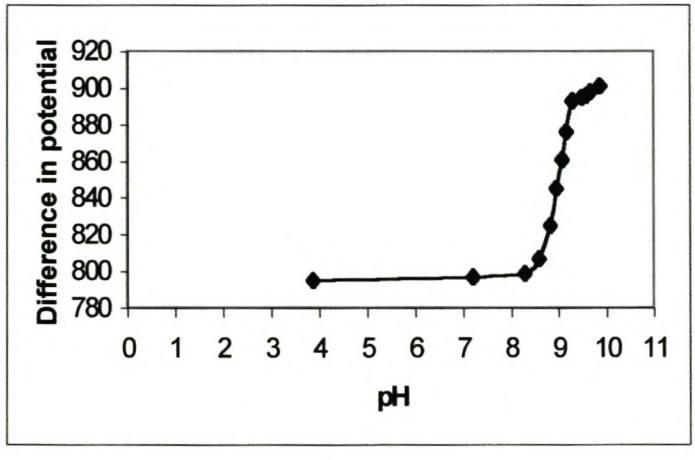

Complex stability constants for complexes between the selected transition metals with ASP and PASP are shown in table 4.2. The literature values were not comparable with the voltammetrically determined values.

Table 4.2:Complex stability constants for ASP and PASP with metals

| Metal | ASP | PASP |
|---|---|---|
| Cd | 10.31 [56] | 1.7 [23] |
| Cu | 15.35 [58] | 4.8 [23] |
| Cr | *3.62 [59] | 7.5 [23] |
| Fe | 11.4 [59] | 18.5 [23] |
| Mn | 4.0 [58] | 2.1 [23] |
| Pb | 7.38 [56] | |
| Zn | 10.4 [58] | 2.2 [23] |

* This is the stepwise formation constant [59]

Table 4.2 shows that ASP reacts more readily with heavy metals (Cd, Cu, Pb and Zn), whereas PASP prefers highly charged metals [60].

### 4.3.2 Speciation of PASP with Cd, Cu, Cr, Fe, Mn, Pb and Zn

It was difficult to predict the speciation data of metal-PASP complexes because they were found to be labile. With this in mind, aspartic acid was used as model to determine

the speciation with heavy metals. This was done because polyaspartic acid is a polymer consisting of aspartic acid units.

Figure 4.13 shows the speciation diagram of aspartic acid. From figure 4.13, as the pH increases the ligand undergoes deprotonation to form $Asp^{2-}$. The reaction starts as $H_3Asp^+$, $H_2Asp$ and $HAsp^-$ then the ligand $Asp^{2-}$. The unprotonated ligand starts forming after a pH of 10.

Figure 4.13: Speciation profile of Asp at T = 25, I = 0.1M.

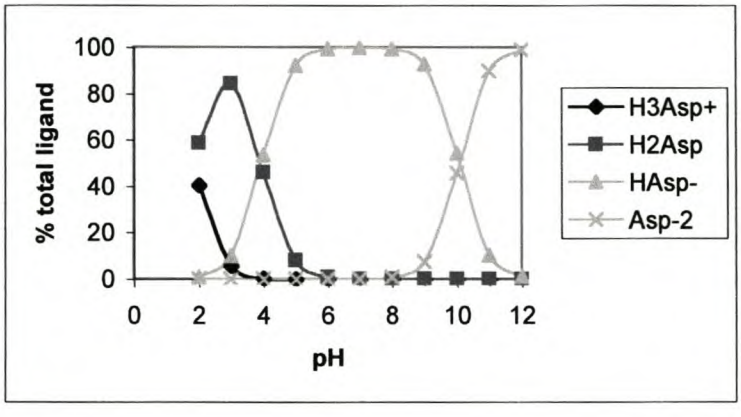


If only one metal and one ligand are present in an aqueous solution, then the following species could be formed: metal-ligand, metal hydroxide, ligand-proton, metal-ligand-proton and metal-ligand-hydroxide. This can be seen in the speciation diagram of CdAsp (figure 4.14a). When interpreting the speciation diagram the following should be noted that is, (i) the species moves from a more positive to a more negative species for example $H_3Asp^+$ to $CdAsp_2^{2-}$ (figure 4.14b) and (ii). hydrolysis should come after the formation of the metal-ligand complex. It is seen from figure 4.14a that at low pH, $Cd^{2+}$ is the main species that exist. The model (figure 4.14a and 4.14b) predicts that as the pH increases, the ligand undergoes deprotonation to form a 1:1 complex between Cd and aspartic acid. Figure 4.14a and 4.14b show that between pH 8 and 10 the main species formed is the CdAsp complex. At low ligand concentration Cd exists as the hydroxide species i.e. at

pH = 11. Cd has a stability constant of 10.31 and a small size. This means that complexation of aspartic acid with Cd is kinetically slow.

Figure 4.14a: Speciation profile of CdAsp at T = 25 °C, I = 0.1M.

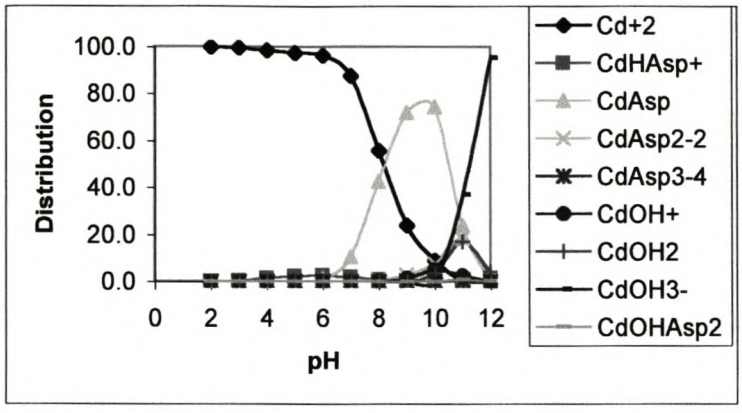


Figure 4.14b: Speciation profile of CdAsp at T = 25 °C, I = 0.1M.

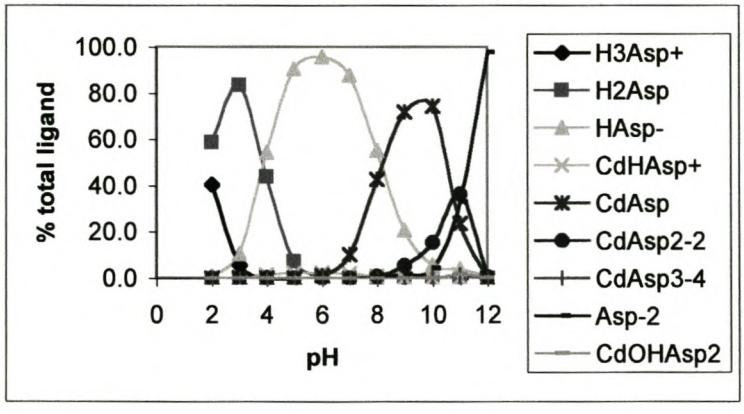

Figure 4.15a shows that the percentage of $Cu^{2+}$ species decreases from pH 2 to pH 8. This is due to the formation of a stable CuAsp complex between pH 5 and 8.2. Above pH 8, hydroxy species of Cu start to form for e.g. $CuOH_2$ that is a very insoluble precipitate.

Figure 4.15a: Speciation profile of CuAsp at T = 25 °C, I = 0.1M.

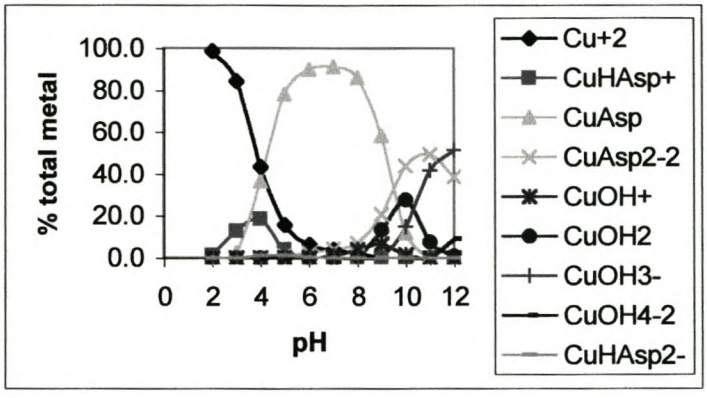


Figure 4.15b: Speciation profile of CuAsp at T = 25 °C, I = 0.1M.

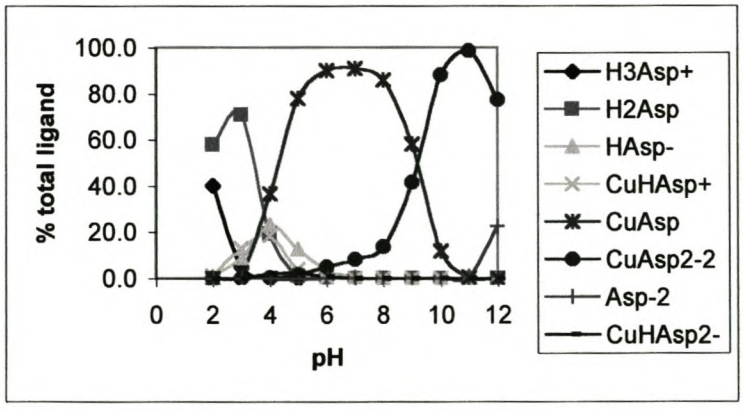

From the figures 4.16a,b below of CrAsp, it can be seen that $Cr^{3+}$ complexes faster with aspartic acid. This might be due to its size, which is larger than other transition metals and since the major complex exist in the pH range of 4 and 8. The $CrAsp^{+}$ complex forms at an earlier pH compared to CdAsp and CuAsp. The stepwise formation constant of 3.62 for $CrAsp^{+}$ is available in literature[59], while the overall stability constant is not. Hydroxy species start to form after the complexation of $Cr^{3+}$ with aspartic acid.

Figure 4.16a: Speciation profile of CrAsp at T = 25 °C, I = 0.1M.

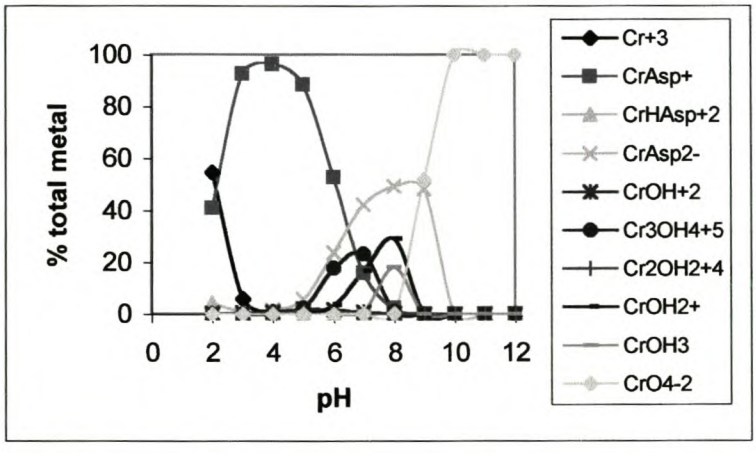


Figure 4.16b: Speciation profile of CrAsp at T = 25 °C, I = 0.1M.

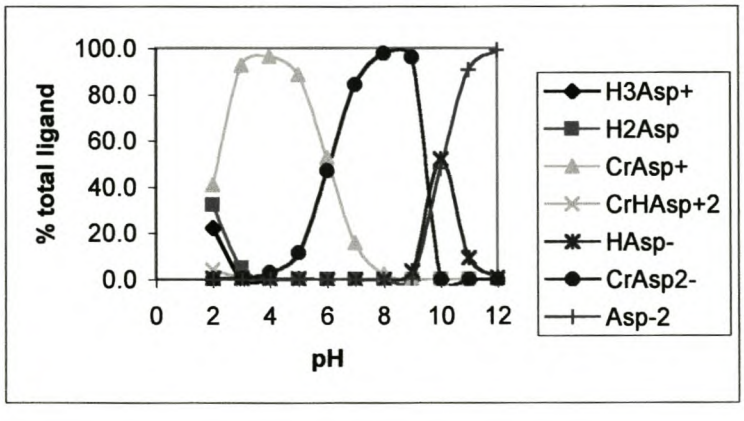

The FeAsp speciation curve shows that optimum complexation occurs between pH 2 and 7. The predominant species i.e. $FeAsp^{+}$ is observed between pH 3 and 5. Fe complexes much faster with aspartic acid compared to other metals except for Cu. This is because of its higher stability constant of 11.4 and large size.

Figure 4.17a: Speciation profile of FeAsp at T = 25 °C, I = 0.1M.

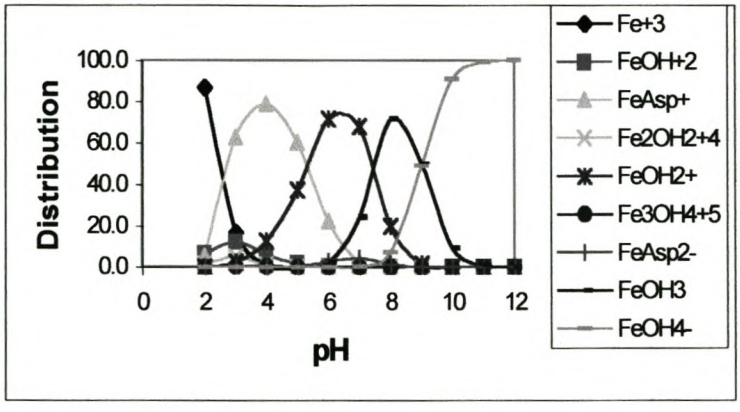


Figure 4.17b: Speciation profile of FeAsp at T = 25 °C, I = 0.1M.

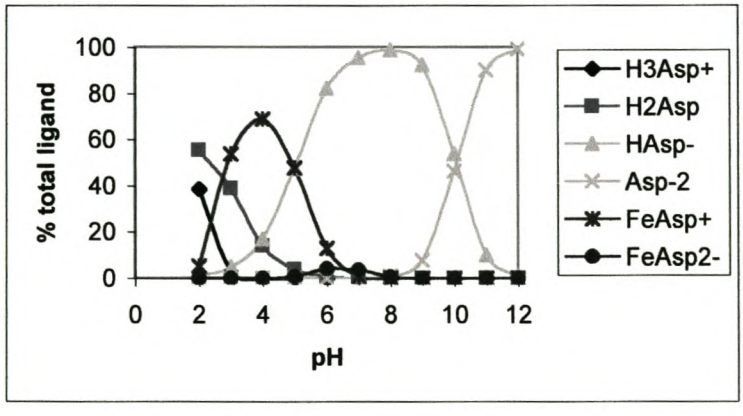

Mn is more stable between pH 2 and 8 (figure 4.18a) and as the main species start to form the Mn species decreases. The MnAsp complex is stable at pH 9. Aspartic acid complex Mn less readily because its stability constant is low i.e. 4.

Figure 4.18a: Speciation profile of MnAsp at T = 25 °C, I = 0.1M.

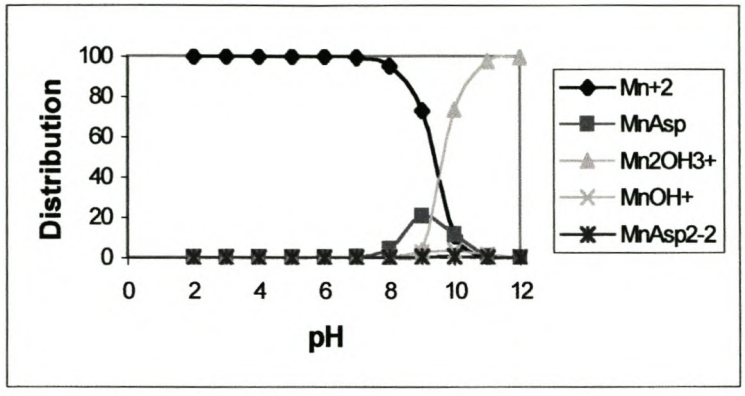


Figure 4.18b: Speciation profile of MnAsp at T = 25 °C, I = 0.1M.

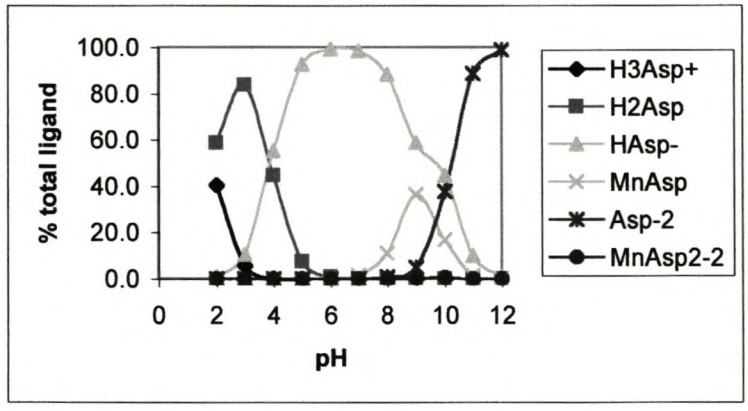

The distribution species-pH diagram of PbAsp is seen in figure 4.19a and 4.19b. PbAsp chelate exists between pH 7 and 9. Pb does not complex faster with aspartic acid because the hydroxy species start to form pH 6. At high ligand concentration, Pb exists as a hydroxide species.

Figure 4.19a: Speciation profile of PbAsp at T = 25 °C, I = 0.1M.

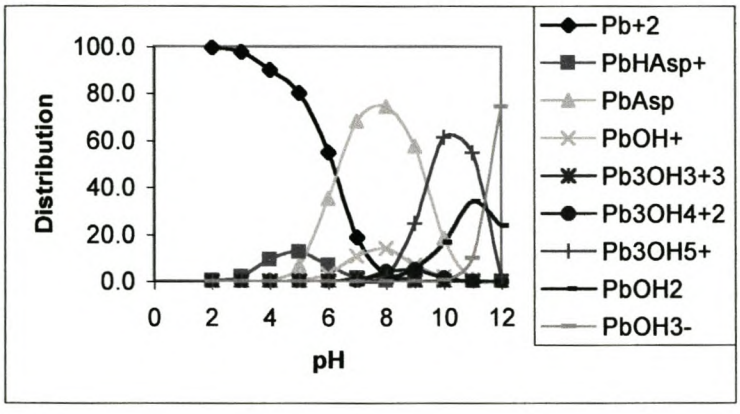


Figure 4.19b: Speciation profile of PbAsp at T = 25 °C, I = 0.1M.

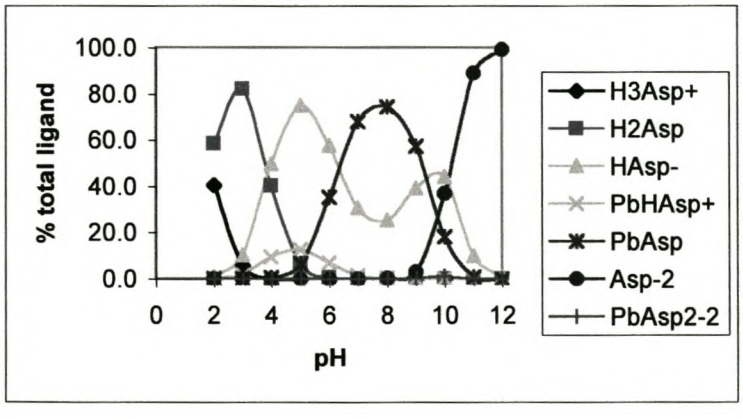

The ZnAsp speciation curve shows a decrease in the percentage of Zn species from pH 6 to 9. Aspartic acid complex Zn completely at pH 8 but the reaction is slow since $Zn^{2+}$ has the stability constant of 10.4. The other reason might be due to the small size of Zn. The hydroxy species are between pH 9 and 12.

Figure 4.20a: Speciation profile of ZnAsp at T = 25 °C, I = 0.1M.

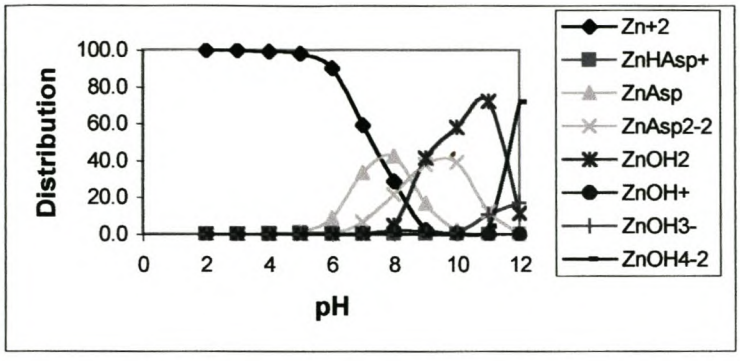


Figure 4.20b: Speciation profile of ZnAsp at T = 25 °C, I = 0.1M.

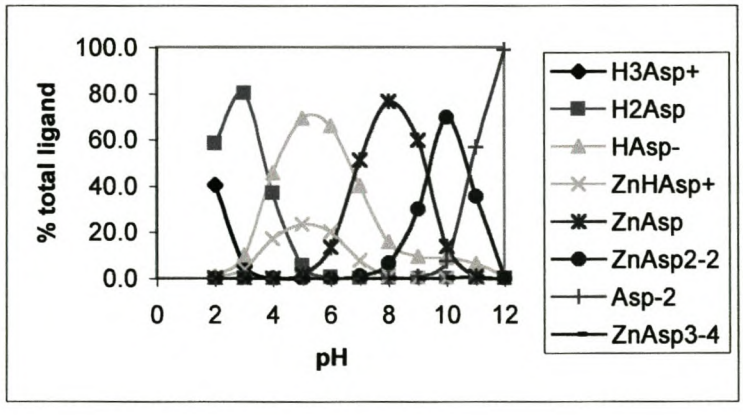

## 4.4 CONCLUSIONS

The results showed to follow the Irving and Williams series. This also agrees well with the literature complex stability values because Zn has the larger logK value than Cd and it implies that PASP will react more readily with Zn than with Cd. The cyclic voltammograms of MnPASP showed that the Mn ion peak decreased its height until it completely disappeared as the PASP was added to the metal. A similar behaviour was observed with the IDS ligand. In the case of IDS with Mn ion a peak was observed, where this peak was due to the Mn and acetate buffer not the IDS.

The complex stability values of PASP are much smaller than IDS and ASP (table 4.2) except for Fe. This is because PASP is a polymeric ligand and it binds in different ratios to the metal ions, whereas IDS has a specific binding mode to the metal ions. Polyaspartic acid exhibit high stability constants with iron (II) and this effect is especially favourable when using polyaspartic acid as dispersant in detergents. Iron form poorly soluble salts that lead to yellowing of laundry and iron interfere with the bleaching process and are thus clearly undesirable[23].

The CV of some of the metals with aspartic acid was studied. The addition of aspartic to the metals did not show the metal-ligand peaks. This is due to the weak binding of aspartic acid with transition metals [60]; ASP prefers metals with higher oxidation states for e.g. $Cr^{3+}$ is larger than $Cu^{2+}$.

# CHAPTER 5

## Separation of Biodegradable complexes by CE

### 5.1 Overview of Electrophoresis

The theoretical foundations of electrophoresis were established 90-100 years ago by Nernst, Whethman and Kohlrausch. A few years later, in 1909, Michaelis first proposed the term electrophoresis [61]. Electrophoresis (In Greek, *elektron* meaning electron and *phoresis* being carrying) is a separation based on the differential rate of migration of charged species in a buffer solution by applying an electric field. The Swedish chemist Arne Tiselius first developed this separation technique in the 1930's for the study of serum proteins. He was awarded the 1948 Nobel Prize for this work [62].

Electrophoresis has been traditionally performed on glass plates coated with anti-convective media, such as agarose gels by Tiselius. This separation technique is used in the biochemical fields. Unfortunately slab gel electrophoresis suffers from long analysis times, low efficiencies and difficulties in detection and automation. This led to the development of electrophoretic separation in narrow-bore capillaries, since these are anti-convective. Hjerten described the initial work in open tube electrophoresis in 1967 [63]. In early 1980's Jorgenson and Lukacs advanced the technique by using 75μm fused silica capillaries. The fundamental theories were fully developed by Jorgensen, i.e. where he

demonstrated the potential for high performance capillary electrophoresis (HPCE) as an analytical technique [64].

There are different modes of CE namely capillary zone electrophoresis (CZE), micellar electrokinetic capillary chromatography (MEKC), capillary gel electrophoresis (CGE), capillary isoelectric focusing (CIEF) and capillary isotachophoresis (CITP). In CZE, ions are separated according to their mobility in free solution [65]. The analytes with different electrophoretic mobility will migrate in separated zones. And the analytes with the same electrophoretic mobility will co-migrate as the same zone in the capillary under the applied electric field [4]. The separation of neutral species as well as charged ones by MEKC is accomplished by the use of surfactants in the running buffer. Neutral compounds can be trapped in micelles of an ionic surfactant and thus can migrate either with or against the electroosmotic flow (EOF), which is the bulk flow of liquid in the capillary (depending on the charge). Addition of cationic surfactants like CTAB is a very convenient method to reverse the direction of EOF [4]. CGE is useful for the separation of oligomers such as oligonucleotides, which have a constant charge-to-mass ratio. Mobility through a gel network decreases as size increases. CIEF is a high resolution electrophoretic technique to separate peptides and proteins on the basis of isoelectric point. CITP is a "moving boundary" electrophoretic technique. In a single ITP experiment either cations or anions can be analyzed.

EOF arises due to electric double layer i.e. formed at the silica interior capillary wall. The capillary surface has a net negative charge owing to the dissociation of the functional

groups on the capillary surface and this depends on the pH of the solution. The EOF determines the time solutes remain in the capillary due to the mobility of the solvent/solute. Mobile positive ions present at the capillary surface are attracted to the negative electrode and solvent molecules are transported concurrently. For fused silica, the EOF is strongly controlled by the numerous silanol groups (SiOH) that can exist in anionic form ($SiO^-$). EOF becomes significant above pH 4. At high pH, where the silanol groups are predominantly deprotonated, the EOF is greater than at low pH where they become protonated. EOF causes movement of nearly all species, regardless of charge, in the same direction. Under normal conditions (i.e. negatively charged surface), the flow is from the anode to the cathode.

Electrophoresis has been found to offer the following advantages, low capital and running cost, separation time is shorter, minimum needs of sample volumes (below attoliter range) can be analyzed and less eluent is consumed, uniform flow profile, high separation, efficiency and the use of sensitive detectors [66-69].

The basic CE system contains of a high-voltage power supply, two buffer reservoirs, a capillary and a detector. This is shown schematically below in figure 5.1. However, the basic instrumentation for CE can be enhanced with the use of autosamplers, multiple injection devices, sample and capillary temperature control, programmable power supply, multiple detectors, fraction collection and computer interfacing [70].

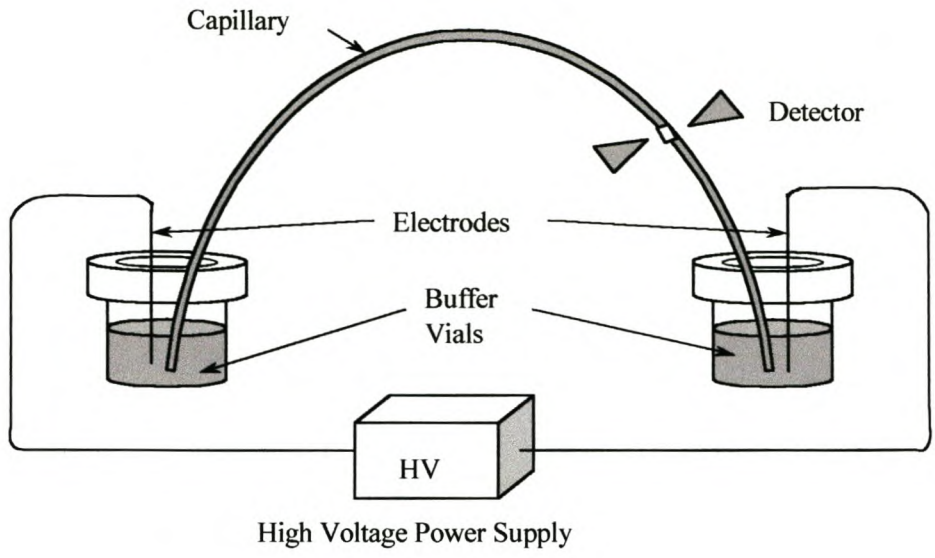


Figure 5.1: Schematic representation of capillary electrophoresis instrumentation

An electrophoretic separation is performed by injecting a small band of the sample into an aqueous buffer solution i.e. contained in a narrow capillary or on a flat porous support medium such as paper or a semisolid gel. A high dc potential is applied across the length of the capillary by means of a pair of electrodes located at either end of the buffer. This potential causes ions of the sample to migrate toward one or the other of the electrodes. The rate of migration of a given species depends upon its charge and also upon its size. Separations are then based upon differences in charge-to-size ratios for the various analytes in a sample. The larger this ratio, the faster an ion migrates in the electrical field [71].

CE has a wide analytical spectrum, i.e. in chemical, biomedical and pharmaceutical applications [65]. It has rapidly evolved as an independent technique, expanding beyond the application field of slab gel electrophoresis, traditionally limited to the separation of biopolymers, to include the analysis of inorganic anions and cations, metal chelates, pharmaceuticals and drugs, hydrocarbons, organic acids, amines, carbohydrates, polymers and particles, fuels, dyes, explosives, DNA sequencing and analysis of neurotransmitters in single cells, etc which traditionally were typical applications of Chromatography [72].

While CE supplements conventional HPLC and GC methods, it offers superior resolution and greater flexibility with regard to separation conditions techniques for metal speciation compared to the latter methods. Since it shows unique promise for speciation purposes by exerting only minor disturbance on the existing equilibrium between different speciation. CE was shown to be the state-of-art in the metal speciation studies because metal speciation has gained importance due to its impact on environmental chemistry, toxicology and biomedical sciences [3]. Certainly CE has a real future in the speciation field, not just for the analysis of trace species but as a technique for studying interactions in the environmental and biological systems. CE methods have also showed to be good alternatives to the potentiometric titration and spectrometric methods developed previously for the determination of stability constants of metal complexes [73].

The most common detectors in HPLC and CE are ultraviolet (UV), fluorescence, electrochemical and diffractometer detectors [74]. CE separation in combination with UV-

and conductivity detection showed to be suitable for speciation analysis of arsenic and selenium [72]. UV-vis and fluorescence detectors are not suitable for direct determination of organic acids (i.e. pentanoic, hexanoic etc) and inorganic ions (i.e. phosphate and carbonate) because most of them do not absorb UV light and do not show fluorescence activity [75].

Indirect UV detection provides a universal means of cation detection because its sensitivity for detecting metal cations is lower than that of direct UV detection [64]. Traditional methods for polyamine detection are mostly confined to HPLC, TLC and sometimes GC. All the methods are tedious and time-consuming since they require that polyamines should be derivatized or labeled before detection since they have no chromophore and cannot be detected within an UV detector. CZE with indirect UV detection has been proved to be a rapid, simple and sensitive method for determination of polyamines in biosamples such as serum and tumor cells [76]. Polyamines mainly putrescine, spermidine and spermine, are low molecular mass aliphatic amines that exist in all living organs and play important roles in cell growth and differentiation. CE has also shown to be a great promise for enantiomeric separations [70]. Indirect UV detection is presently the most versatile method to solve the problem of universal detection for metal speciation by CE [3].

Electrochemical (EC) detectors can offer some advantages over the latter detectors. If ultramicroelectrodes (10 μm) are used, detector responses will not be limited by a small detection volume [77]. EC detection also offers sensitivity for oxidised or reduced analytes

that often rivals that of laser-induced fluorescence, which is currently the method of choice for many CE applications [78]. Although UV-vis, fluorescence and electrochemical detectors provide sensitive and simple detection with these techniques. Electrospray MS (ESI-MS), in which the analyte is protonated or deprotonated, has proven highly successful for the analysis of peptides, proteins and nucleotides [79].

CE is unique among liquid-phase separations in its utility for fast separations. The development of such fast separations has opened many new applications and this includes real time chemical monitoring, detection of short-lived species and rapid multi-dimensional separations. Other applications currently being developed include high-throughput assays for clinical laboratories or screening combinatorial libraries.

However, historically CE lacks sufficient concentration detection sensitivity (low $mgl^{-1}$ range), which is a serious limitation for its application to metal speciation using commercial instruments [3]. As a result, the use of CE in speciation is still not widespread. More new applications and developments can be expected in future. It is believed that novel detectors will be developed and become more viable to the users of commercial CE instrumentation. At the present stage of development, CE represents a valuable alternative to HPLC in differentiating species from relatively concentrated samples.

## 5.2 EXPERIMENTAL PROCEDURES

### 5.2.1 Instrumentation

All separations were performed on a $HP^{3D}CE$ system. A bare fused silica coated capillary of 75μm i.d. was used. The total length of the capillary was 86cm, with the detection window burned 8.5cm from the capillary end. A separation potential of -25kV was applied during all separations. Samples were introduced by applying a 50mbar pressure for 2.5 seconds. UV detection at 200nm and 214nm was used. The pH of solutions was measured with a Jenway 4330 pH meter. All experiments were conducted at 20°C.

### 5.2.2 Reagents and solutions

All chemicals were of analytical grade. Ultrapure water was used throughout. The stock solutions of 1000ppm $Cd^{2+}$, $Cu^{2+}$, $Cr^{3+}$, $Fe^{3+}$, $Mn^{2+}$, $Pb^{2+}$, $Zn^{2+}$ and two ligands (IDS and PASP) were used to prepare dilute metal-chelate solutions. The working electrolyte was prepared daily from stock solutions containing 20mM borate buffer. 0.3mM CTAB (Cetyltrimethylammonium bromide) was used as a surfactant. The electrolyte was filtered through a 0.45-μm membrane filter prior to use.

### 5.2.3 Standard preparations

**Borate Buffer solution**, 20mM $Na_2B_4O_7.10H_2O$. Dissolve 0.4775g of borate with an amount of distilled water and dilute to a 250ml volumetric flask using the same solvent.

**CTAB as a surfactant**, 0.3mM Cetyltrimethylammonium bromide. 0.01823g of CTAB was dissolved and diluted to 50ml with borate buffer in a volumetric flask.

**Stock solutions of $Cd^{2+}$, $Cu^{2+}$, $Cr^{3+}$, $Fe^{3+}$, $Mn^{2+}$, $Pb^{2+}$ and $Zn^{2+}$**, 10ppm of each metal. Dilute 0.25ml of metal ion with borate buffer in a 25ml volumetric flask.

**IDS**, 1mM. Dilute 0.02095ml of IDS with an appropriate amount of 20mM borate buffer in a 25ml volumetric flask.

**PASP**, 1mM. Dilute 0.1202ml of PASP with borate buffer in a 25ml volumetric flask.

### 5.2.4 Procedure for Electrophoresis

The fused silica capillary was rinsed with 0.1M NaOH for 10 minutes, then with deionized water for another 10 minutes and equilibrated with the borate buffer solution for another 10 minutes. Between each injection the capillary was filled with the buffer solution by flushing the entire capillary for 5 minutes at 50mbar. The flush cycle is used to wash the capillary in order to remove the traces of old sample and buffer. Both ends of the capillary were dipped into two separate beakers filled with the same buffer solution. The sample solution was introduced into the anodic end of the capillary by hydrodynamic injection. A voltage of –20kV was then applied.

## 5.3 RESULTS AND DISCUSSIONS

The metal-ligand complexes were studied at different pH's using CZE as a mode of separation. This technique was used because of its ability to separate both anionic and cationic species in a single operation [4]. Cations migrate in the same direction as the electroosmotic flow (EOF) whereas anions migrate opposite to the direction of the EOF. EOF causes the movement of nearly all species, regardless of charge, in the same direction. The electrophoretic mobilities of metal-IDS are in the opposite direction to those for EOF. Therefore, to control the EOF-rate, a separation mode was performed by addition of a cationic surfactant (0.3mM CTAB) to the carrier electrolyte, which has the effect of reversing the direction of the EOF so that it flows from negative electrode to the positive electrode. Padarauskas et.al showed that using a cationic surfactant namely tetradecyltrimethyl ammonium hydroxide (TTAOH) at a concentration above 0.3mM, the EOF is reversed [80] (shown in figure 5.2) [4]. The effectiveness of CTAB, in reducing the EOF, in addition to the buffer decreased EOF and gave a rapid migration of the complexants in less than 7 minutes. An improvement in the peak shapes and shorter migration times are also achieved.

Figure 5.2: Elimination and reversal of EOF using a cationic surfactant [4]

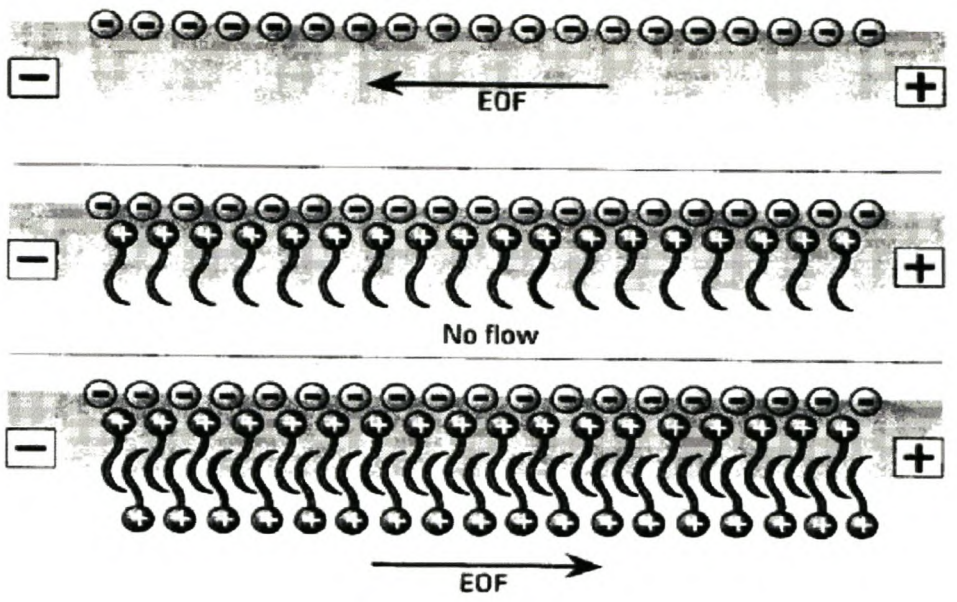


### 5.3.1 Separation of metal-IDS complexes

Common anions such as chloride and nitrate did not interfere directly with the detection of the ligands studied here or with their metal complexes since their charge density is much larger [7] and these anions therefore eluted more rapidly (typically less than 6 minutes). The $Cl^-$ peak is shown in figure 5.3.

Figure 5.3: Electropherogram of $Cl^-$ at pH 2.259

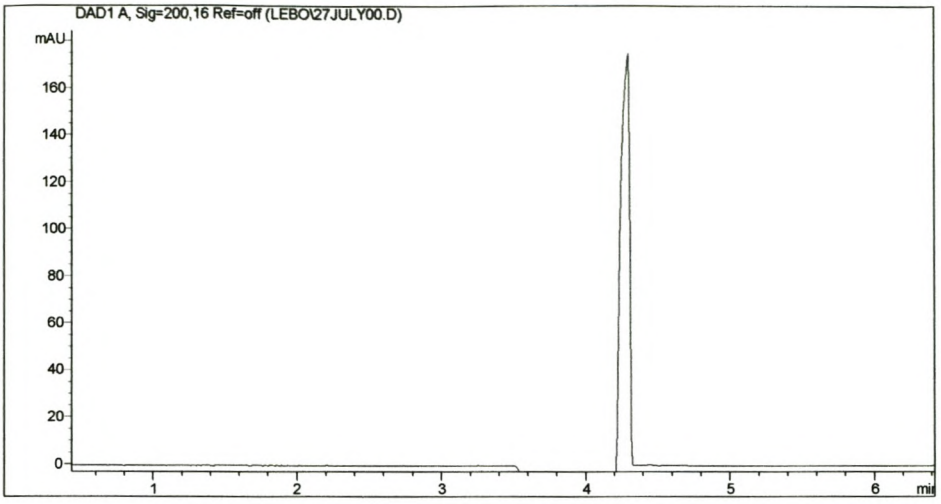


Figure 5.4 show the nitrate peak. This peak was detected when potassium nitrate solution was electrophoresed. The metal solutions used in this work are in the nitrate form for e.g. Cd $(NO_3)_2$; therefore there was a need to establish the migration of the nitrate peak.

Figure 5.4: Electropherogram of $NO_3^-$ at pH 5.982

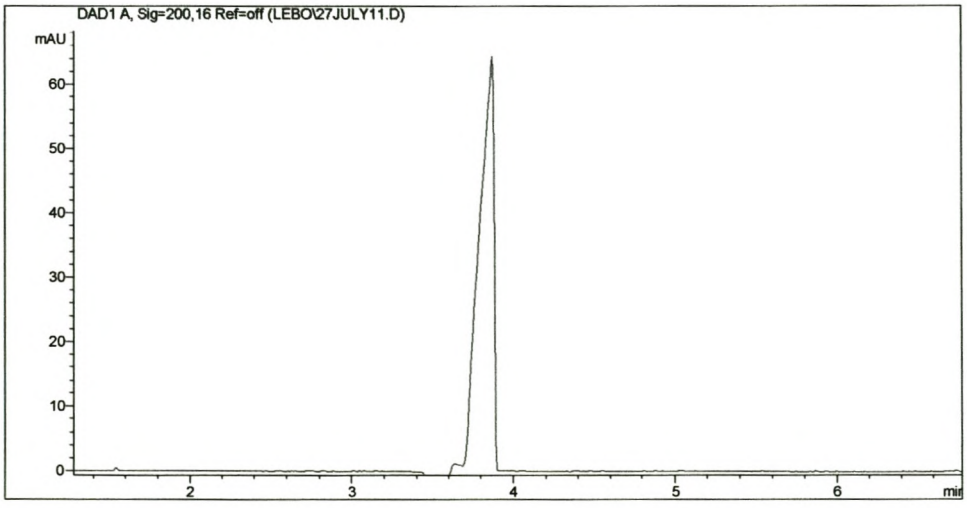

An EOF marker i.e. mesityl oxide was used as the mobility reference peak that is, EOF can be measured using a neutral marker that moves at a velocity equal to the EOF. The EOF time $t_{eof}$ was taken to be the elution time of a neutral mesityl oxide peak that eluted at 7.230 minutes. A peak seen in figure 5.5 relates to the marker peak.

Figure 5.5: Electropherogram of mesityl oxide at pH 8.730

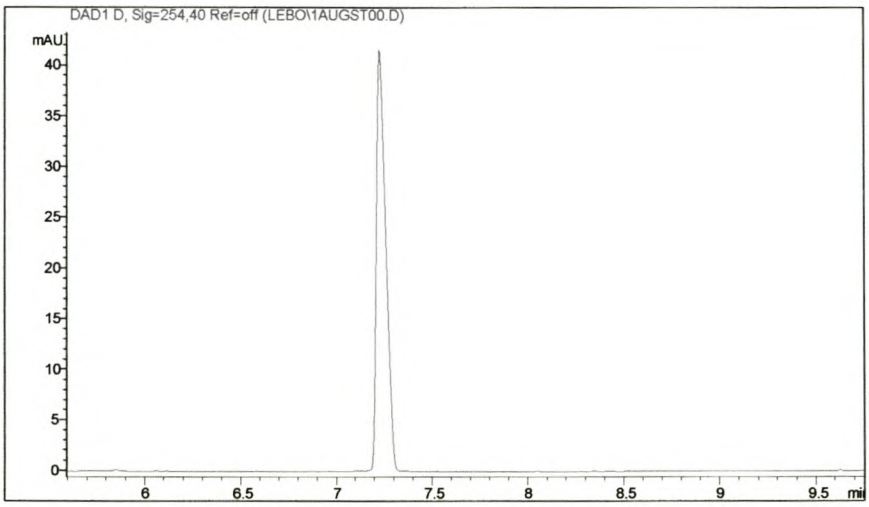


The metal-IDS complexes were prepared by mixing the cation stock solution with IDS in a 1:1 ratio of metal to ligand. The chelates absorb less at wavelengths higher than 220nm and are stable over a broad range of pH. When IDS complexes with bivalent and trivalent cations, metal-IDS chelates possess a negative net charge and can be thus separated in the anionic separation mode. An electropherogram that demonstrates the separation of the $CdIDS^{2-}$ is shown in figure 5.6.

Figure 5.6: Electropherogram of CdIDS at pH 11.070

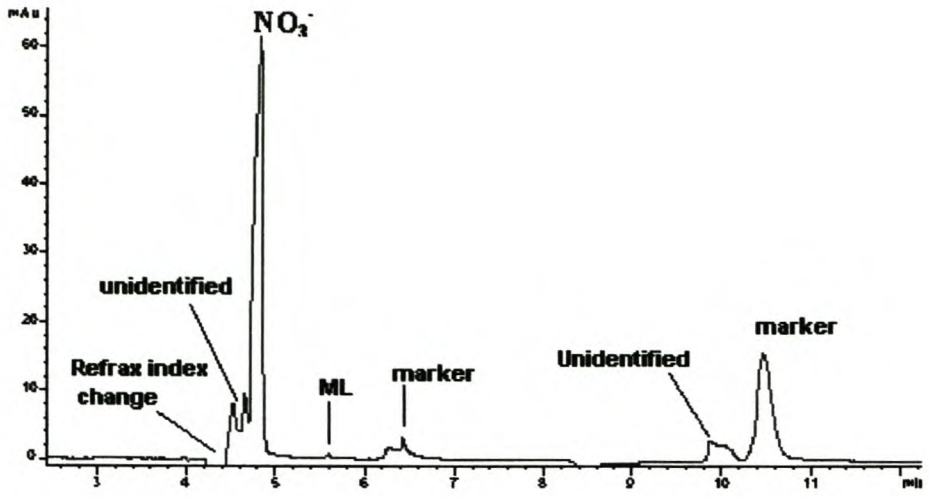


At high pH i.e. at full complexation of the metal with IDS there is only one peak that is of our interest i.e. the metal-ligand (ML) peak. At pH 11.070 the CdIDS peak is not clearly seen due to the formation of other hydroxo species present. The peak depicted by $NO_3^-$ in the above figure at 4.830 min corresponds to the nitrate anion, followed by a CdIDS (ML) peak (5.605 min) which is very small at this pH. The pH of the electrolyte was varied over the range from 11.070 to 2.843 by the addition of 0.1M HCl. A decrease in the pH resulted in the formation of the $Cl^-$ peak. This peak is eluted before nitrate.

The metal-ligand complexes were detected only at 200 and 214 nm (figure 5.7a) and the neutral marker (mesityl oxide) showed a higher absorbance at 254 and 225nm (figure 5.7b). The marker showed to elute as two peaks when mixed with metal-ligand complexes, i.e. at 7.406 min and 12.557 min in figure 5.7b. They (ML species and anions) will elute before EOF. The following was observed in figures 5.7-5.15.

Figure 5.7a: Electropherogram of CdIDS and marker at pH 10.828(214nm)

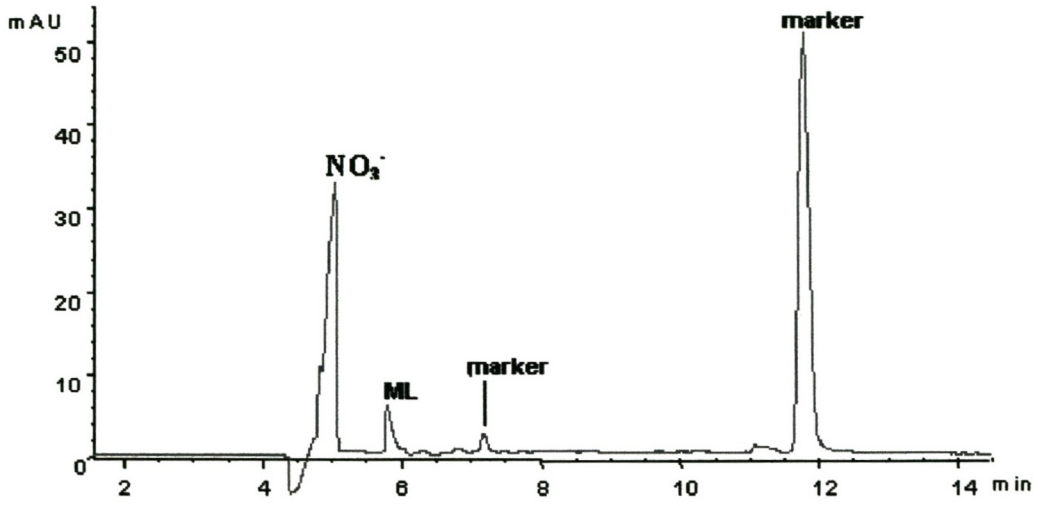


Figure 5.7b: Electropherogram of CdIDS and marker at pH 10.828(225nm)

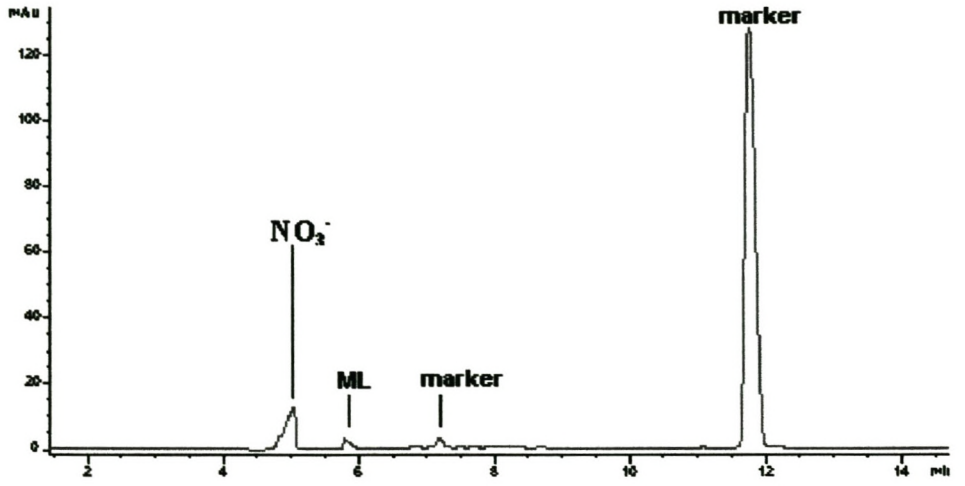

Figure 5.8: Electropherogram of CdIDS and marker at pH 9.826(214nm)

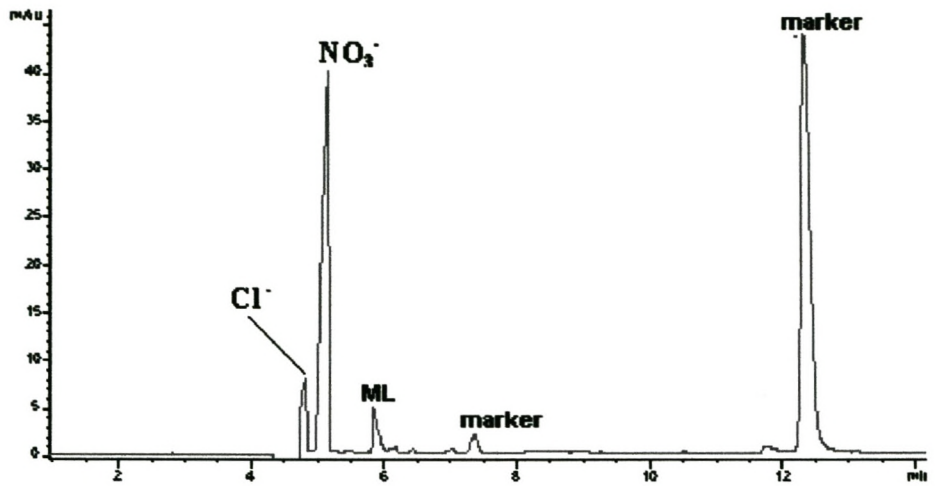


Figure 5.9: Electropherogram of CdIDS and marker at pH 8.751(200nm)

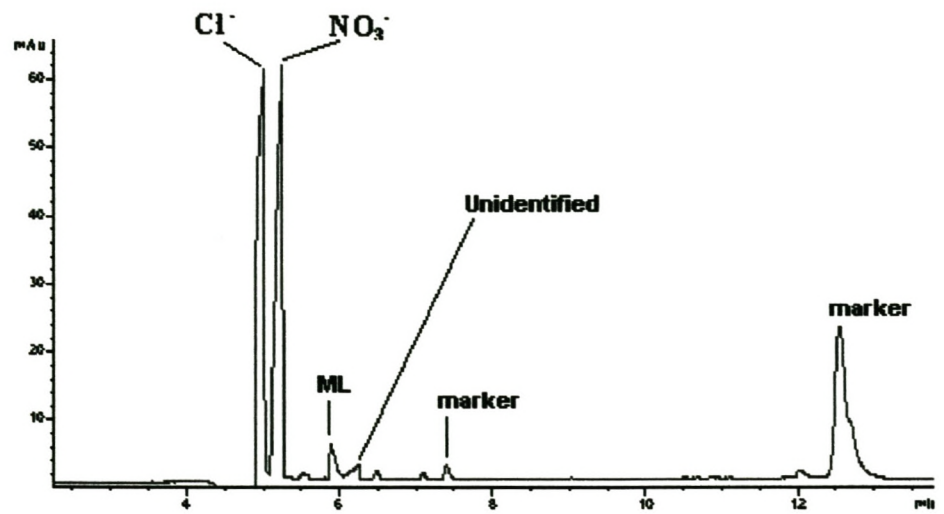

Figure 5.10: Electropherogram of CdIDS and marker at pH 7.136(214nm)

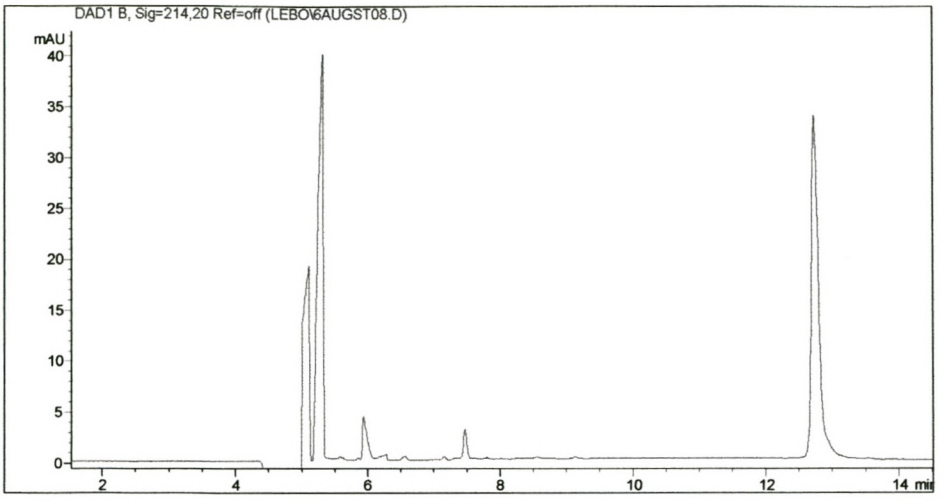


Figure 5.11b: Electropherogram of CdIDS and marker at pH 6.569(214nm)

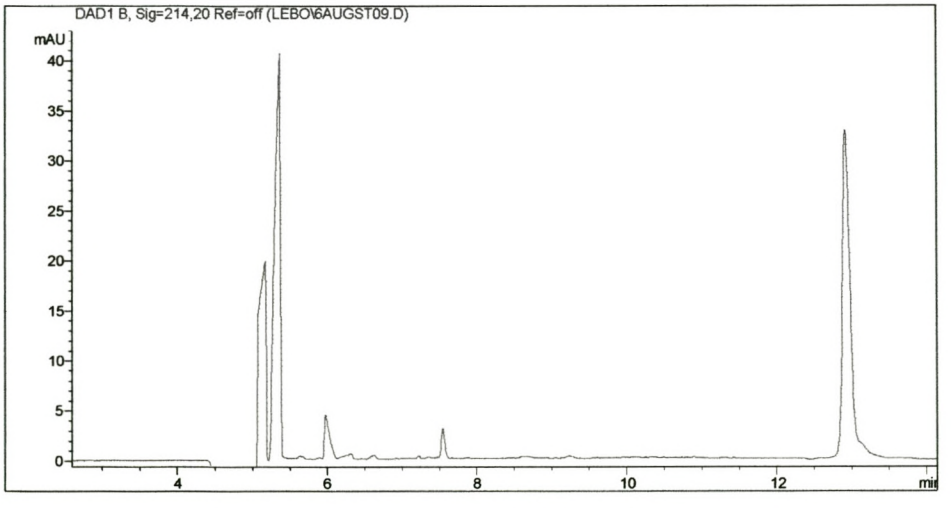

Figure 5.12: Electropherogram of CdIDS and marker at pH 5.555(214nm)

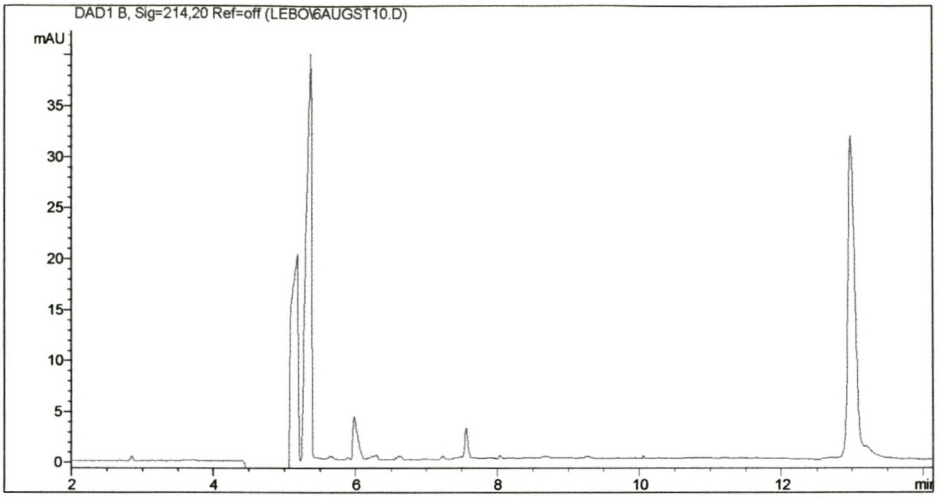


Figure 5.13: Electropherogram of CdIDS and marker at pH 4.613(214nm)

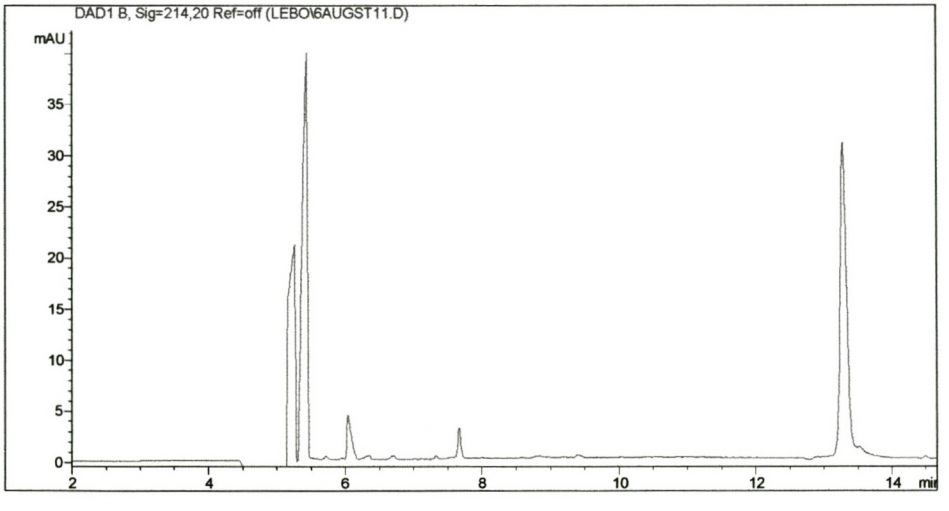

Figure 5.14: Electropherogram of CdIDS and marker at pH 3.801(214nm)

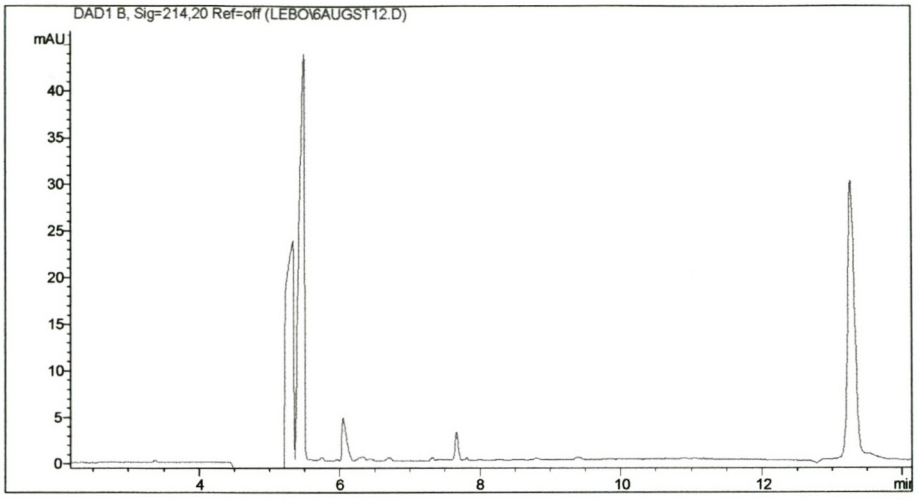


Figure 5.15: Electropherogram of CdIDS and marker at pH 2.843(200nm)

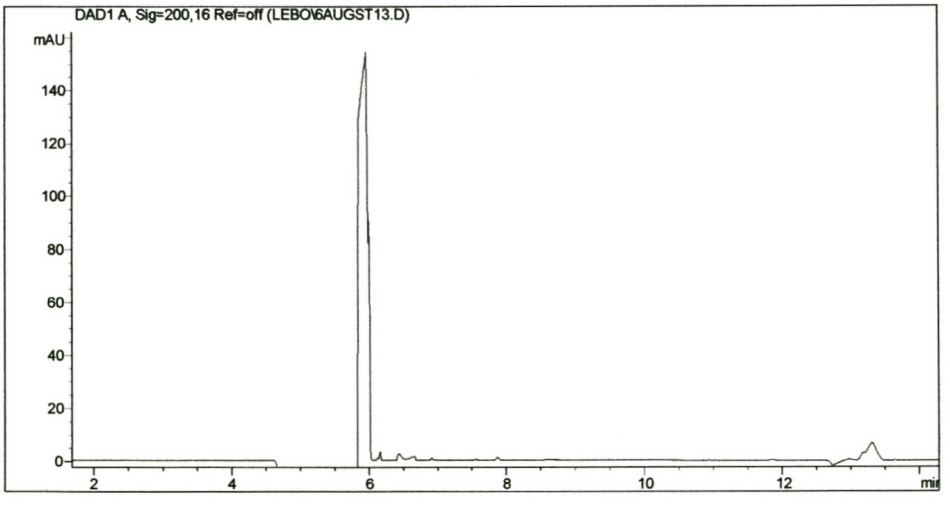

A similar behaviour was observed for all metal-IDS complexes (see annexure figure).

The plot of pH vs log peak area was constructed to predict the effect of pH on the equilibrium between metal-ligand complexes. Figure 5.16a and 5.16b show the plot for CdIDS.

Figure 5.16: Graph of pH vs log peak area of CdIDS

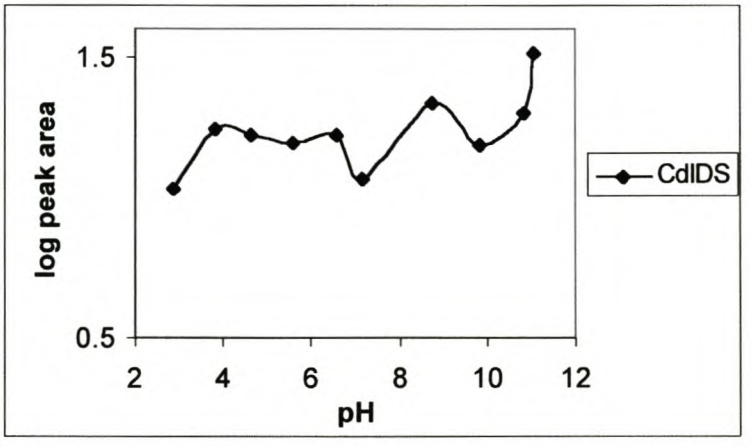


The CdIDS complex is highly labile; thus the varying concentration $CdIDS^{2-}$ complex over the pH range. This is shown in figure5.16. From the speciation profile of CdIDS (figure 3.19), its evident that there is an increase in $[CdIDS^{2-}]$ starting at pH 4-11 and a decrease in $[Cd^{2+}]$. This implies that complexation has taken place within this range. Some other hydroxides species of the metal are also existing, but at a low concentration. A decrease in $[CdIDS^{2-}]$ at pH 6.8-7.5 is seen because of the lability of the complex i.e. the equilibrium between Cd and IDS is attained rapidly because of its higher stability constant at 13.5.

Figure 5.17: Graph of pH vs log peak area of CuIDS

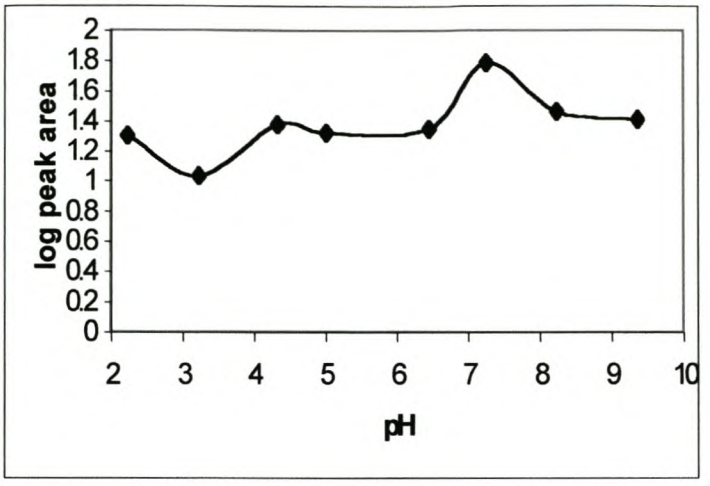


For the chelation of $Cu^{2+}$ with IDS, an equilibrium between the Cu ion and CdIDS exists. CuIDS behaves differently from CdIDS because of its higher stability compared to Cd. The [CuIDS] increases with increasing pH. This follows the prediction that at high pH, the complex $CuIDS^{2-}$ will predominate. No other complexes i.e. $CuH_3IDS$, $CuH_2IDS$, CuHIDS could be observed, showing that an overall complexation of $Cu^{2+}$ takes place and exist predominantly as the CuIDS species. The varying of [$CuIDS^{2-}$] over the pH range also show the $CuIDS^{2-}$ complex is labile. The lability of the complex can be determined from the increase in the concentration of the CuIDS peak area with pH. This can be seen in figure 5.17 that between pH 3.3 and 7.2, CuIDS is the main predominant species.

Figure 5.18: Graph of pH vs log peak area of CrIDS

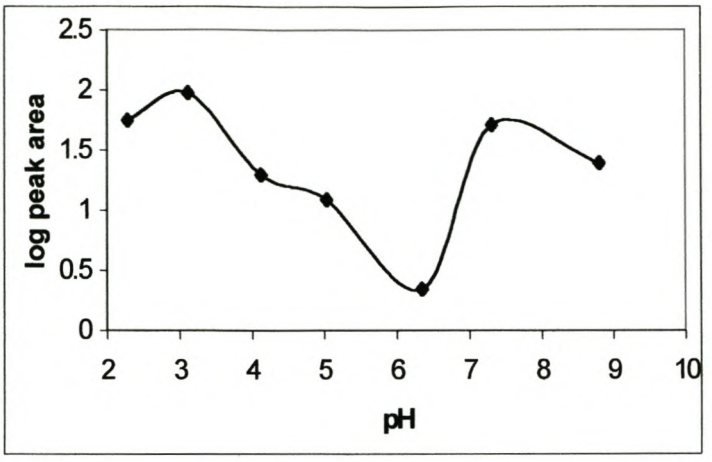


As the pH increases, the CrIDS complex starts to form as the main species at pH 2-3. A variation of [CrIDS] in the above figure is observed. This might be due to the stability constant of Cr with IDS of 9.3, which shows that Cr does not react strongly with IDS.

Figure 5.19: Graph of pH vs log peak area of FeIDS

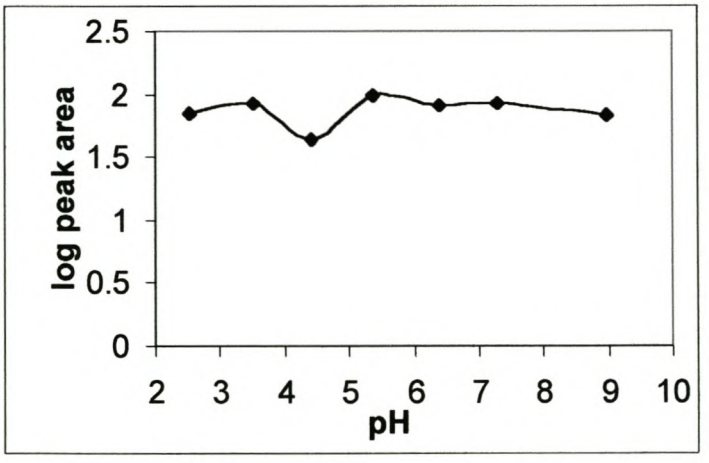


A similar behaviour is observed for FeIDS complexes.

Figure 5.20: Graph of pH vs log peak area of MnIDS

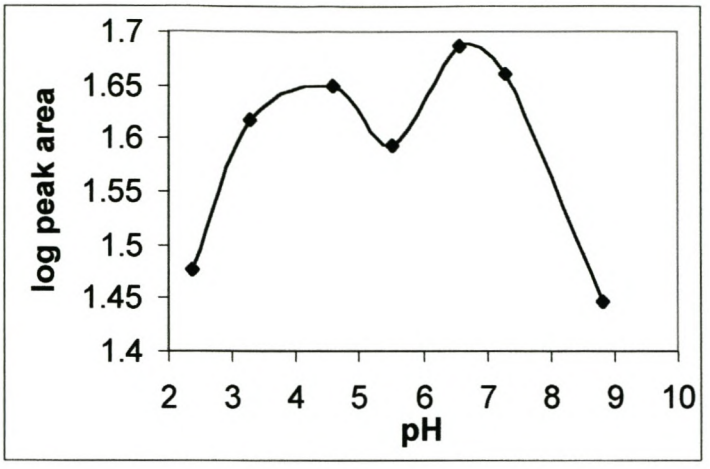


MnIDS complex exists at pH 2-4.8, as the predominant species. The formation of other species present is evident by a decrease in $[MnIDS^{2-}]$ within a pH range of 6.8-9.

Figure 5.21: Graph of pH vs log peak area of PbIDS

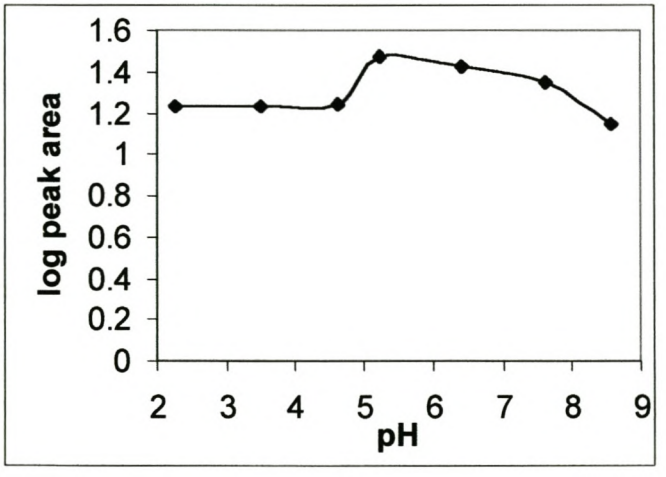

The behaviour of Pb with IDS is shown in figure 5.21. The PbIDS complex exists between the pH of 4.8 and 6.3. The decrease in the concentration of PbIDS might be due to the hydroxy species present in the solution. Speciation of curve of PbIDS (figure 3.22) agrees with the later information mentioned.

Figure 5.22: Graph of pH vs log peak area of ZnIDS

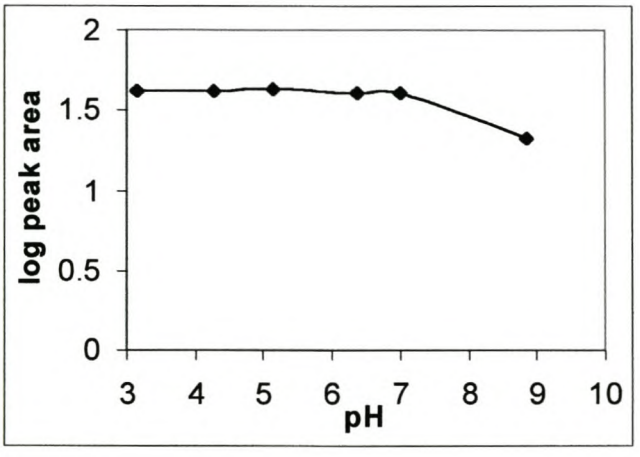


From the formation constant of ZnIDS, it is expected that Zn would complex more readily. In aqueous environment, the interaction of a metal with a ligand is competing with many reactions since other metal ligands (e.g. protons and hydroxide species) are all present. The ML is stable until pH 7.2 and then decreases afterwards. A decrease in the ZnIDS complex might be due to the formation of hydroxy species. This was seen in the speciation diagram of ZnIDS (figure 3.22).

## 5.3.2 Complexation of metals in excess of IDS

Figure 5.23 and 5.31 shows the electropherograms of CuIDS and PbIDS in the presence of excess IDS. The metal-IDS complexes were in a 1:3 ratio. Four peaks were observed when excess IDS complexes with Cu ion. The first and second peaks are known, i.e. the nitrate and metal-ligand peaks. In this case the metal-ligand peak is higher than the CdIDS on a 1:1 basis (see figure 5.17). The third peak and the fourth peaks might be due to other species present in the solution (i.e. hydroxide, IDS and ML proton species) as seen in the speciation graph of PbIDS. As the pH was decrease by the addition of HCl, the $Cl^-$ peak was evident. This was also seen as in a 1:1 ratio of CuIDS.

Figure 5.23: Electropherogram of CuIDS in a 1: 3 at pH = 9.567

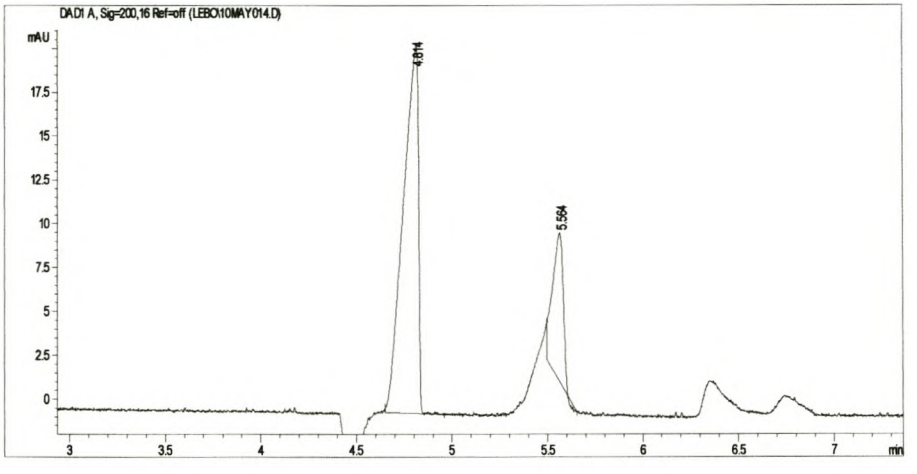

Figure 5.24: Electropherogram of CuIDS at pH = 8.496

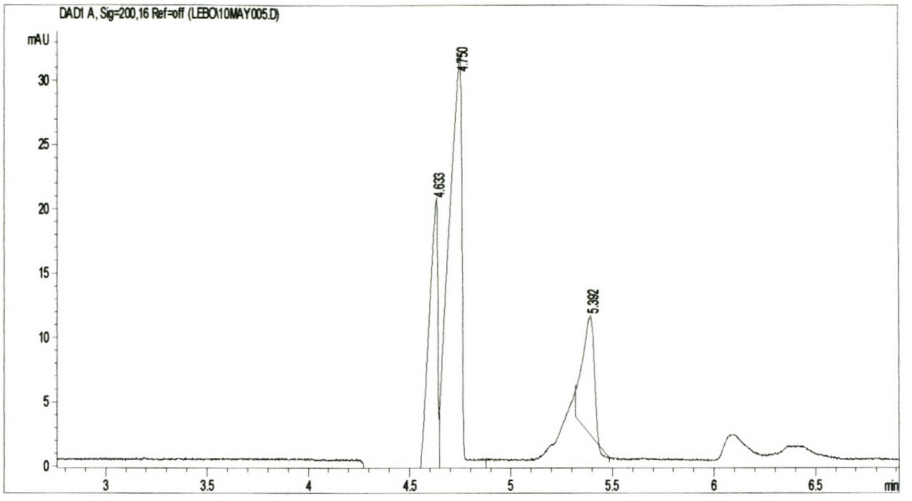


Figure 5.25: Electropherogram of CuIDS at pH = 7.404

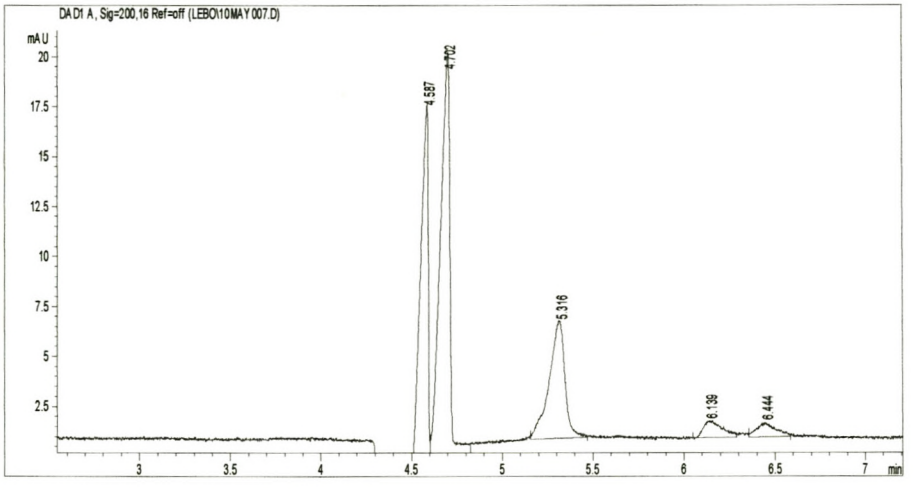

Figure 5.26: Electropherogram of CuIDS at pH = 6.346

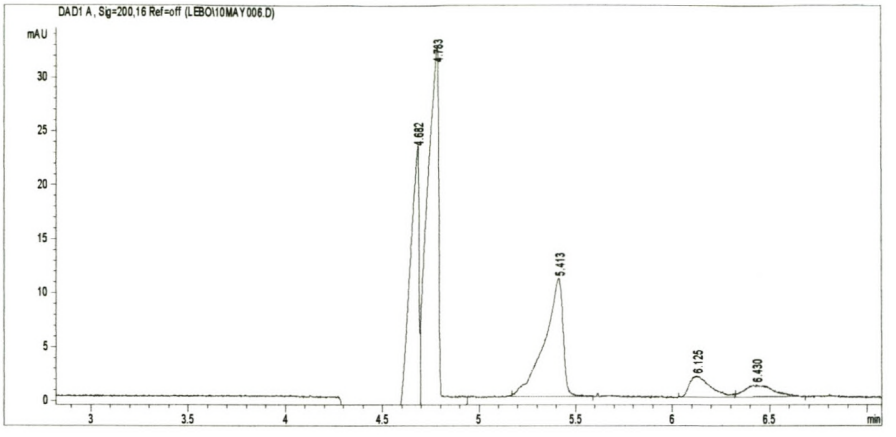


Figure 5.27: Electropherogram of CuIDS at pH = 5.086

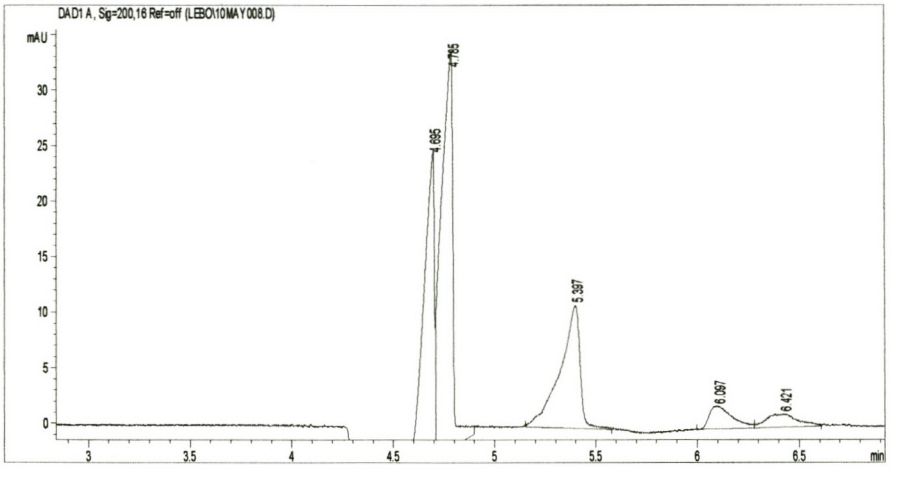

Figure 5.28: Electropherogram of CuIDS at pH = 4.685

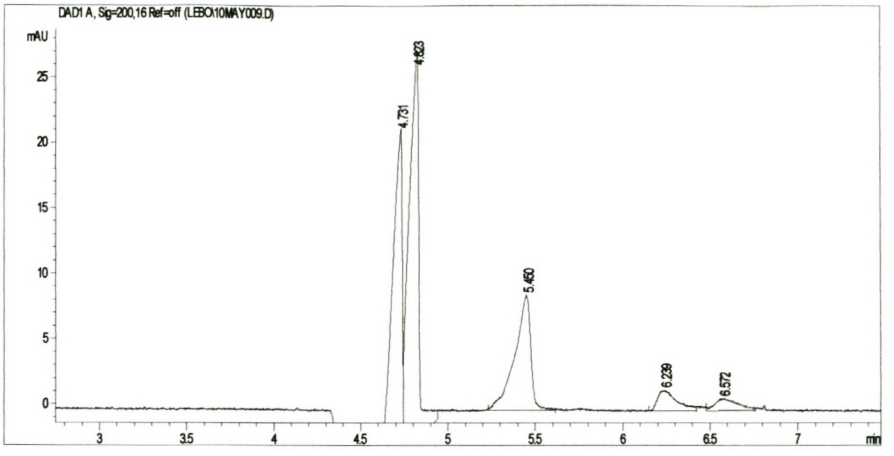


Figure 5.29: Electropherogram of CuIDS at pH = 3.601

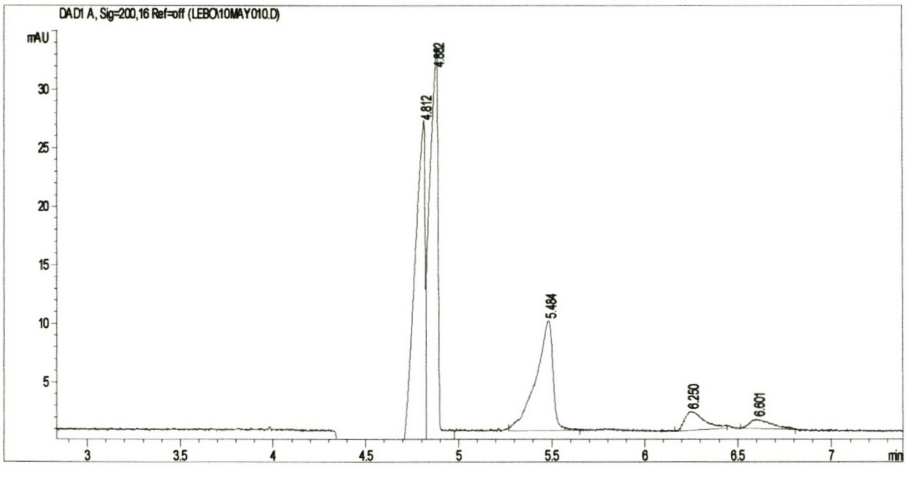

Figure 5.30: Electropherogram of CuIDS at pH = 2.545

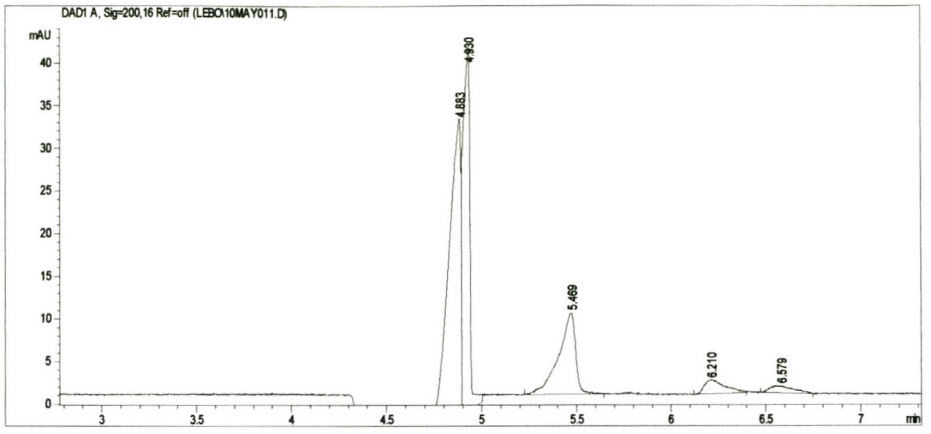


Figure 5.31: Electropherogram of PbIDS at pH = 9.700

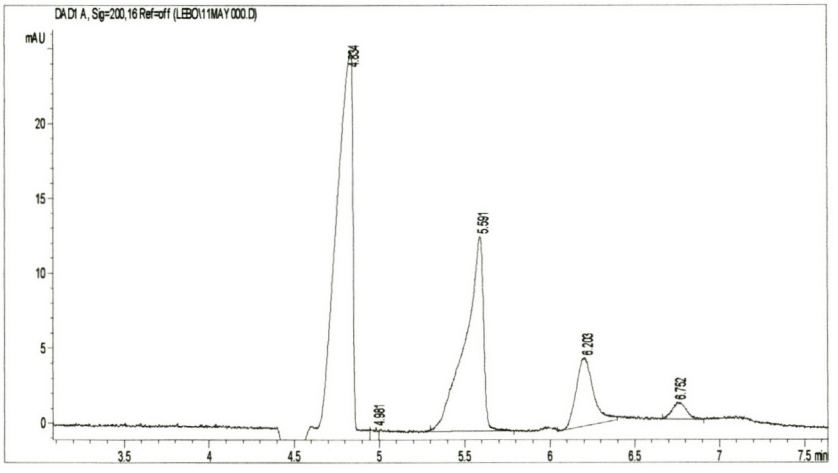

Figure 5.32: Electropherogram of PbIDS at pH = 8.402

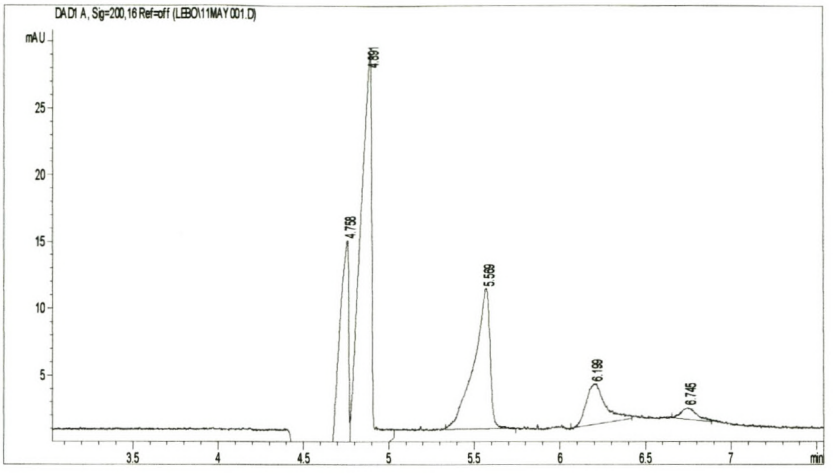


Figure 5.33: Electropherogram of PbIDS at pH = 7.583

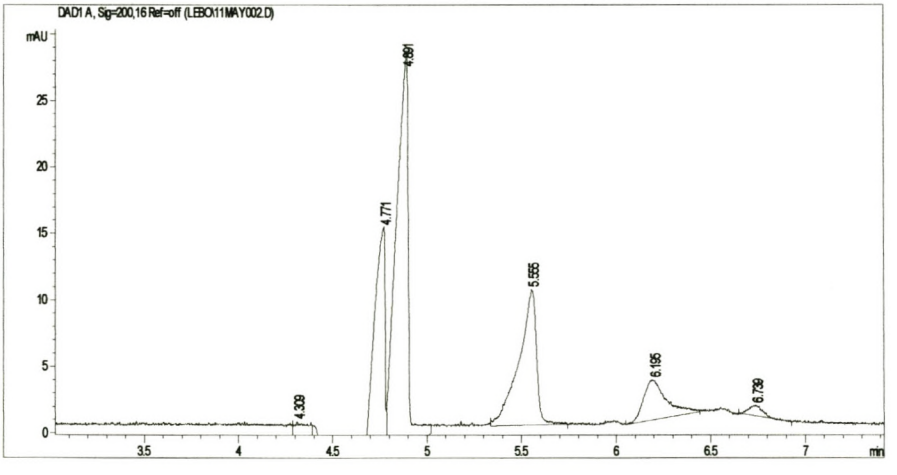

Figure 5.34: Electropherogram of PbIDS at pH = 6.128

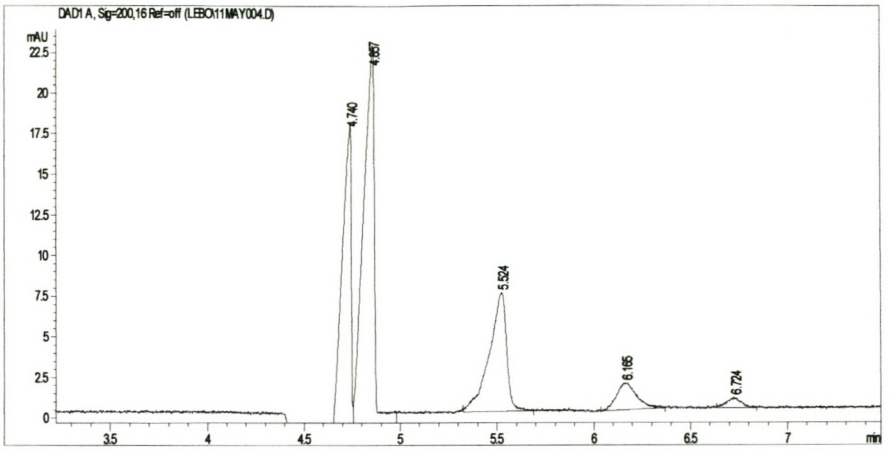


Figure 5.35: Electropherogram of PbIDS at pH = 5.262

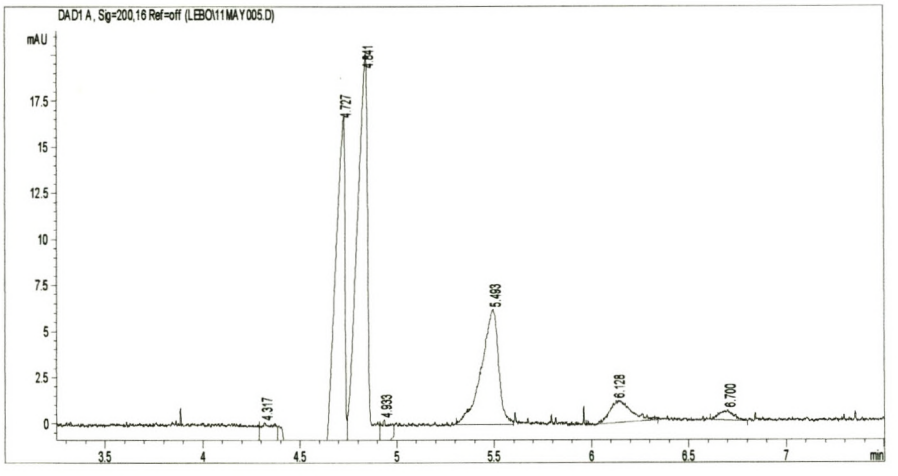

Figure 5.36: Electropherogram of PbIDS at pH = 4.495

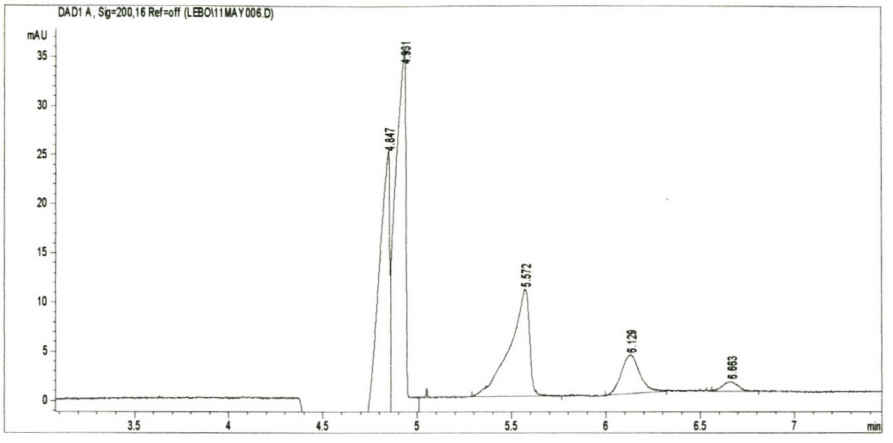


Figure 5.37: Electropherogram of PbIDS at pH = 3.651

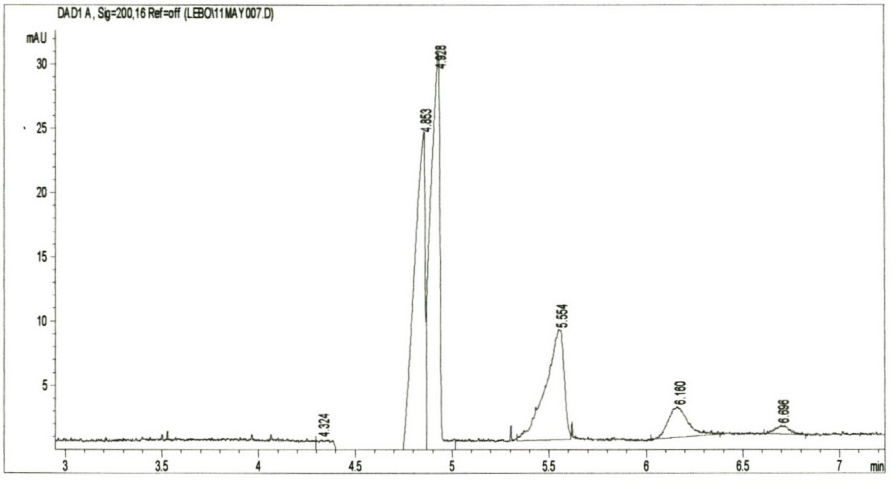

Figure 5.38: Electropherogram of PbIDS at pH = 2.545

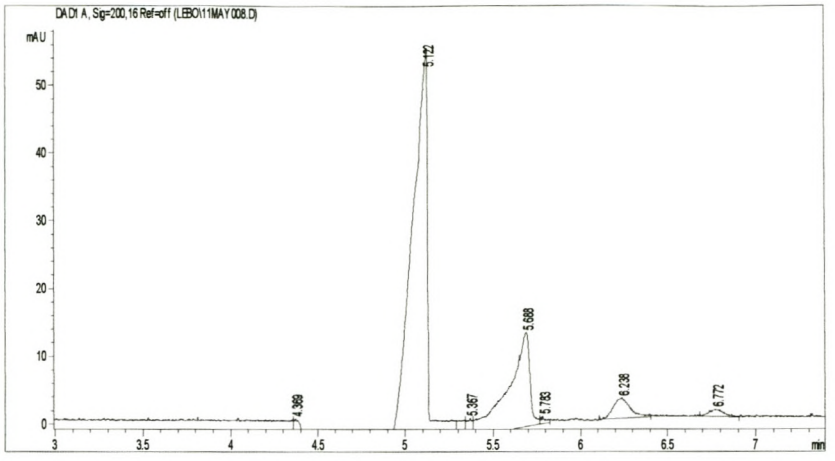


The plots of pH vs log peak area were constructed to predict the effect of pH for CuIDS and PbIDS. This can be seen in figure 5.39 and 5.40

Figure 5.39: Graph of pH vs log peak area of CuIDS

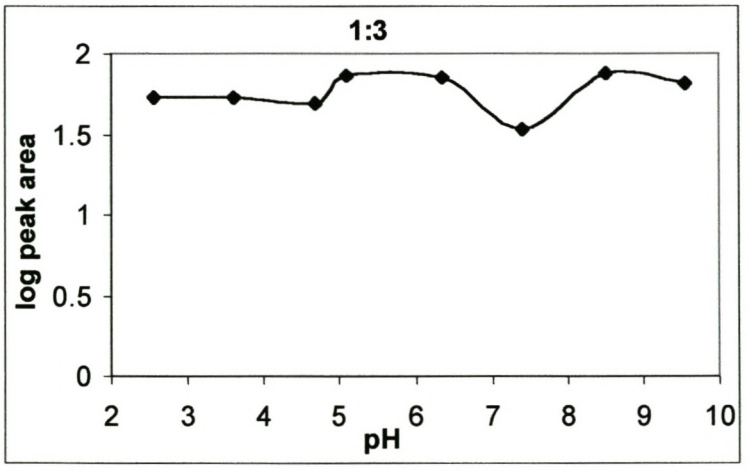

In the presence of the excess ligand, CuIDS showed a more stabilised behaviour compared to the 1:1 basis (figure 5.17) i.e. between pH 2 and 5. The ligand affected the equilibrium of the chelate formation. From pH 4.8 to 6.2 there is an increase in [CuIDS], which shows that the main species exist.

Figure 5.40: Graph of pH vs log peak area of PbIDS

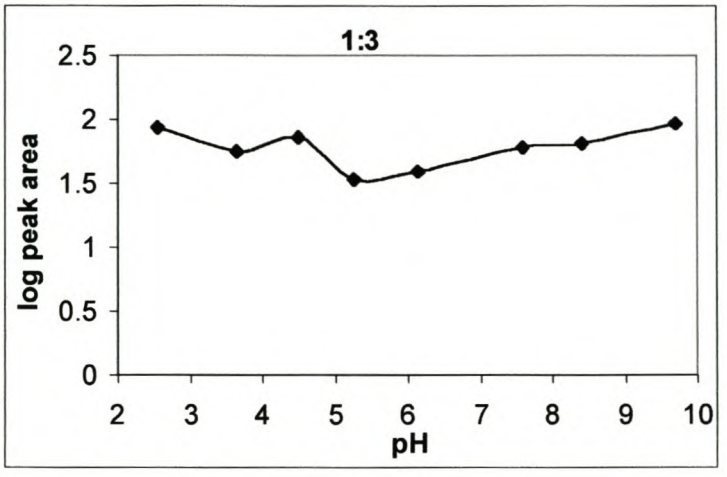


When excess IDS was added to Pb ion, the equilibrium favoured the formation of the PbIDS complex. This is can be seen by an increase in the [PbIDS] between the pH of 5 to 9.8. The concentration of PbIDS for a 1:1 ratio was found to be more labile than the 1:3 basis.

### 5.3.3 Separation of metal-PASP complexes

The CZE (anionic separation mode) was also used for the metal-PASP complexes, since they possess a negative net charge. The complexes were studied in a 1:1 ratio. The

chelates absorb at the wavelength of 200nm. CE showed a separation of only CdPASP and FePASP.

An electropherogram of CdPASP is shown in figure 5.41. The same two peaks were seen for CdPASP as in metal-IDS complexes, i.e. where the first peak is the nitrate peak and the second is metal-ligand. In the case of metal-PASP complexes, as the pH was decreased with HCl, the metal-ligand peak became broader. This caused a breakdown of the current. PASP is a polymer compared to IDS. It is difficult for the metal ions to be complexed with PASP because of their low stability constant. The interaction between metals and PASP is slow; thus broad separated peaks for ML were seen. This could also be due to the agglomeration of the polymer on protonation at low pH.

Figure 5.41: Electropherogram of CdPASP at pH = 8.922

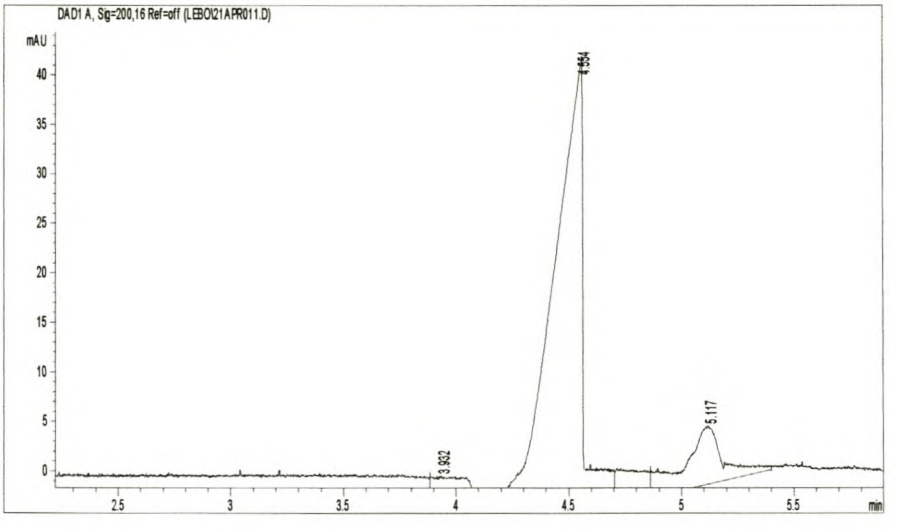

Figure 5.42: Electropherogram of CdPASP at pH = 3.388

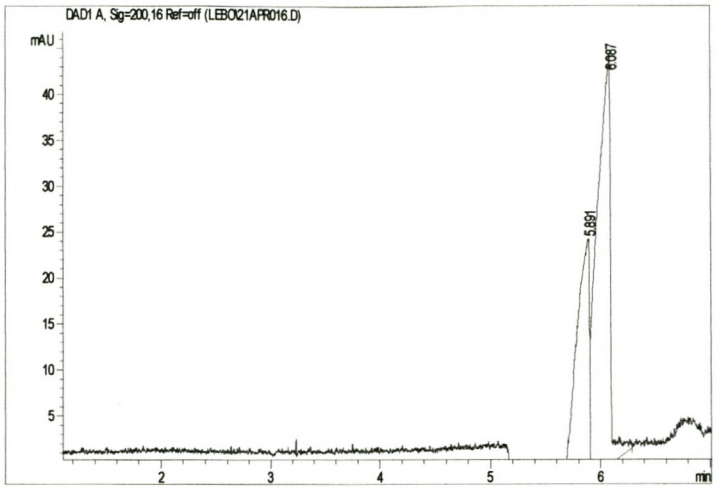


Figure 5.43 shows the electropherogram of FePASP. The same peaks were observed as in the latter complex.

Figure 5.43: Electropherogram of FePASP at pH = 8.758

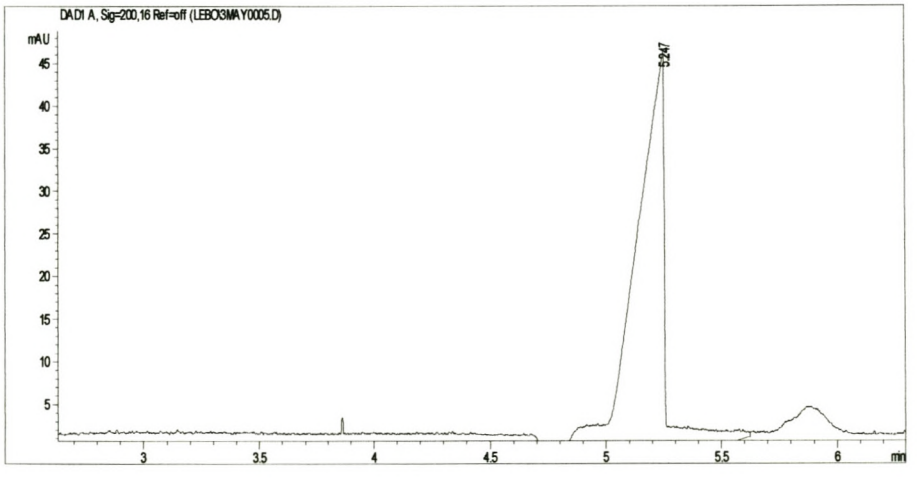

Figure 5.44: Electropherogram of FePASP at pH = 4.549

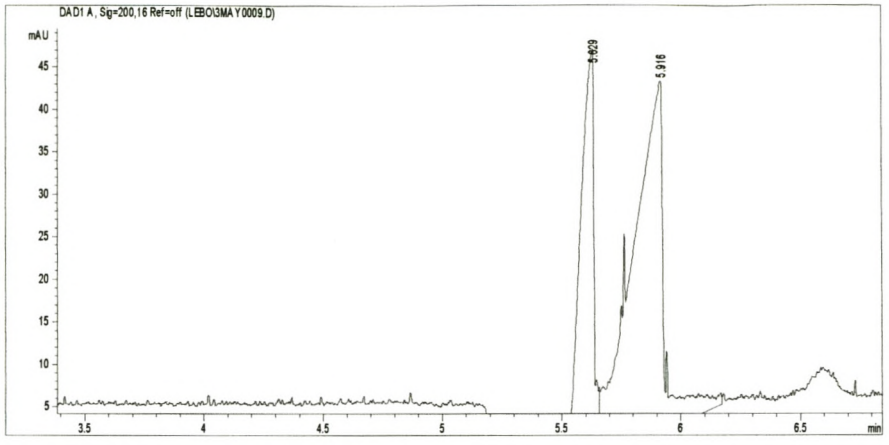


The plots of pH vs log peak area were constructed to predict the effect of pH for CdPASP and FePASP.

Figure 5.45: Graph of pH vs log peak area of CdPASP

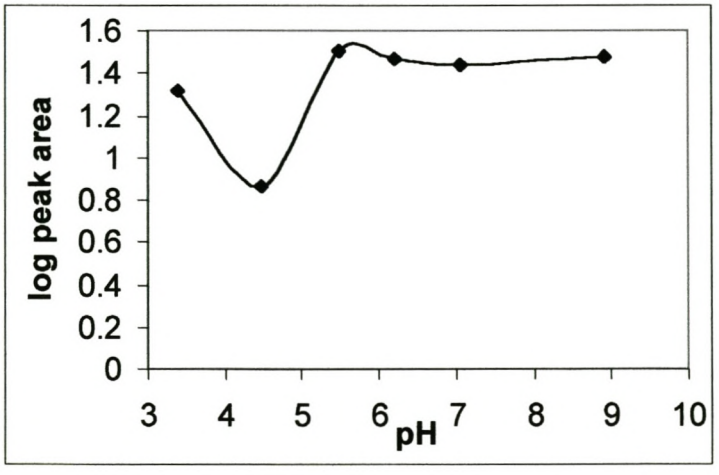

The above figure shows that [CdPASP] is constant between pH 5.5 to 9 and forms the predominant species. CdPASP show a higher stability than the CdIDS complex, even though it has the lowest stability constant.

Figure 5.46: Graph of pH vs log peak area of FePASP

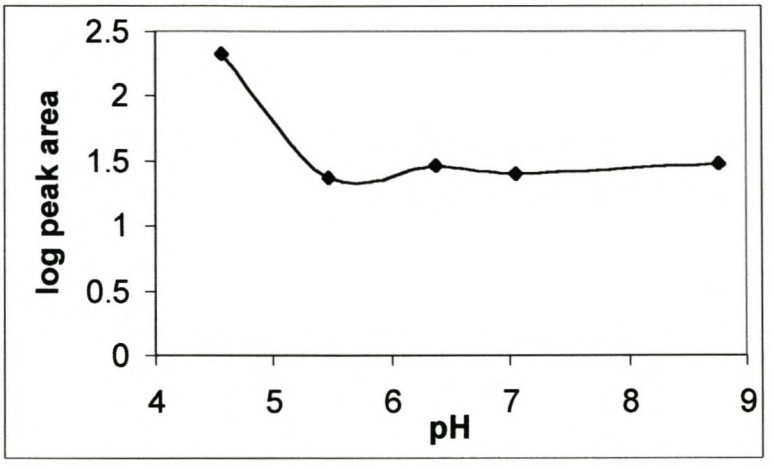


PASP has a high stability constant with Fe ions. This implies that iron would complex more readily with PASP, thus the stabilization observed in figure 5.46.

### 5.3.4 Separation of a mixture of metal ions with IDS

An electropherogram, which demonstrates the separation of a mixture of seven metal ions as complexes (i.e. Cd, Cu, Cr, Fe, Pb, Mn and Zn) with excess IDS, is shown in figure 5.47.

Figure 5.47: Electropherogram of metals with IDS + marker at pH 9.729(200nm)

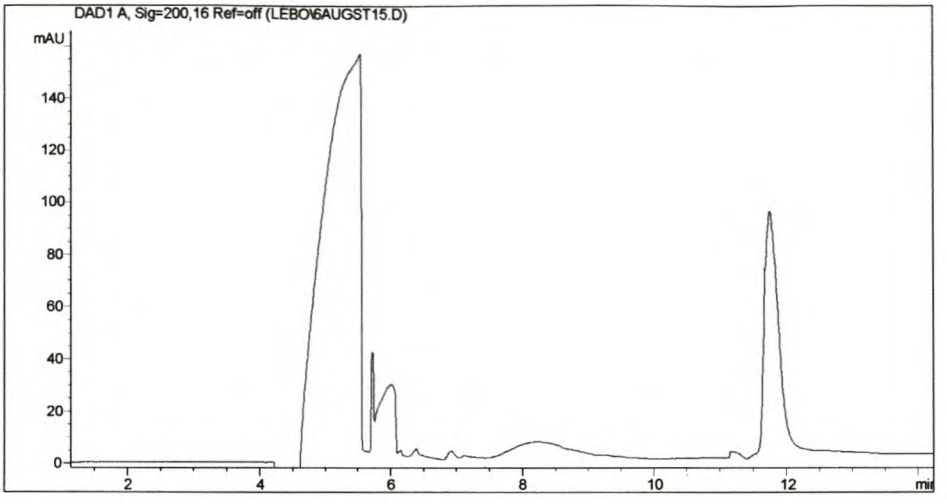


It was not possible to separate all of the metal-IDS complexes at a high pH of 9.729. An alternative reason is the broadening of the peak resulting from adsorption of the complex to the capillary wall [81]. Separation of these complex species could possibly be achieved using a longer capillary. However, none of these options were investigated because our primary concern was initially to distinguish between free and complexed ligand.

The separation of a group of metal-IDS complexes showed to elute before the marker peak (11.770 min). Metal-IDS chelates have the migration behaviour that generally follows the charge number and the mass of the chelate. That is, metal-IDS complexes with higher charge show significantly shorter migration times. The complexation of metals with IDS results in the competition with many other reactions since other metal ions and ligands (e.g. protons and hydroxide species) are all present. The free hydroxy groups in the metal complexes might affect the migration behaviour because the hydroxy

groups interact with the ionized silanol groups on the capillary wall. This will lead to broader peaks as evident in figure 5.47. The other reason of poor peak shapes is due to slow complexation equilibria in the capillary [82]. Therefore the expected separation of complexes was not observed, even though most of the highly charged complexes migrated faster. The separation of these species can be achieved by using a greater length and changing the wavelength and the applied voltage [83].

Table 5.1 lists the migration times ($t_m$) of the MIDS chelates.

Table 5.1: Migration times of metal-IDS chelates

| Metal-IDS | $t_m$ (minutes) |
|---|---|
| Zn | 3.638 |
| Mn | 3.793 |
| Cd | 4.188 |
| Pb | 4.326 |
| Cu | 4.567 |
| Cr | 4.665 |
| Fe | 5.058 |

The migration behaviour of the metal-IDS complexes was investigated and the order of elution was as follows: Zn ≈ Mn < Cd ≈ Pb < Cu < Cr< Fe. This is shown in the table above. The largest peak might correspond to nitrate, MnIDS and ZnIDS. This was evident in all the electropherograms for all the metals with IDS obtained. The second and

third peaks are due to CdIDS and FeIDS. CuIDS, CrIDS PbIDS and $IDS^{4-}$ can be assigned to the fourth broad peak.

From the electropherogram (figure 5.47) it is shown that Cu, Cr and Pb with IDS are eluted as one peak (fourth peak), preceded by a much smaller peak corresponding to the $FeIDS^-$complex. The same trend was also observed for EDTA with the metals (Cu, Pb, Cr and Fe) except for the three metals were well separated. The chelating complexes for EDTA showed the following order of mobility: $CuEDTA^{2-}$>$PbEDTA^{2-}$>$CrEDTA^-$ >$FeEDTA^-$[83].

## 5.4 CONCLUSIONS

The applicability of CE as a useful tool for the analysis of ML complexes is demonstrated. This work demonstrated that CE provides fast and fairly efficient method for the separation of metal chelates of IDS and PASP, which absorb in the UV range. The simplicity and small sample volume requirements make it advantageous to other chromatographic techniques. CZE is a technique complementary to the HPLC of metal ions, due to its different selectivity.

Common inorganic anions such as $NO_3^-$, $NO_2^-$, $Br^-$ and $Cl^-$ show higher mobilities, compared to most of metal-chelate complexes that show lower mobilities [84]. The expected order of separation was seen i.e. Cu, Cd and Zn migrate faster than Cr, Pb and Fe because of their small atomic size. This was also observed in the metal-EDTA

chelates in different electrolyte systems. When the pH is decreased the nitrate peak increases and becomes broader. This was seen because at low pH, metal is the predominant species.

It was shown that it is possible to separate the metal-ligand chelates using CE. The obtained results from CE were proved and compared with speciation models predicted by the JESS program. A reasonable agreement between the data obtained from the speciation diagrams and the peaks of the electropherograms of metal-IDS complexes were observed. The CE for PASP with other metals shows poor broad peaks. This could be connected with slow complexation equilibria in the capillary.

Most of the MIDS complexes showed a highly labile behaviour. This behaviour is caused by the low stability constants of the complexes compared to EDDS and EDTA complexes (table 3.2). MEDTA chelates have much higher stability constant values than MIDS; thus their complexes are relatively inert.

# CHAPTER 6

## Evaluation and suggestions for further study

The utility of cyclic voltammetry for determining the complex stability constants of metal-ligand complexes was established. The results obtained from voltammetric analysis of $H_4$IDS and metal-IDS complexes were able to validate the predicted speciation models obtained using JESS. The speciation distribution diagrams were found to correlate well with the voltammetric $\Delta E$ vs pH curves, showing that this approach is useful for labile complexes at low pH. The speciation and complex stability constants associated with a ligand and its metal ion complexes are responsible for determining the possible application of these sequestering agents.

The CV of some of the metals with aspartic acid and polyaspartic acid was studied. The complex stability values of PASP are much smaller than IDS and ASP except for Fe. This is because PASP is a polymeric ligand and it binds in different ratios to the metal ions, whereas IDS has a specific binding mode to the metal ions. Polyaspartic acid exhibit high stability constants with Fe ions and this effect is especially favourable when using polyaspartic acid as dispersant in detergents

CE showed the possibility to separate cations and metal-ligand chelates using CE. The obtained results were validated with the speciation diagrams obtained from JESS. A good correlation between the data obtained from the speciation and the peaks of the

electropherograms of metal-IDS complexes were observed. Unresolved broader peaks were observed when the CE was run for PASP with other metals, and this could be attributed to slow complexation equilibria in the capillary.

A further investigation is needed to improve the separation efficiencies of the metal-ligand chelates. The separation of metal ligand complexes using other separation techniques like HPLC and MS is also necessary. The rate of photodegradation of IDS and PASP would be studied.

# REFERENCES


1. Robinson. J. W, Rhodes. I. A. L, ***Spectroscopy***, 1980, 13 (2 and 3), 93-116.
2. Antonio. B, et al, ***Anal Chem***, 1993, 65, 3137-3142.
3. Dabek-Zlotorzynska. E, et al, ***Anal Chim Acta***, 1998, 359, 1-26.
4. Heiger. D. N, ***High performance Capillary Electrophoresis***, Hewlett Packard Company, 1992, 3rd edition, Printed in France.
5. Van Leeuwen. H. P, Buffle. J, ***J.Electroanal.Chem***, 1990, 296, 359-370.
6. Hatland. S. M. I, Radzuk. B, Tomassen. Y, ***Anal.Sci***, 1991, 7, 1029.
7. Jianguo. C, Chakrabrti. C. L, Back. M. H, Schoroender. W. H, ***Anal Chim Acta***, 1994, 288, 141-156.
8. Merian. E, ***Metals and their compounds in the environments***, VCH, Weinheim, 1991.
9. Florence. T. M, ***Talanta***, 1982, 29, 345.
10. Sirover. M. A, Loeb. L. A, ***Science***, 1976, 194, 1434.
11. Ebbing, ***General chemistry***, 4th edition, Houghton Mifflin Company, 1993, 981-983.
12. Basset. J., Denney. R. C, ***Vogel's textbook of quantitative inorganic analysis***, 4th Edition, Inc, New York, London, 1978.
13. Hart. J. R, ***J.Chem.Educ***, 1984, 61, 1060.
14. Hart. J. R, ***J.Chem.Educ***, 1985, 62, 75.
15. Vema. P. S, Saxena. R. C, Jayaraman. A, ***Fresenius J.Anal.Chem***, 1997, 357, 56-60.
16. Harrison. P.G, Healy. M.A, Steel. A.T, ***Inogarnica Chim.Acta***, 1982, 67, L15-L16.
17. Sillanpaa. M, Sihvonen. M, ***Talanta***, 1997, 44, 1487-1497.

18. Crouch. A. M, Polhuis. M, ***J.Molecular Structure***, 2000, 530, 171-176.

19. ***Technical Bulletin***, 23, The Associated Octel Company Limited, Performance Chemicals Group.

20. Loonen. H, et al, ***Environ.Toxic and Chem***, 1999, 18(8), 1763-1768.

21. Williams. D. R, Crouch. A. M, Polhuis. M, Khotseng. L. E, ***To be published***.

22. Mashihara. M, Ando. T, Murase. I, ***Bulletin of the Chemical Society of Japan***, 1973, 46, 844-847.

23. PASP, "A new biologically degradable dispersant", ***Product Information Brochure***, Bayer (Germany). Information Brochure, Bayer (Germany).

24. IDS, "A new biologically degradable dispersant", ***Product Information Brochure***, Bayer (Germany).

25. Inczedy. J, ***Analytical applications of complex equilibria***, Ellis Horwood Limited, Chinchester, 1976.

26. Christensen. J. M, ***Sci.Total Environ***, 1995, 166, 89-135.

27. Esteban. M, et al, ***Anal Chim Acta***, 1994, 285, 193-208.

28. Baoxin. Y, Shuxun. Y, ***Talanta***, 1994, 41, 537-540.

29. Sander. S, Steiner. B, ***Electrochemical Seminar*** (Metrohm, Swiss Lab), May 2000.

30. Florence. T. M, ***Analyst***, May 1986, Vol. 111.

31. Adeloju. S. B, Bond. A. M, ***Anal Chim Acta***, 1983, 55, 184.

32. Cheng. J. et al, ***Anal Chim Acta***, 1994, 288, 141-156.

33. Hirose K, ***Anal Chim Acta***, 1994, 284, 621-634.

34. Apostoli. P., ***Fresenius J.Anal Chem***, 1999, 363, 499-504.

35. Szpunar. J, Lobinski. R., ***Fresenius J.Anal Chem***, 1999, 363, 550-557.

36. Ozaki. S, Ichimura. T, ***Arch Toxicol***, 1993, 67, 268-276.

37. Williams. D. R, ***Coordination Chemistry Reviews***, 1999, 185-186, 177-188.

38. Williams. D. R, ***Chem Br***, 1998, 48-50.

39. Williams. D.R, ***European Brewery Convention***, 6-10 June 1993, 24th International Congress.

40. Hill. S., ***Chemical Society Reviews***, 1997, 26, 291-298.

41. Timerbaev A.R, Talanta, 2000, 52, 573-606.

42. Xue. B, Sigg. L, ***Anal Chim Acta***, 1994, 284, 505-515.

43. Turoczy. N. J, Sherwood. J. E, ***Anal Chim Acta,*** 1997, 354, 15-21.

44. Khotseng. L, ***Master's thesis***, University of Stellenbosch, South Africa, 1999.

45. Crouch. A. M, et.al, ***Accepted for publication in Analytica Chimica Acta***, 2000, 16 March.

46. Lingane. J. J, ***J.Chem.Soc***, 1940, 1-35.

47. Cukrowski. I, et.al, ***Polyhedron***, 1995, 14, 1661.

48. May. P. M, ***Talanta***, 1991, 38(12), 1409-1417.

49. May. P. M, ***Talanta***, 1991, 38(12), 1419-1426.

50. May. P. M, ***Talanta***, 1991, 40(6), 819-825.

51. Crouch. A. M, Polhuis. M, Katata. L, ***To be submitted for publication***.

52. Sawyer. C. T, ***Experiments for Instrumental Method***, A Laboratory Manual, McGraw-Hill Book Co.

53. Nakato. T, et al, ***Pure Appl.Chem***, 1999, A36 (7 and 8), 949-961.

54. Suau, et al, ***United States Patent***, 7 Dec 1999, 5, 998.

55. Hayashi. T, Iwatsuki. M, ***Biopolymers***, 1990, 29, 549-557.

56. Pearson. R.G, ***Inorg.Chem***, 1972, 11, 3146.

57. Lee J.D, ***Concise Inorganic Chemistry***, Chapmann and Hall, London, 1994.

58. ***The Chemical Society***, Stability constants Supplement No.1, Special Publication 25, London, Burlington House, 1971.

59. ***The Chemical Society***, Stability constants, Organic ligands (Part 1), London, Burlington House, 1957.

60. ***The Chemical Society***, Stability constants Supplement No.1, Special Publication No.17, London, Burlington House, 1964.

61. Brown. P. R, et al, ***LC-GC INTL***, 5 (1), 20-26.

62. Tiselius. A, ***Trans.Faraday Soc.***, 1937, 33, 524.

63. Hjerten. S, ***Chromatogr.Rev***, 1967, 9, 122.

64. Jorgenson. J.W, Lucacz. K.D, ***Anal Chem***, 1981, 53, 1298-1302.

65. Goodall. D, et al, ***LC-GC***, 8 (8), 788-799.

66. Ying-Sing. F, Ho-Shan. T, ***Electrophoresis***, 1999, 20, 1832-1841.

67. ***Analytical Chemistry News and Features***, 1999, May 1.

68. Cassidy. L. W, Baranski. R. M, ***Journal of Chromatography***, 1993, 640, 433-440.

69. Gottlicher. B, Bachmann. K, ***Journal of Chromatography A***, 1997, 780, 63-73.

70. Szpunar-Lobinska, et al, ***Fresenius J Anal Chem***, 1995, 351, 351-377.

71. Skoog, ***Principles of instrumental analysis***, 1998, Holler, Nieman, Harcourt Brace college, 5th edition.

72. Tagliaro. F, et al, ***Journal of Chromatography B***, 1998, 713, 27-49.

73. Chang. C. A, et al, ***Journal of Chinese Chemical Society***, 1999, 46, 519-528.

74. Korhammer. S. A, Bernreuther. A, ***Fresenius J. Anal Chem***, 1996, 354, 131-135.

75. Poels. I and Nagels. L. J, ***Anal Chim Acta***, 1999, 401, 21-27.

76. Lin. B, et al, ***Clinical Applications of CE***, 27, 189-198, Humana Press Inc., Totowa, NJ.

77. Lu. W., Cassidy. R. M., Baranski A. S., ***Journal of Chromatography***, 1993, 640, 433-440.

78. Voegel. P. D., et al, ***Anal Chem***, 1997, 69, 951-957.

79. Gfroer. P, et al, ***Analytical Chemistry News and Features***, 1999, May 1, 315A-321A.

80. Padarauskas. A, Schwedt. G, ***Journal of Chromatography A***, 1997, 773, 351-360

81. Owens, et al, ***Environ.Sci.Technol***, 2000, 34, 885-891.

82. Pacakova. V, et al, ***Journal of Chromatography A***, 1999, 834, 257-275.

83. Baraj. B, et al, ***Journal of Chromatography A***, 1995, 695, 103-111.

84. Kuban. P, ***Journal of Chromatography A***, 1999, 836, 75-80

# Annexures

Figure 1: Cyclic voltammogram of PASP at pH = 10.31, T =21.5°C.

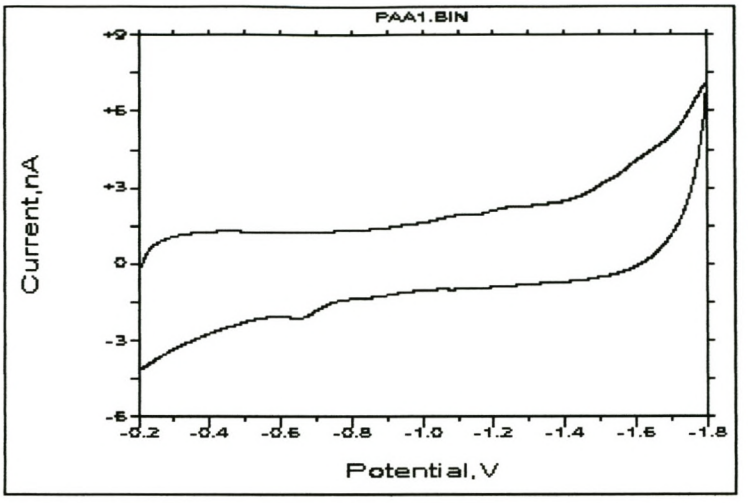


Figure 2: Electropherogram of CuIDS at pH = 9.365

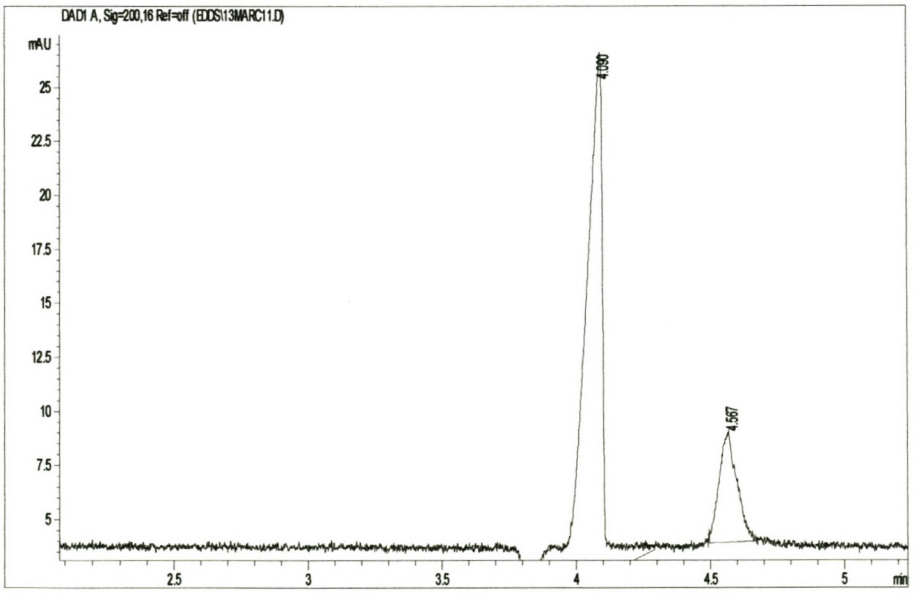

Figure 3: Electropherogram of CuIDS at pH = 8.233

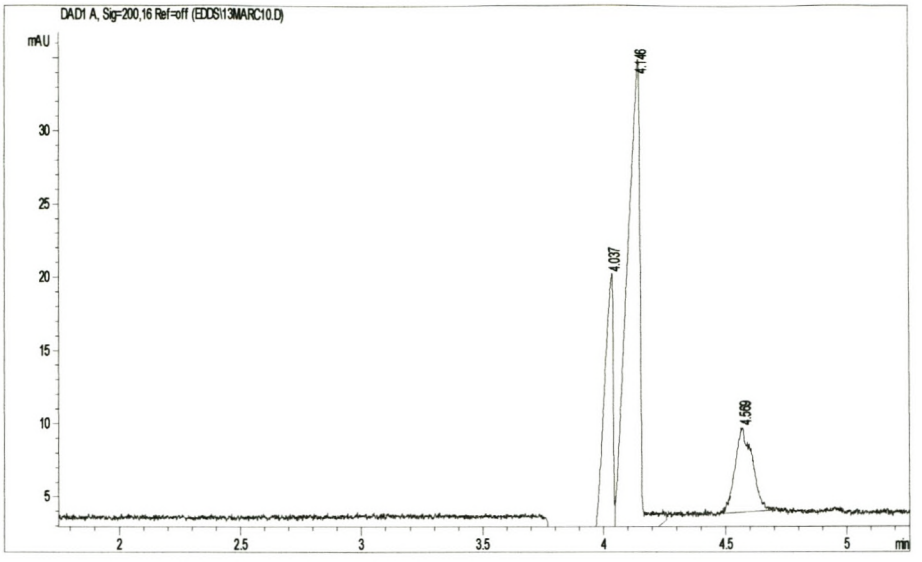


Figure 4: Electropherogram of CuIDS at pH = 7.244

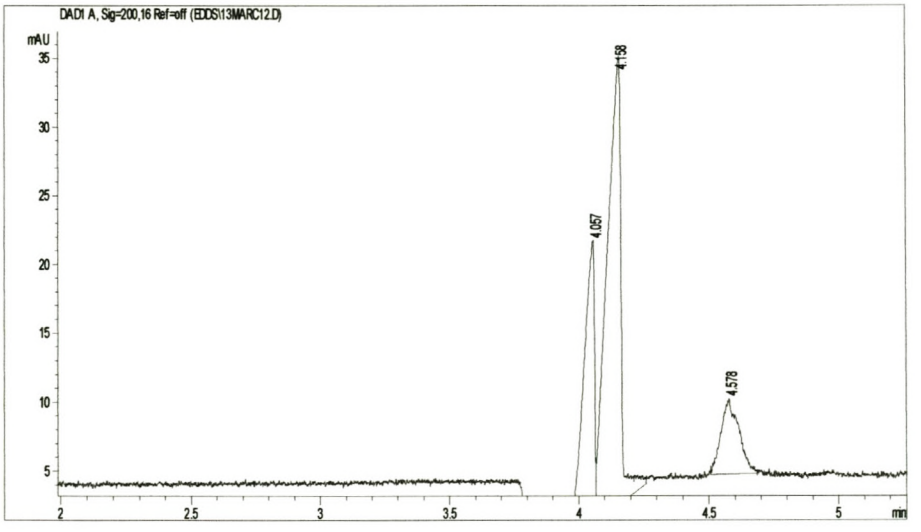

Figure 5: Electropherogram of CuIDS at pH = 6.449

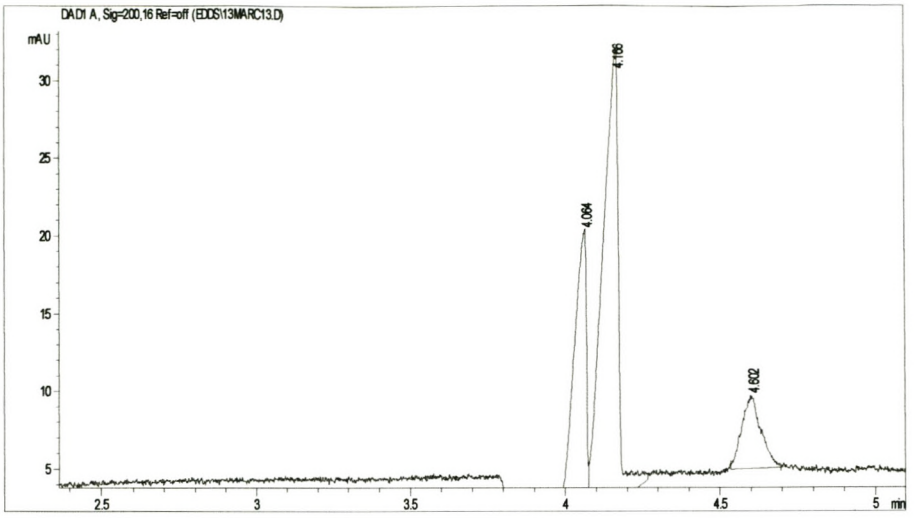


Figure 6: Electropherogram of CuIDS at pH = 5.015

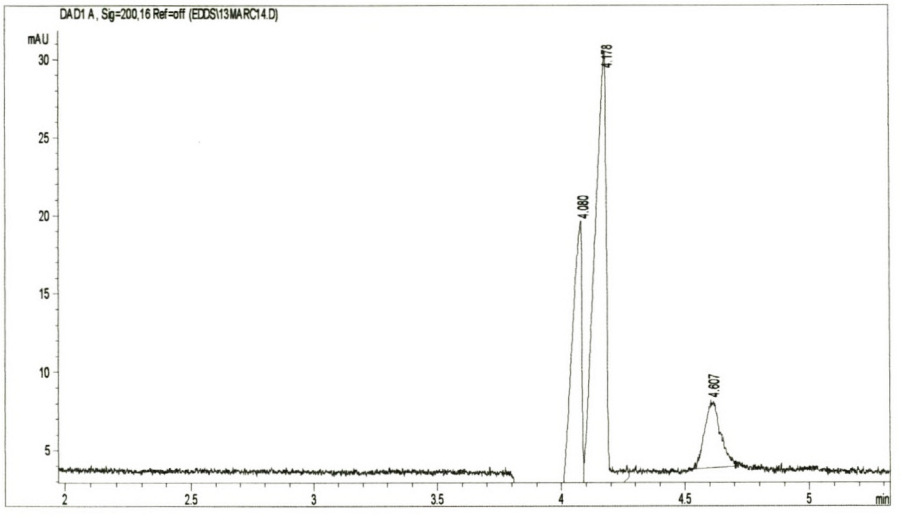

Figure 7: Electropherogram of CuIDS at pH = 4.331

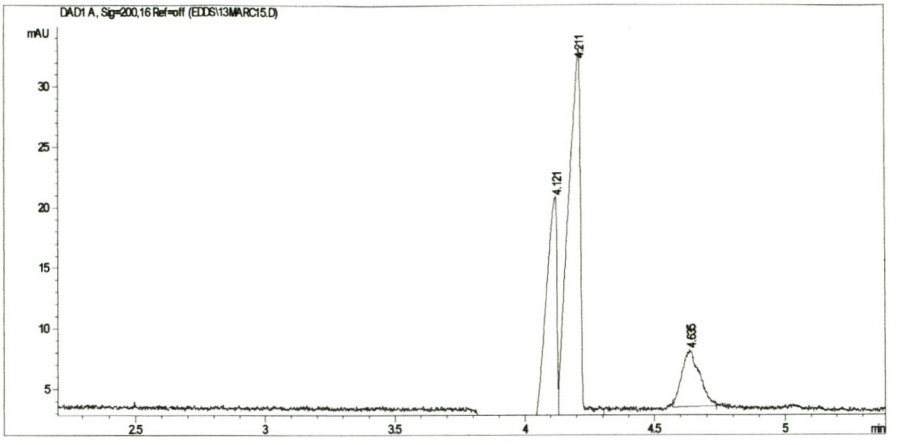


Figure 8: Electropherogram of CuIDS at pH = 3.227

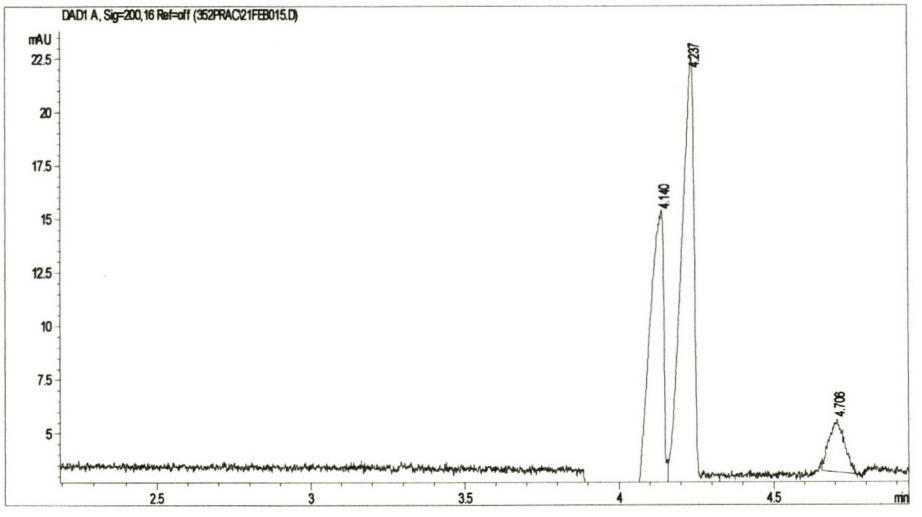

Figure 9: Electropherogram of CuIDS at pH = 2.223

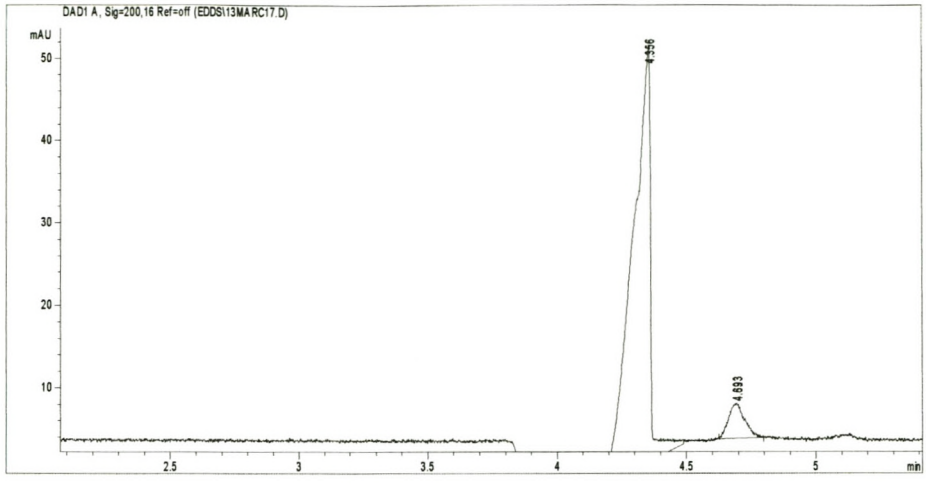


Figure 10: Electropherogram of Cr at pH = 8.513

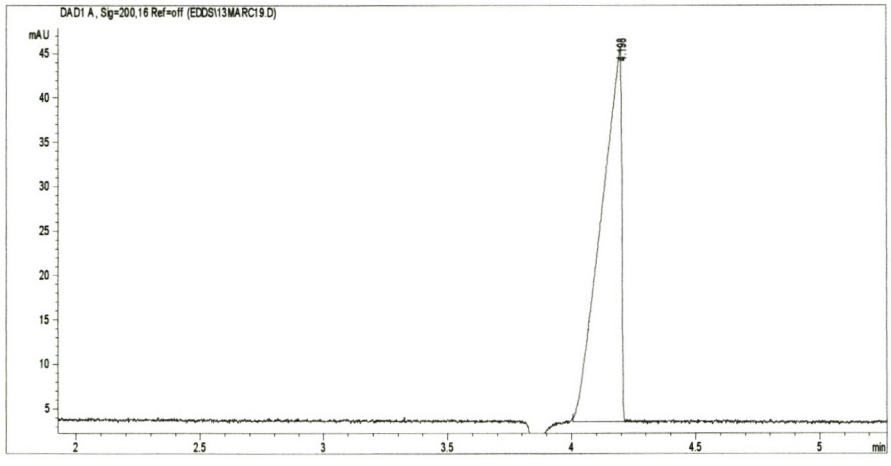

Figure 11: Electropherogram of CrIDS at pH = 8.801

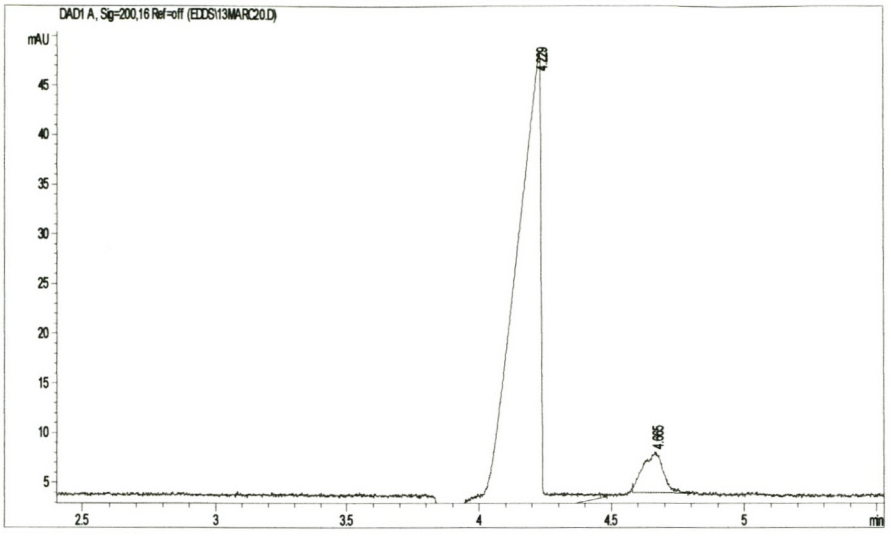


Figure 12: Electropherogram of CrIDS at pH = 7.310

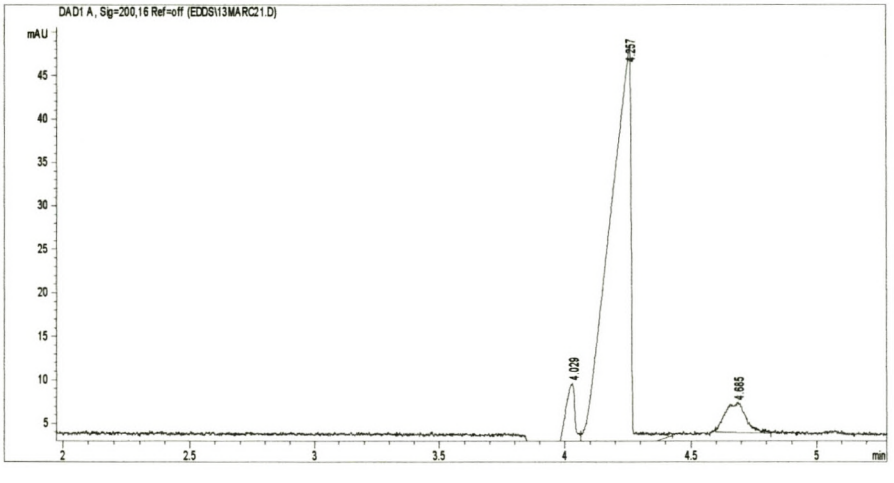

Figure 13: Electropherogram of CrIDS at pH = 6.341

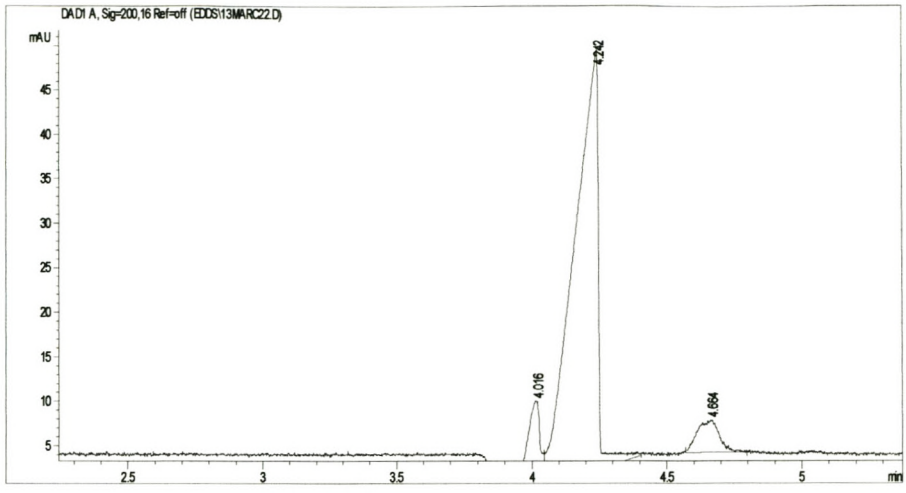


Figure 14: Electropherogram of CrIDS at pH = 5.029

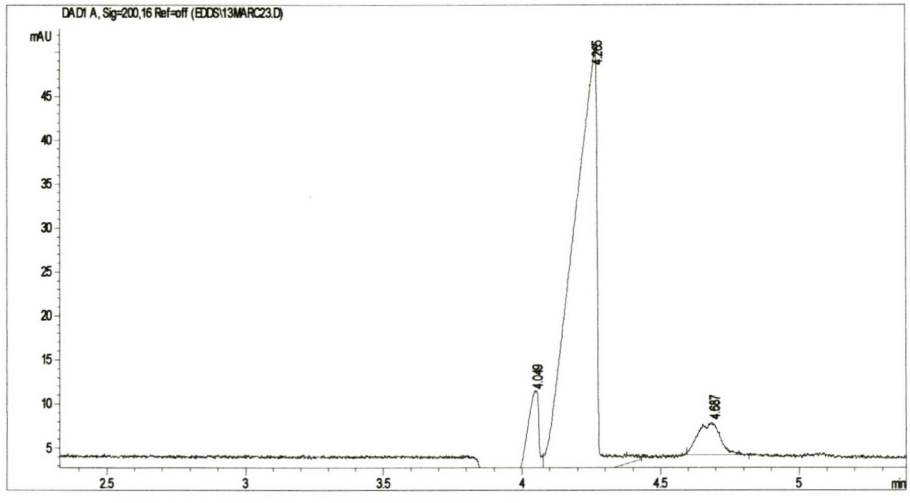

Figure 15: Electropherogram of CrIDS at pH = 4.120

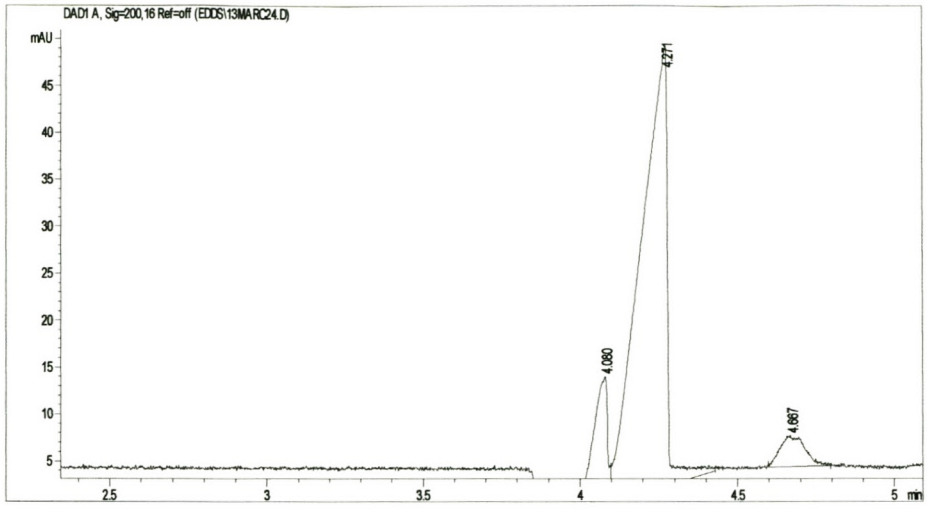


Figure 16: Electropherogram of CrIDS at pH = 3.113

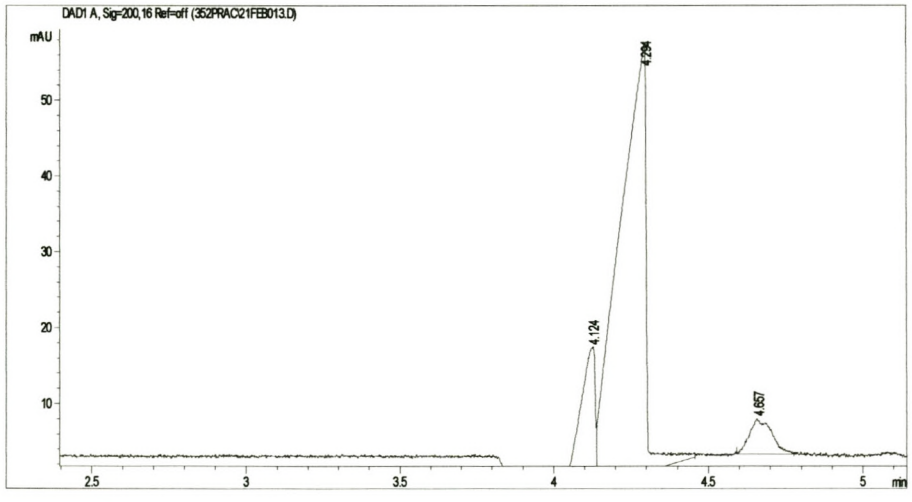

Figure 17: Electropherogram of CrIDS at pH = 2.278

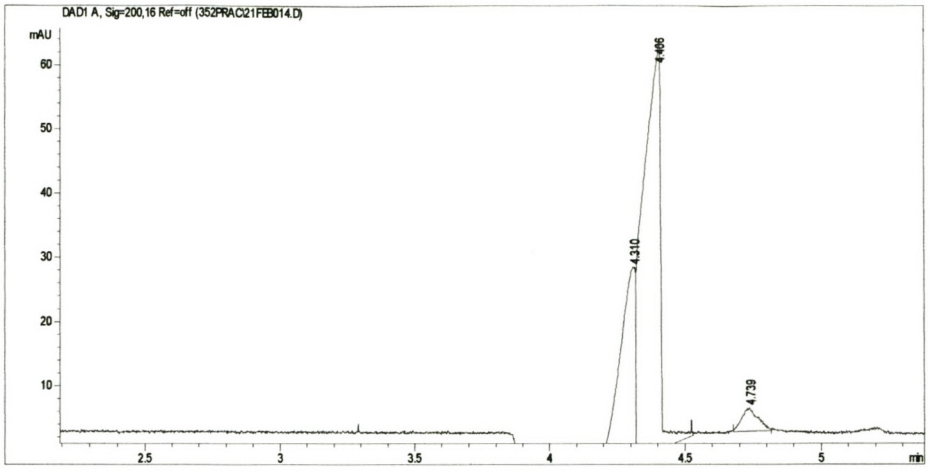


Figure 18: Electropherogram of Fe at pH = 8.547

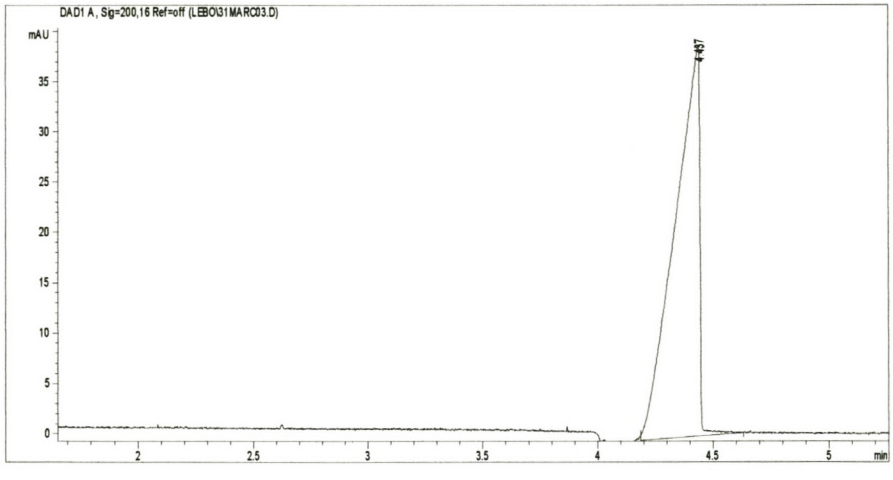

Figure 19: Electropherogram of FeIDS at pH = 8.991

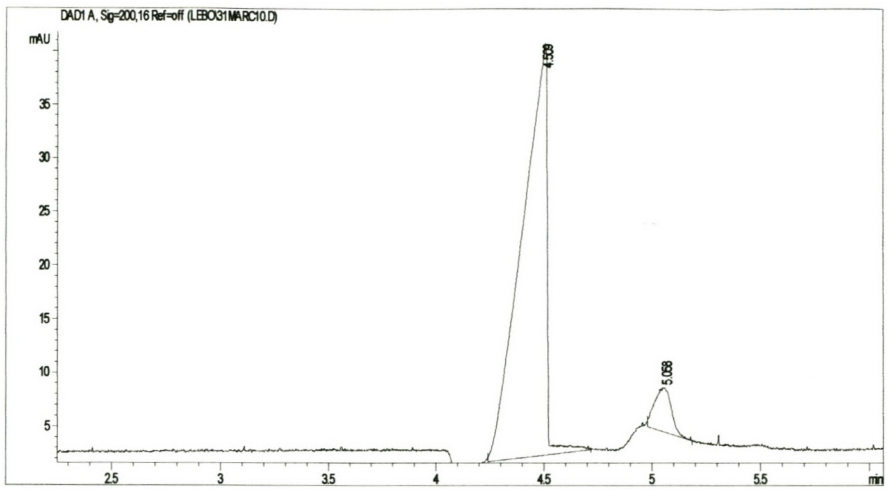


Figure 20: Electropherogram of FeIDS at pH = 7.282

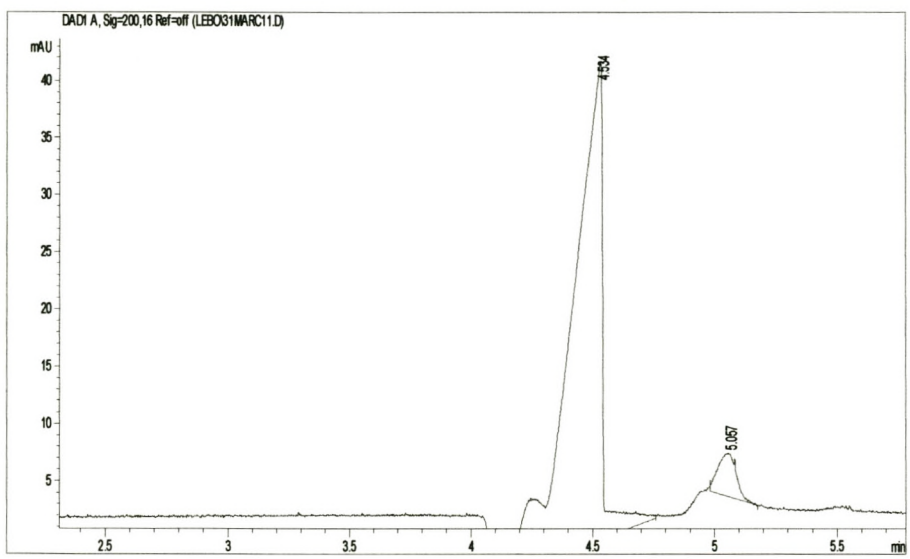

Figure 21: Electropherogram of FeIDS at pH = 6.379

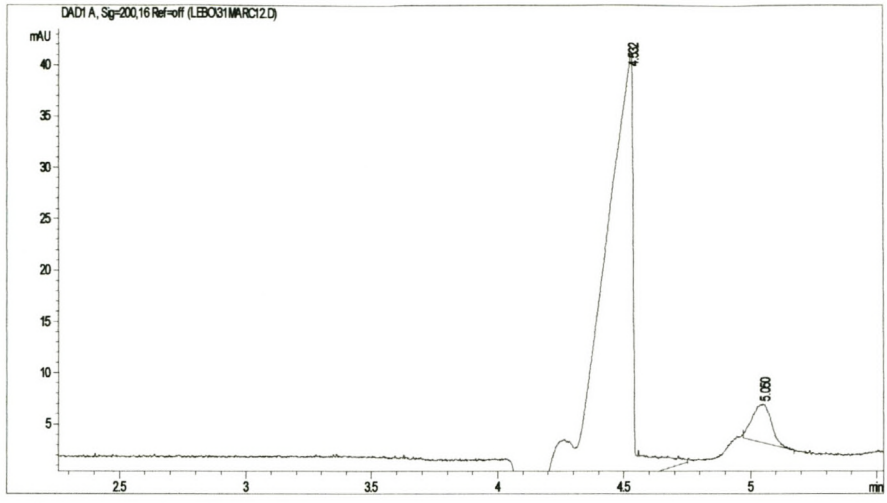


Figure 22: Electropherogram of FeIDS at pH = 5.379

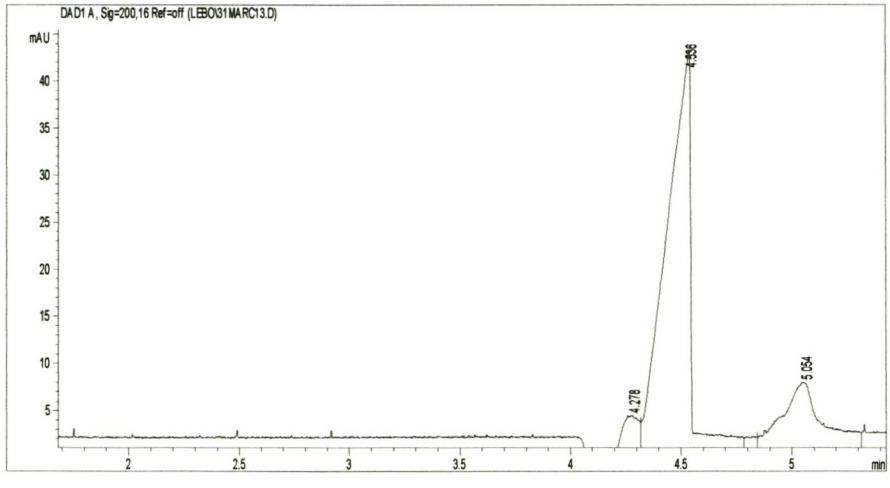

Figure 23: Electropherogram of FeIDS at pH = 4.404

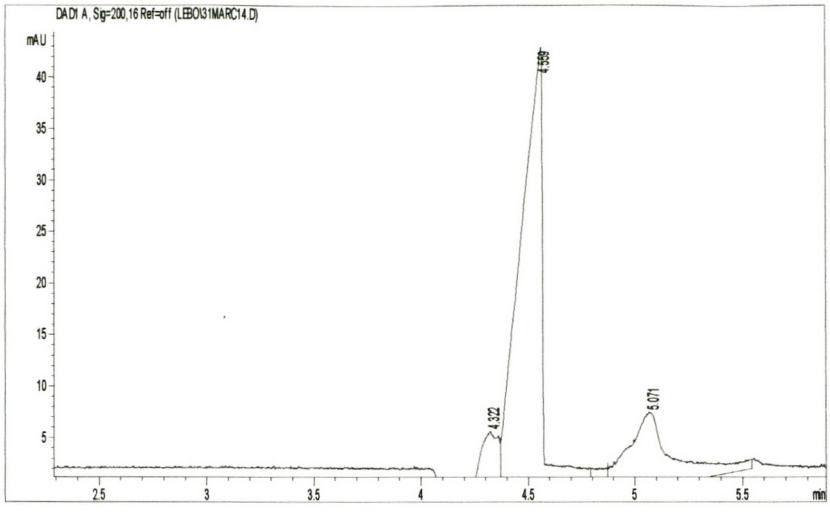


Figure 24: Electropherogram of FeIDS at pH = 3.521

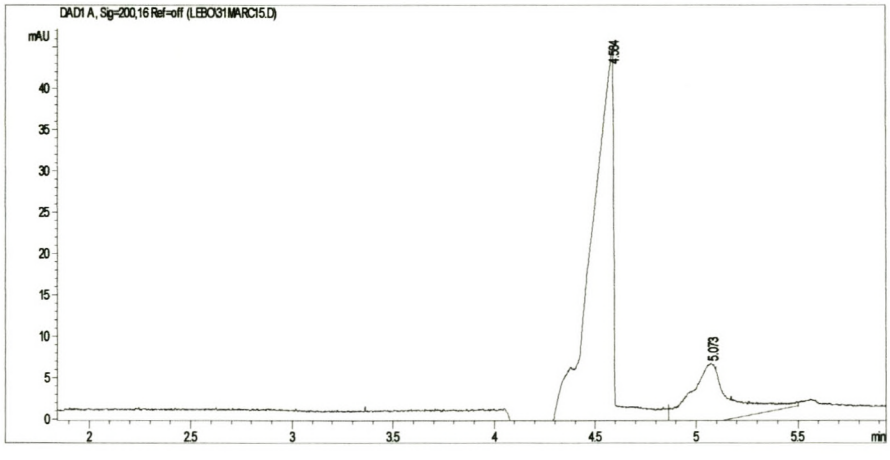

Figure 25: Electropherogram of FeIDS at pH = 2.520

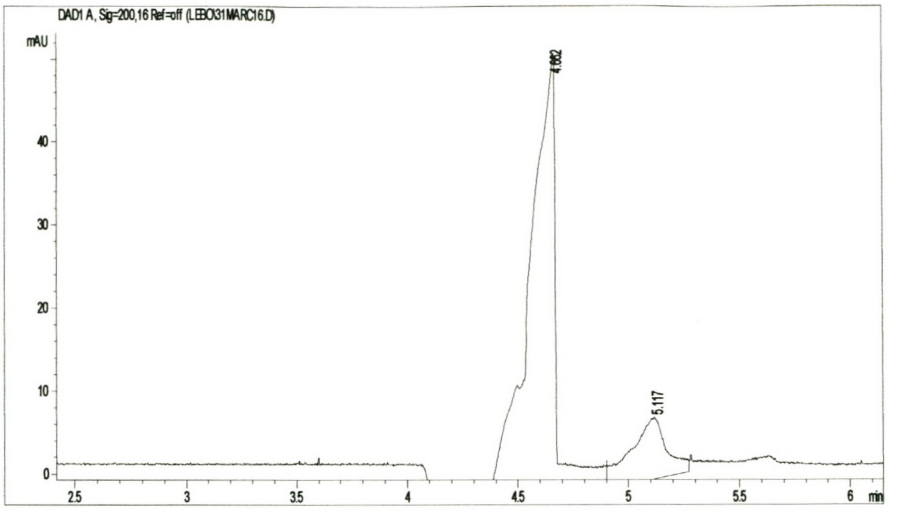


Figure 26: Electropherogram of Mn at pH = 8.527

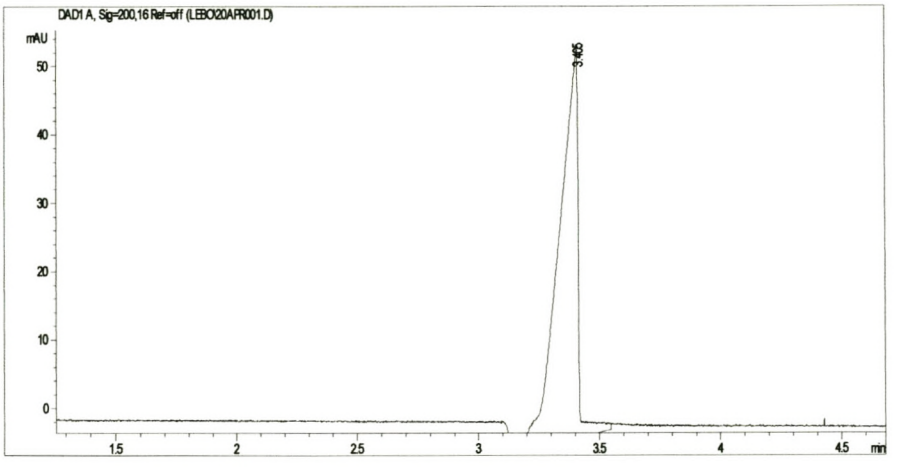

Figure 27: Electropherogram of MnIDS at pH = 8.825

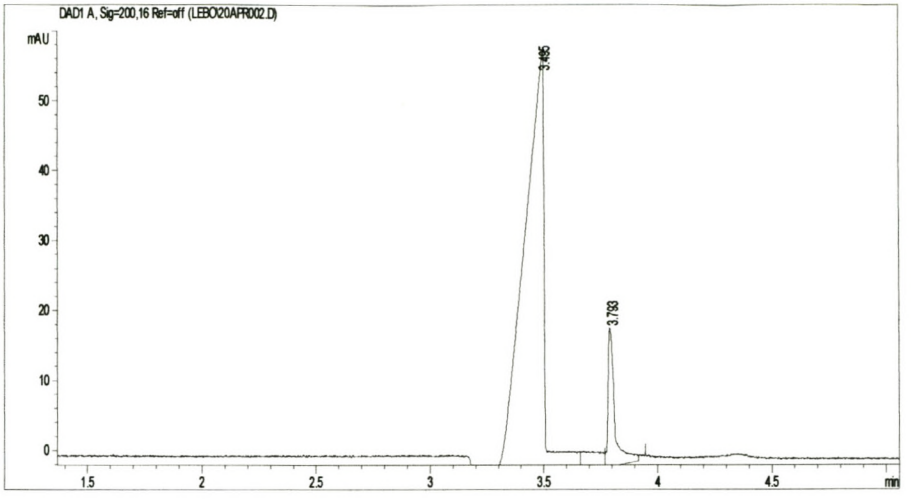


Figure 28: Electropherogram of MnIDS at pH = 7.302

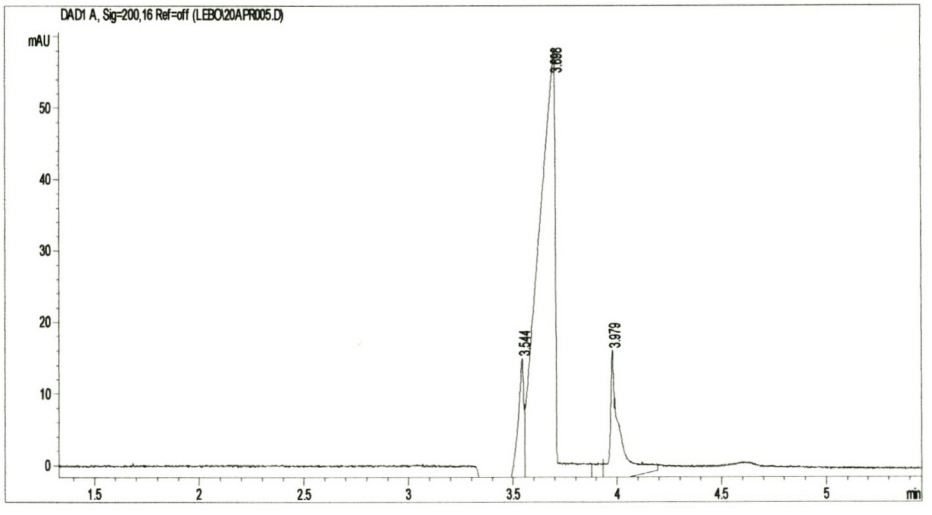

Figure 29: Electropherogram of MnIDS at pH = 6.589

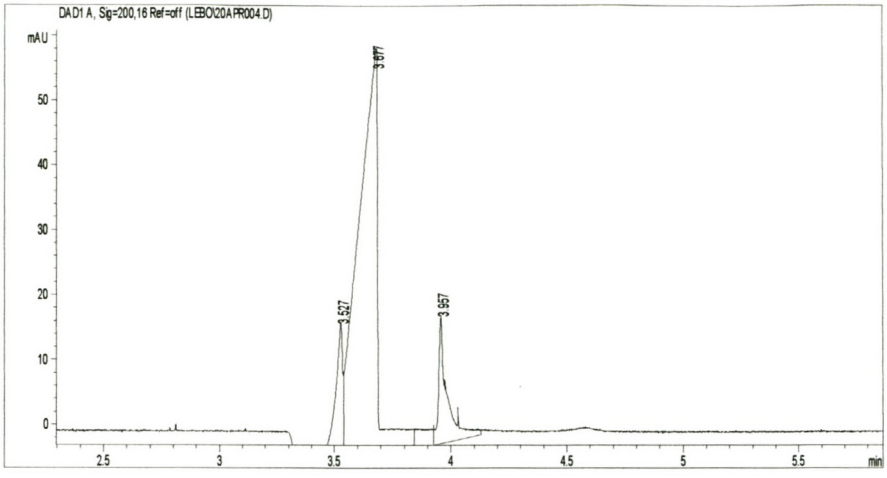


Figure 30: Electropherogram of MnIDS at pH = 5.523

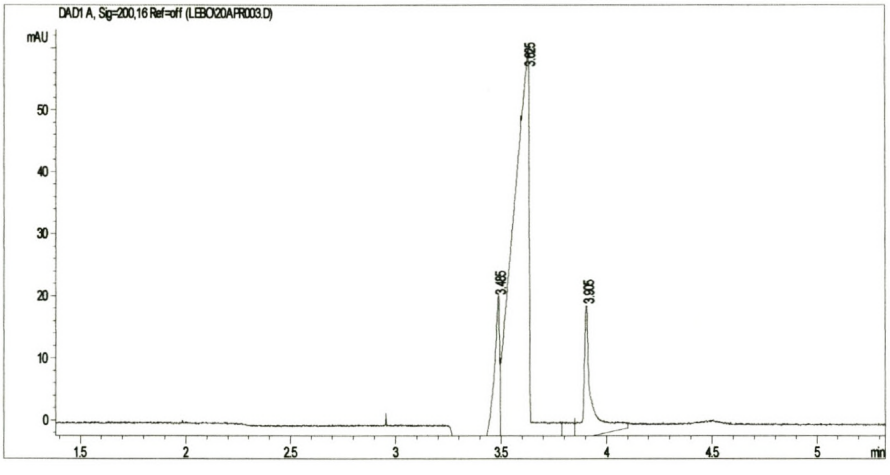

Figure 31: Electropherogram of MnIDS at pH = 4.586

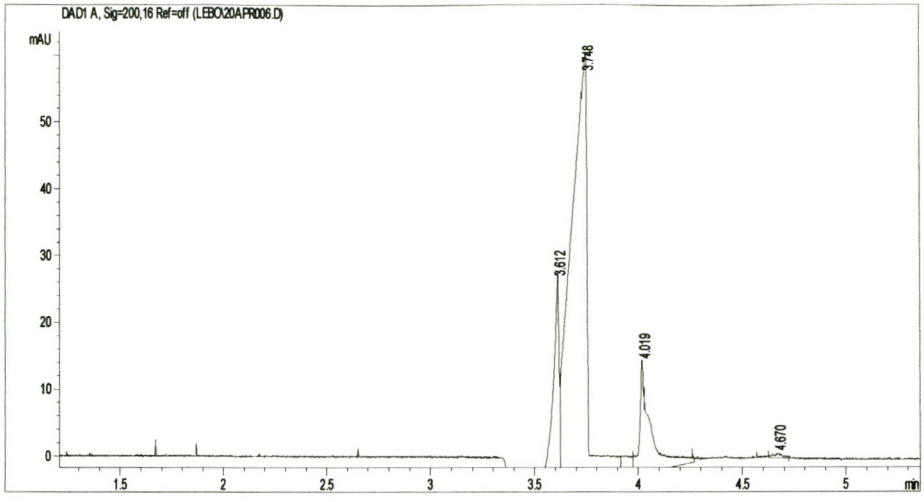


Figure 32: Electropherogram of MnIDS at pH = 3.278

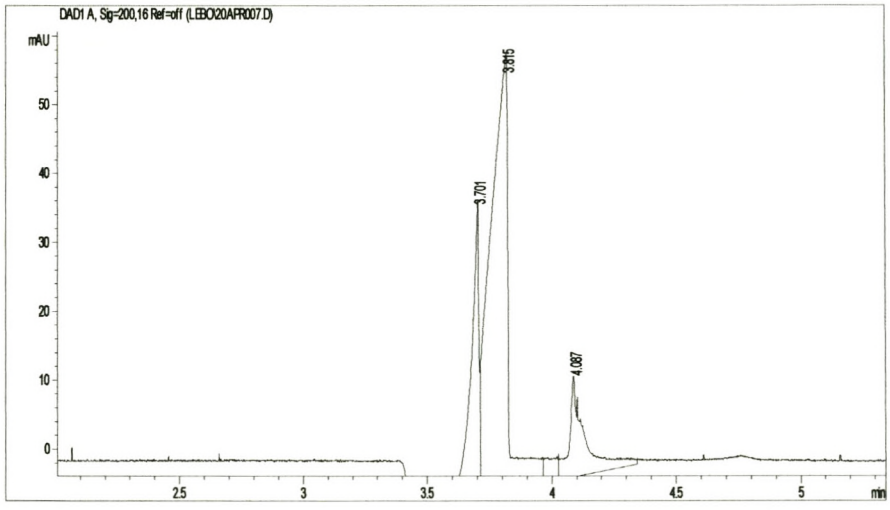

Figure 33: Electropherogram of MnIDS at pH = 2.375

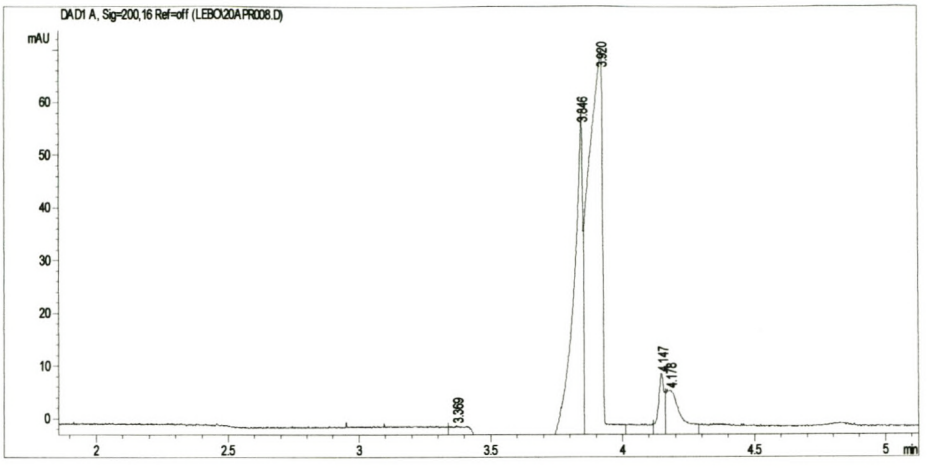


Figure 34: Electropherogram of Pb at pH = 9.003

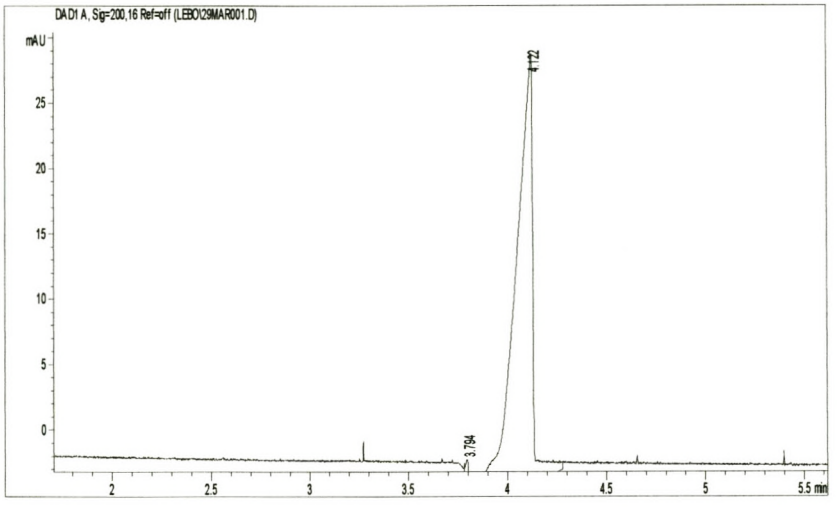

Figure 35: Electropherogram of PbIDS at pH = 8.570

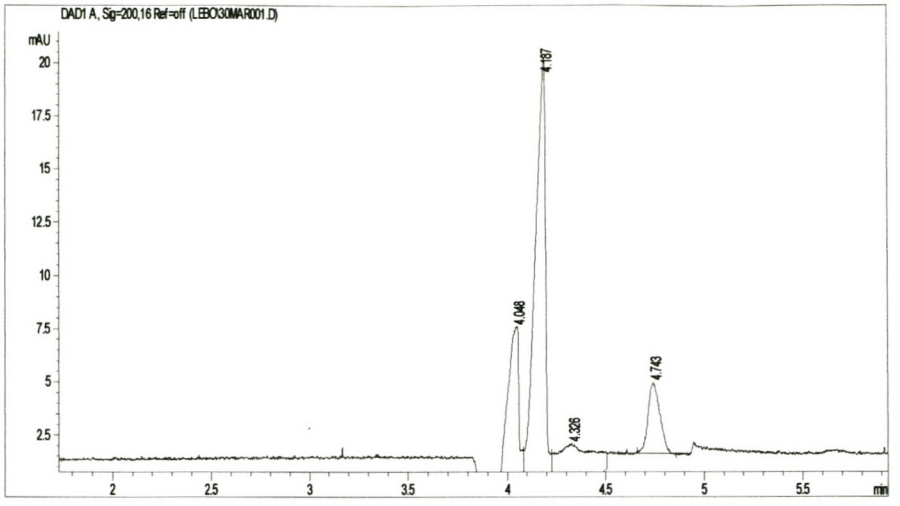


Figure 36: Electropherogram of PbIDS at pH = 7.610

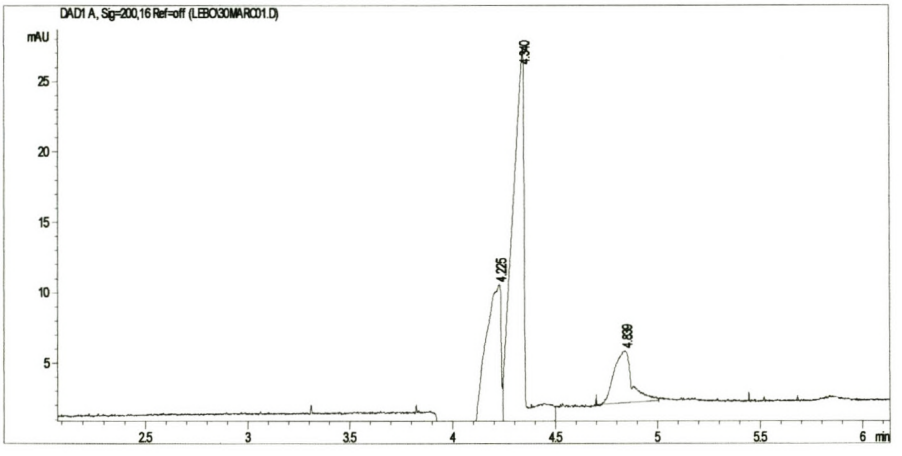

Figure 37: Electropherogram of PbIDS at pH = 6.405

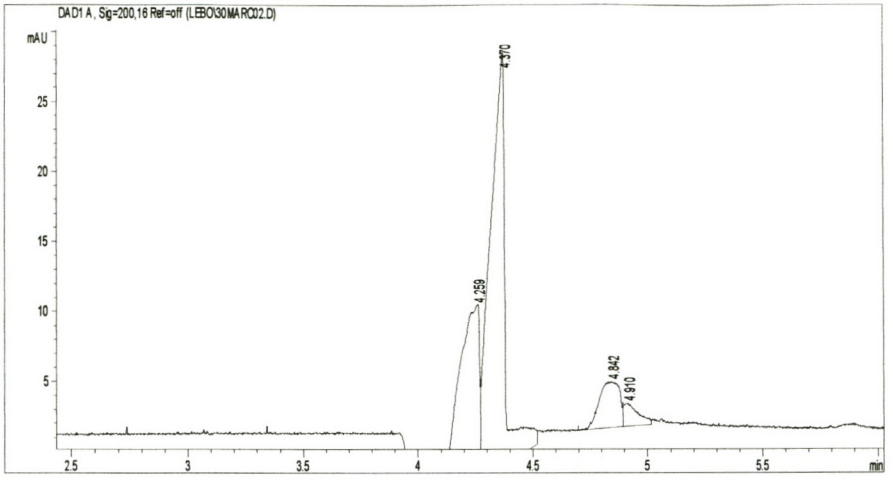


Figure 38: Electropherogram of PbIDS at pH = 5.223

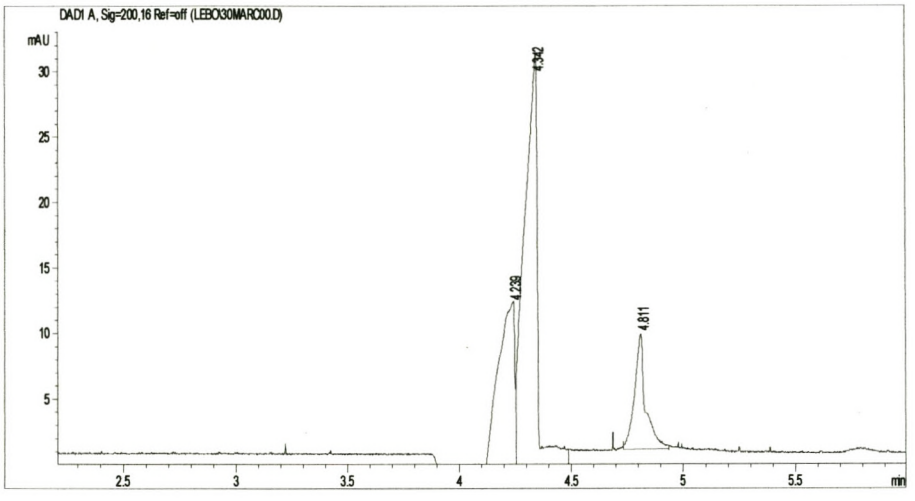

Figure 39: Electropherogram of PbIDS at pH = 4.609

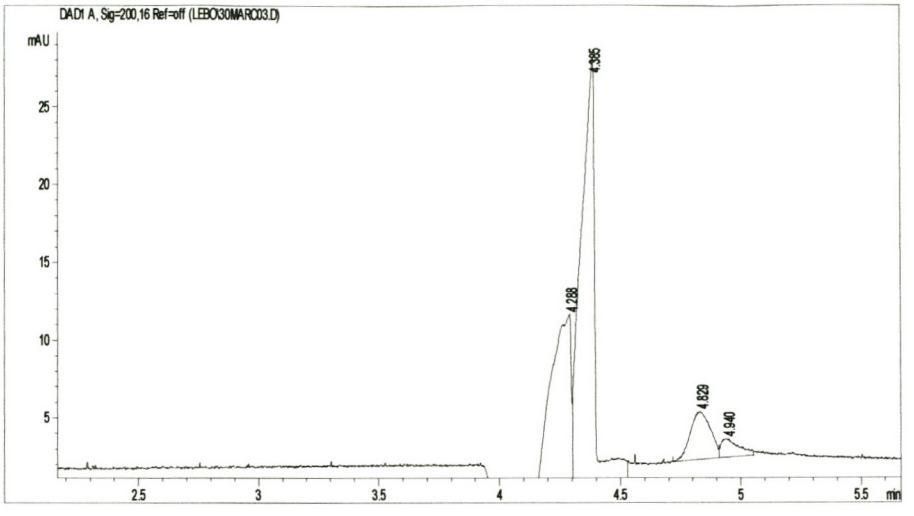


Figure 40: Electropherogram of PbIDS at pH = 3.486

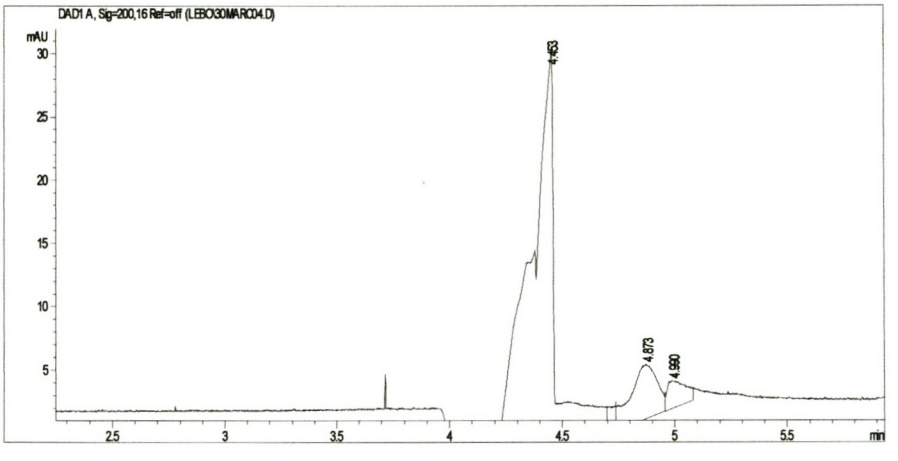

Figure 41: Electropherogram of PbIDS at pH = 2.248

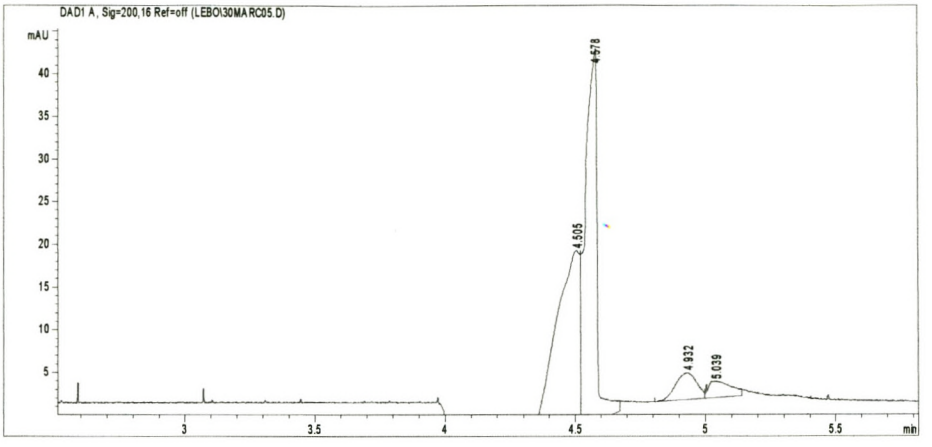


Figure 42: Electropherogram of Zn at pH = 8.348

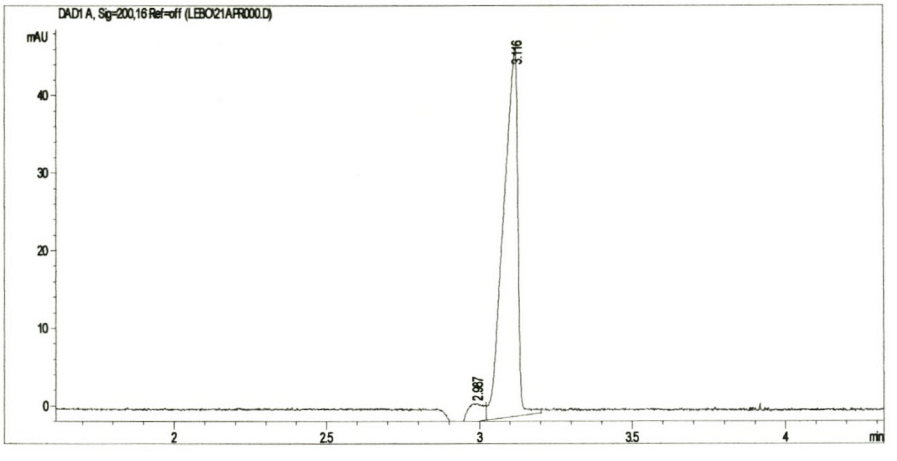

Figure 43: Electropherogram of ZnIDS at pH = 8.837

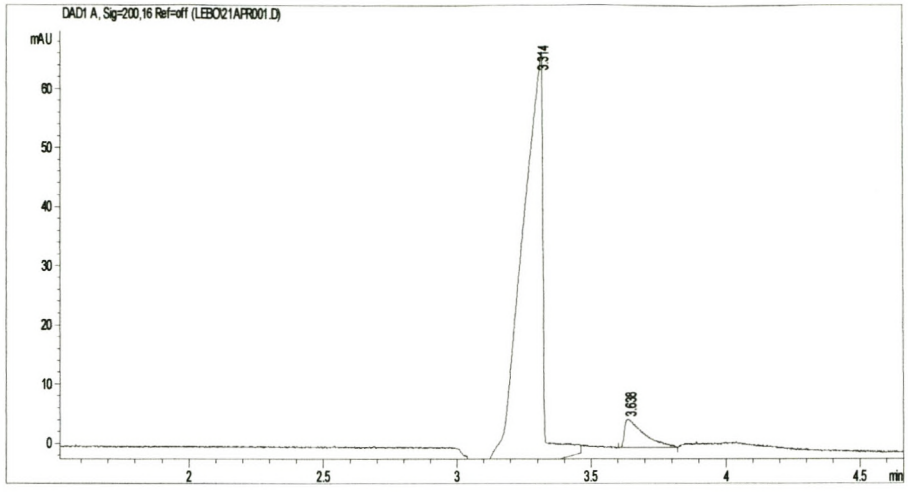


Figure 44: Electropherogram of ZnIDS at pH = 7.011

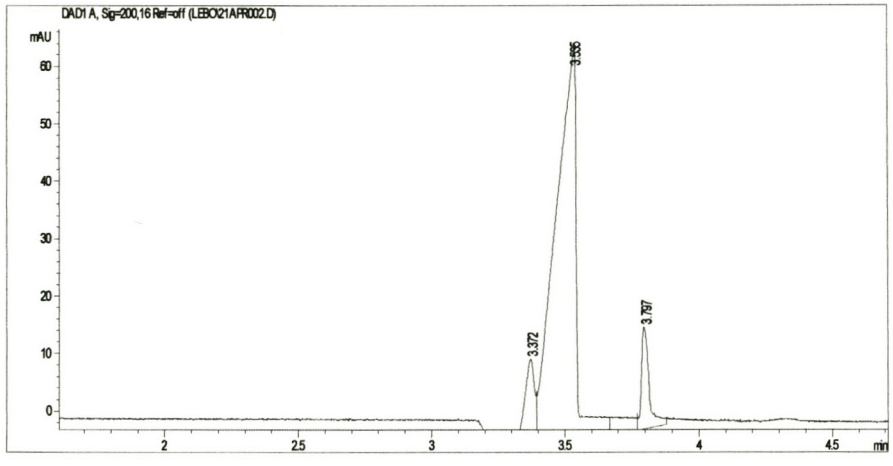

Figure 45: Electropherogram of ZnIDS at pH = 6.371

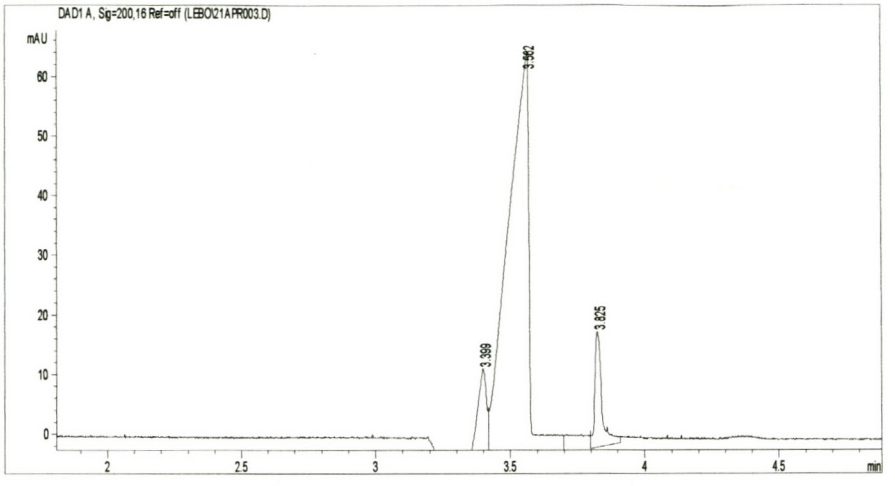


Figure 46: Electropherogram of ZnIDS at pH = 5.139

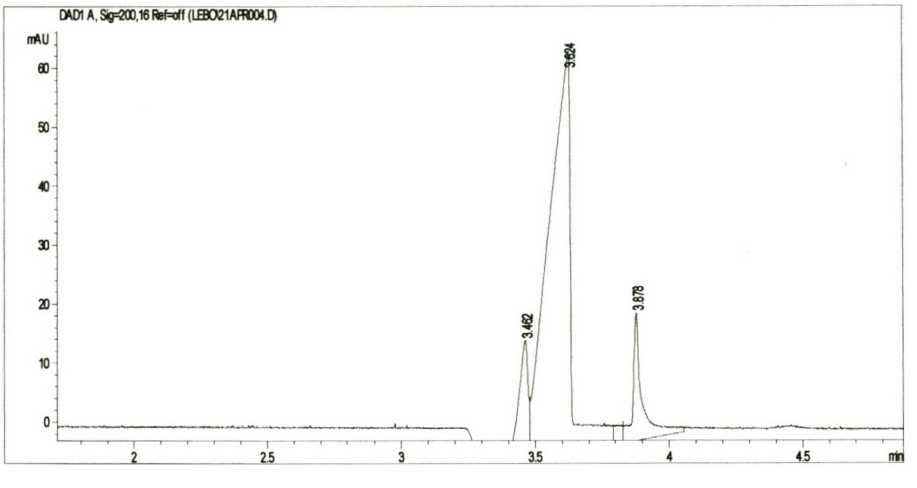

Figure 47: Electropherogram of ZnIDS at pH = 4.276

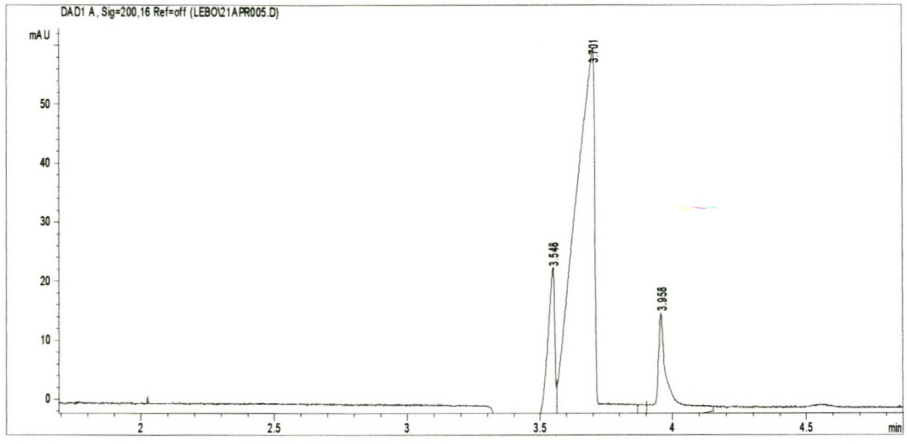


Figure 48: Electropherogram of ZnIDS at pH = 3.156

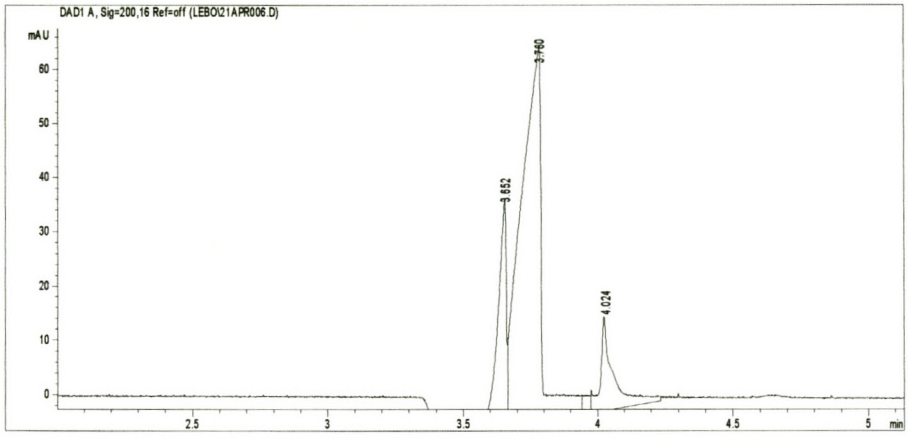

Figure 49: Electropherogram of CdPASP at pH = 7.060

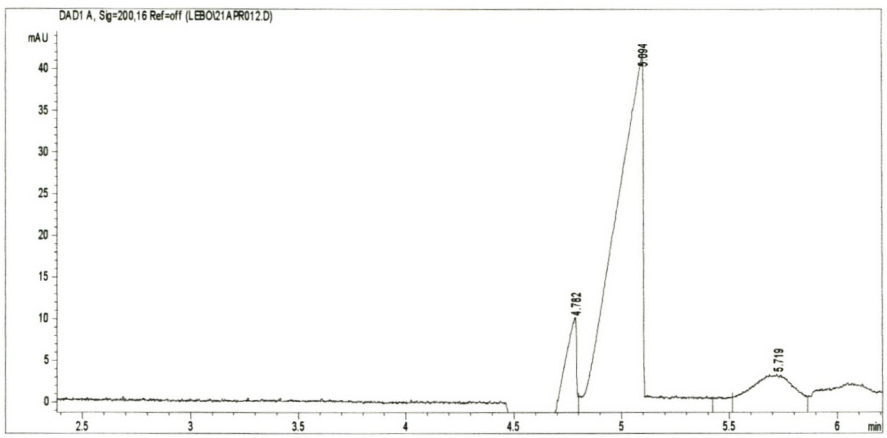


Figure 50: Electropherogram of CdPASP at pH = 6.202